Politecnico di Torino
Corso di Laurea Magistrale in Ingegneria Energetica e Nucleare

# Preliminary modeling of a plasma gasification system for marine transportation


Politecnico di Torino

**Supervisors:**
Prof. Maurizio Repetto
Prof. Hossam Gaber

**Candidate:**
Davide Lisi

A.A. 2020/2021

# Abstract

Cruise ships are complex systems that strongly resemble municipal communities, as they must manage a significant and diversified amount of waste streams, often while far away from the shore. Different waste management techniques are employed on vessels, such as storage and off-loading, discharge at sea (if possible) and incineration. The scope of this study was to develop a model for a plasma gasification system and to simulate the treatment process of different feedstock compositions, based on the waste date obtained from the literature. A parallel model for an RF plasma torch as part of plasma generation system, i.e. plasma generator was also developed, to assess quantities which are needed by the gasification model. The two models were used to investigate the possibility for the system to operate in conditions of electricity net gain, to assess the efficiency of the gasification process through the cold gas efficiency parameter, but also the emissions generated, the heat that can be recovered, the sorbent consumption of the gas cleaning system. In the first section, the environmental issues and the current waste management techniques were investigated, with some references to international regulations. In addition, the different waste-to-energy approaches were described, focusing on the advantages and disadvantages of plasma gasification; subsequently, the modeling phase was carried out, starting from the development of the plasma generator model. Finally, the overall gasification system, comprising of waste pre-treatment, gasification, syngas cleaning, energy conversion, heat recovery sub-models was modeled. Four different feedstock composition scenarios were investigated. The results of the simulations have shown that the system developed is able to treat variable compositions of the waste feedstock, in a mixture of solid wastes, plastics and sewage sludge, while also maintaining a positive balance in terms of electric energy in a suitable range of mass flow rates of feedstock. The heat recovered is reduced for higher contents of sewage sludge, up to -12% in scenario 2 (integration of sewage sludge only) compared to the scenario with only solid wastes. The introduction of plastic allows for a higher heat recovered, up to +23.6% in scenario 4 (integration of sewage sludge and plastic). The cold gas efficiency is increased for higher plastic and sewage sludge contents, up to a maximum value of 58.65%. Emissions are within the limits prescribed by the MARPOL Annex VI regulation (6 gSOx/kWh and 7.84gNOx/kWh) and strongly linked to sewage sludge

content. The results of the torch modeling provide expected results in terms of temperatures and air mass flow rates. This preliminary study suggests potential feasibility of such systems. However, in future research works, the models will need validation through experimental setups. Improvements to the model will also be needed, to increase the complexity of the physics involved and to investigate some additional plasma gasification issues, like tars formation, clogging and dioxins formation.

## Acknowledgements

I would like to thank ProFlange and OCE for the support on this research work, as well as the members of the Plasma team at the University of Ontario Institute of Technology (UOIT) for warmly integrating me in their research group and for the knowledge they shared on plasma technologies and gasification processes. In particular, I would like to thank Prof. Gaber, Dr. Vahid, Isaac and Mohamed. I would like to thank my family for encouraging me and always supporting me in this journey, thank you Mamma, Papà and Ale! Finally, I would like to thank my girlfriend Laura for always being there in times of need and for always cheering me up, when I was down; thank you for everything.

# Contents

# List of Figures

# List of Tables

# 1 Introduction

## 1.1 Background challenges of the cruise industry

The cruise industry is one of the most rapid growing tourism sectors, accounting for 30 million passengers worldwide only in 2019; the number of cruise ships in operation, up to 2019, is 272 and expected to grow, according to the CLIA (Cruise Lines International Association) [1]. The cruise market is showing a steady growth in both passengers and operating cruise ships since the early 2000s and, according to this development, major concerns regarding the sustainability of the industry are raised. In the context of sustainable development, a sustainable industry should be able to meet the needs of the present without hindering the necessities of the future generations. In particular, the three main fields in which these necessities can be categorized, are the economical, societal and environmental fields. According to the CLIA reports, the global economic impact of the industry amounts to $134 Billion Worldwide in 2017 and to $150 Billion in 2018, where the global impact was calculated considering direct, indirect and induced economic contributions [2]. The direct contribution is represented by the expenditures of the cruise industry, including the expenditures of the crew and the passengers. In turn, the cruise industry, which provides these services, affects indirectly the secondary businesses existing on the territory due to the increased demand of goods, utilities and services like electricity, water, raw food, raw materials. Finally, the induced contribution is represented by the general expenditures of the employees of cruise lines and the secondary suppliers. In 2017 the direct contribution to the whole global economic impact amounted to $61 billions, while the induced and indirect contributions amounted to $73 billions; $45.6 billions were payed to the directly and indirectly involved workers, the number of which adds up to 1108676 full-time jobs required [2]. While this data would suggest strong positive economic and social impacts on the affected regions by cruise tourism, it would be important, in any case, to investigate more in details these societal dynamics to find possible criticalities and shortcomings. As an example, MacNeill and Wozniak analyzed the effects of cruise tourism on a local community in Trujillo, Honduras through the use of mul-

tidimensional indicators and control groups, before and after the opening of a cruise ship port [3]. The study shows that the creation of the port did not benefit the local population. In fact, while improvements to cultural capital and security were observed, increased corruption and reduced capacity for residents to provide for their primary needs were other consequences [3]. The conclusions of MacNeill and Wozniak are that, in order to reach high levels of sustainability the cruise industry must not overlook these dynamics and provide means to protect the communities, by investing in infrastructures such as sewage/garbage treatment and collection plants, and by involving the local populations in open consultations. Furthermore, government regulations, where missing, could definitely aid in reducing these potential impacts. On this regard, destinations planning is a fundamental phase of the sustainable development of a new route. In fact, ports need to be able to receive larger ships to embrace the cruise market expansion but at the same time they should be able to satisfy the needs of the local communities and minimize the environmental impacts on the affected territory. Indeed, besides societal and economic impacts, the cruise industry, and more in general the marine transportation industry, can impact the environment in different ways and it is not often easy to quantify the magnitude of these impacts. Johnson employed a Life Cycle Assessment (LCA) approach to identify and characterize the various sources of impact, by dividing them in separate stages defined by their inputs and outputs. These are infrastructure impacts, comprehending construction and operations, transport impacts, use and consumption impacts, disposal impacts [4]. Infrastructure impacts are related to the construction of the vessels and all the necessary auxiliary facilities and their operations; they include electricity, water, raw materials consumption, soil occupation, local environment modifications and exploitation, air and noise pollution. The transport impacts are related to the logistics and the distribution of passengers and supplies to the facilities and the vessels. The use and consumption impacts are related to the overcrowding of destination areas by passengers, the consumption of local resources such as water, electricity, various goods such as detergents and food, and impacting activities such as littering. Lastly, disposal impacts are linked to the management of waste streams produced on the vessels and in the facilities. This last category is the one that will be analyzed more in depth in the next chapter, as the wastes produced on cruise ships will be the focus of this work. Indeed, the environmental impacts of the

main ship-generated wastes will be described, in order to give the readers an idea of the importance of the correct management of these streams. On this specific issue the International Marine Organization (IMO) has produced an international regulation, the International Convention for the Prevention of Pollution from Ships (1973) as modified by the Protocol of 1978 (MARPOL 73/78), to control the disposal and the management techniques for certain types of wastes, as detailed in the six annexes of the convention, which will be referenced inside the manuscript. The characterization of the waste production on cruise ships is important not only to give the reader a grasp on the issue, but also because the following chapters will make use of relevant and related data collected from the literature.

## 1.2 Objectives and document structure

The main scope of this work is to develop a comprehensive model for a small scale plasma gasification system conceived to be installed on relatively large cruise ships for the treatment of ship-generated waste streams, rivaling existing techniques such as incineration. The idea is fairly novel and a very low number of papers exist in literature on the topic. Notably, the most comprehensive study was performed by Pyrogenesis that developed a system for the treatment of solid waste, called PAWDS (Plasma Arc Waste Destruction System) [5]. The study provides insights on the design of such systems and provides experimental results for a specific waste composition and feedstock mass flow rate. The model developed in this study aims to aid the design of such systems, allowing the investigation of different scenarios through simulations and in terms of waste composition, quantity of feedstock treated, operating conditions at the gasifier (gasification temperatures, plasma air mass flow rates), at the syngas cleaning step (quantity of sorbent involved) or at the energy conversion step (combustion temperature, combustion air quantity). Indeed, the model will be used to run a series of simulations for the treatment of different compositions of feedstock, which were based on the data extracted from literature. In particular, two sub-models are developed: a plasma generator model and a plasma gasification system model. The objective of the plasma generation model is to investigate the possibility to produce air plasma at the conditions required by the plasma gasification system, in terms of temperature and mass flow rate at steady state. The objective of the plasma gasification model is to show that the system modeled

can operate without the need of external sources of electric energy, by exploiting the syngas produced to generate internally the electric power needed to maintain the plasma generators operating. Moreover, the system should also be able to operate under different conditions of feedstock compositions since waste on cruise ships comes in different varieties. The flexibility of using different varieties should be investigated. The cruise ship waste generation and characterization was analyzed in chapter 2. In chapter 3 the various Waste-to-energy approaches and their pros and cons were described, to justify the plasma gasification choice. In chapter 4 the plasma torch is modeled, using the software COMSOL. In chapter 5 the plasma gasification system is modeled, using the software Aspen Plus. In chapter 6 the conclusions of this work are presented.

# 2 Waste generation and management on cruise ships

Cruise ships can be considered to all effects small floating cities. While the number of passengers may vary depending on the dimensions of the ship and the type of voyage (by river or by sea), in the last few decades this maximum capacity has been almost doubled with the construction of "megaships", long about 350 meters and capable of carrying about 5400 passengers. According to the numbers provided by cruise lines, the average number of passengers amounts to 3000 guests for sea cruises and 150 for river cruises, while the biggest ship, up to 2018, is the "Symphony of the seas" of Royal Caribbean Cruises Ltd. long 361 meters and capable of hosting a maximum of 6680 guests [6, 7]. While 2020 was not an ordinary year for the cruise industry (and a lot of other industries) due to the COVID-19 pandemic, according to the CLIA, 270 cruise ships are projected to be operational in 2021 and as such every single one of these ships will need to be able to provide certain services and goods to its passengers and the crew [8]. While the destination tourism generally represents a significant part of the cruise experience, it is also true that a big factor playing in the cruise market success is the "shipscape" or the ship itself. In fact, since the 90' cruise ships evolved more and more towards the "Hotel" business model, by implementing innovations such as restaurants, bars, spas, fitness centers, pools, casinos, theaters and sometimes even full-sized basketball courts to stimulate the on-board experience [9]. This increase in ship dimensions and passenger's capability, coupled to the shift of the business model from just the shipping of people to the cruise vacationing, led to an increase of the pressures on the local environment and the destination ports. The main environmental pressures induced by the cruise industry are generally region-specific and also depend on the types of technologies adopted by the different cruise ships; these key issues are related to the air emissions, ballast waters, hazardous wastes, solid wastes, gray and black waters, bilge waters and the impacts on coral reefs [10], which will be described briefly one by one in the next sections.

## 2.1 Air emissions

Air emissions are mainly generated by the diesel engines whose task is

to produce enough mechanical energy to rotate crankshafts that are in turn connected to the ship propellers. In reality, newer ships adopt main diesel engines to power generators to produce electric energy that can be in turn used to power motors for the needed mechanical power; this system is often preferred since the large main diesel engines can thus operate in their optimum conditions regardless of the ship velocity [11]. Smaller and independent diesel engines or gas turbines are used to produce the electric energy necessary for the correct functioning of the ship during normal operations, while small and redundant back-up diesel are employed to maintain the vital functions of the ship in case of offshore emergencies. While there are cases of ships being able to move for 30 minutes by only using electric batteries [12], diesel fuels are still the main source of energy for the engines and therefore the moving capabilities of the cruise ships depend on it. In fact, the majority of cruise ships run on HFOs (Heavy Fuel Oil), a low-grade product of petroleum thermal cracking with a high Sulfur content. This type of fuels enhance SOx emissions due to their composition, but other types of emissions, such as $NOx$, VOCs (Volatile Organic Compounds) and $CO$ are also significant, since the combustion quality is low due to generally relatively poor atomization characteristics [13]. Beside these types of emissions, particulate matter and GHGs (Greenhouse Gases) are also produced, such as $CO_2$ and in some cases $CH_4$, due to methane slips, which are typical of LNG (Liquid Natural Gas) powered ships. Air emissions due to cruising contribute to different notorious issues. GHGs contribute to global warming and climate change, $NOx$ and $SOx$ play a fundamental role in rain acidification while also being toxic to human, together with certain types of VOCs, particulate matter and $CO$. $NOx$ are also strongly linked to eutrophication processes of water bodies, issue that is most relevant when linked to marine transportation. The emissions from the shipping industry represent a significant share of the global emissions but the cruise industry make up just for a small fraction of that. For example, while shipping accounts for 2.2% of the global emissions of $CO_2$, cruising accounts to just 5% of that share [14]. Nevertheless, due to the intrinsic nature of cruising, which is based on the concept of weekly repetitions of the same itinerary for entire seasons, cumulative effects on regional small scales could be of significant impact for the local environment. As it will be described in more details in the next sections, incineration of wastes on-board of cruise ships contributes, in a small fraction, to the generation of

air emission: for this reason, it would be beneficial to investigate alternative solutions to reduce these impacts.

## 2.2 Coral reef impact

Coral reefs are underwater ecosystems home to an estimate of 25% of worldwide marine species while also occupying less than 1% of the ocean surface [15]. From the point of view of biodiversity richness, coral reefs are often compared to rainforests. These reefs are generally constituted by stony corals colonies held together by calcium carbonate and are often found in shallows waters close to the coastlines. Corals provide food and protect a large number of marine species from predators and waves meanwhile algae, sea grasses and mangrove protect the corals from various harmful pollutants. These complex ecosystems, while of significant importance to the biosphere, are also extremely fragile and are often threatened by human activities. Besides the important contribution do biodiversity, coral reefs provide a significant amount of the seafood consumed globally and their impact on local tourism is substantial. The reefs act also as barriers against coastline erosion by slowing down waves. While the main contributors to coral reefs decline are ocean warming, ocean acidification and overfishing (in particular blast-fishing and cyanide-fishing), mining practices, sea pollution and irresponsible tourism represent a threat to these ecosystems as well [15]. In particular, the cruise industry contributes to these pressures in different ways: cruise ships can directly damage coral structures by accidentally hitting them with the hull or the anchor, and indirectly by transporting to the destinations tourists that may damage or disturb these delicate habitats [10]. Furthermore, due to the growing nature of the industry new ports may be constructed and old ports may be fitted to receive bigger vessels, directly damaging the sea floor and indirectly increasing air and water pollutants in the affected regions. In fact, the movements of the large ships generate turbidity plumes in inter-reef waters while ship hull's paint can contaminate sediments preventing marine organisms settlement [16]. In order to reduce the impact on coral reefs, cruise lines are adopting preventive measures such as the anchoring in predetermined safe zones and the release of treated wastewater at sufficient distances from the reefs; also, guests are sensitized and educated in order to minimize their impacts [10].

## 2.3 Ballast waters

Ships use ballast waters to maintain ship stability and compensate reductions in weight due to fuel consumption, wastewater discharges, cargo and/or passengers unloads. These large quantities of water are removed from a location and subsequently discharged into a different area. Often, ballast waters may contain animals, viruses, bacteria and plants native of a specific zone, therefore when these are discharged in different locations disruptions to the local ecological equilibrium may happen by introduction of non-native invasive species. Cruise ships generally discharge ballast waters outside of ports because no big changes of weight happen when docked. While this type of environmental impact is much bigger for ships that travel long distances crossing different ecosystems, it is still non-negligible for cruise ships that follow the same routes multiple times. There is still no widely spread solution to the issue, but different technologies are being tested for the elimination of non-native species. The employment of chemical biocides, heat, filtration, ozone, deoxygenation are some of the main approaches followed [10].

## 2.4 Wastewaters

Wastewaters are generally classified as gray waters and black waters. These two types of liquid wastes are normally produced intensively by human activities and their nature and impact to the environment can strongly differ. Gray water, also called washwater, is a type of wastewater with low levels of pathogens and bacteria. Its main source, in human agglomerates, are showers, sinks, washing machines, dishwashers. It can be generally reused for toilet flushing, to reduce water consumption, or for irrigation, thanks to its abundance of nutrients. To do so, it is generally treated beforehand, and the complexity of the treatment depends strongly on the specific application and the quality needed. Black water is mainly generated from toilet flushing and medical facilities, and may contain a mixture of urine and feces diluted into a water matrix. It can generally carry a much bigger quantity of pathogens, bacteria and have a higher content of organic compounds with respect to gray water, therefore the two streams are generally separated. Both types of wastewaters are generated on cruise ships and the average quantities esti-

mated, for a ship transporting 3000 passengers, are 57 to 114 $m^3/day$ of black waters and 341 to 965 $m^3/day$ of gray waters [17]. The main risks associated to wastewaters are related to human health and the potential environmental impact in case of open discharge into the sea; in fact, both wastewaters may contain different types of pollutants, ranging from heavy metals and chemical compounds such as Chromium, Copper, Zinc, Nickel, Lead, Ammonia, Chlorine, but also fecal coliforms and viruses, hazardous to human health and marine ecosystems. MARPOL 73/78 annex IV regulates sewage discharges from ships but no specific indications are provided for grey water removal. Some national regulations exist to control untreated gray water discharges, such as the 2008 VGP (Vessel General Permit) issued by the EPA (US Environmental Protection Agency). The regulation prohibits discharges of untreated gray water unless the vessel is operating at least one nautical mile from the shore and at a speed of minimum 6 knots [18]. On the other hand, the dispositions issued by MARPOL 73/78 for black water are precise: if sewage is treated and disinfected, it can be discharged between 3 and 12 nautical miles; if sewage is not treated, it can only be discharged 12 nautical miles away from the shore. In both cases the vessel must proceed at a speed of at least 4 knots and the waters cannot be released instantaneously [19]. Wastewater nutrients can enhance and over-stimulate the growth of algae and plants reducing the oxygen content in the water. This process is called Eutrophication and can strongly impact marine life and coral reefs ecosystems. It is clear than how important is for the cruise industry to develop sustainable methods and advanced technologies to dispose of sewage in a clean and affordable way.

### 2.5 Oily Bilge Waters

The issue related to the generation of bilge waters is characteristic of ships, and cruise ships are not an exemption. The bilge is the lowest part of a ship and because of that, small quantities of water tend to accumulate there, generally due to condensation. Often, this type of wastewater mixes with spills or leaks of fuel, and lubricants of the various machinery present in the lower decks of the ship, creating a collection of oily water that must be disposed of. According to estimates, the quantities of oily bilge waters produced depend on the ship dimensions and can vary from 5 to 140 $m^3/day$

[17], and the risk associated to these waste streams is linked to the possibility of having accidental spills of such oily mixture. The impact of oil spills on the marine environment can be significant and the residence times of these oils depend on the their composition: while light oils may evaporate or dilute and diffuse more easily in water, heavy oils can accumulate and even form tar balls, and some oil agglomerates can last even 20-25 years [20]. These substances can be extremely harmful for the sea life, killing turtles, fish, seabirds, seaweed, crustaceans and, due to the accumulation on the surface of the sea, can hinder the development of larvae and fish eggs [10]. MARPOL 73/78 Annex I regulate the collection by pumping, stocking, treatment and eventual sea discharge/port disposal/incineration of the oily bilge waters [19].

### 2.6 Hazardous and non-hazardous solid wastes

Cruise ships can be generally considered as huge floating luxurious resorts and as such the quantities of solid wastes produced by the passengers and the crew can be substantial. It is estimated that while belonging to just 1% of the global shipping fleet, the cruise industry generates up to 24% of the total share of waste produced on ships [17, 21]. This is mainly due to the nature of cruising itself, in which a large number of passengers is engaged in the most various activities: buffets, sports, social events, shopping, spa treatments and more. Solid wastes are divided in two sub-streams: hazardous wastes and non-hazardous wastes, as function of the potential hazards to human health and the environment, if not correctly handled. Typical hazardous wastes generated on cruise ships are x-ray development fluids produced by photo processing, print shops waste fluid such as inks, outdated and unused pharmaceuticals, chlorinated dry-cleaning fluids, batteries, fluorescent and mercury vapor lamp bulbs. Hazardous wastes can be solid as well as liquid or gaseous and must show at least one of the following characteristics: ignitability, corrosivity, toxicity, reactivity [22]. Since this kind of wastes, if mishandled, can pose a significant threat to human health and to the environment, cruise lines are actively working on reducing their generation by developing alternative and sustainable ways to provide the same type of services, such as photo digitalization, filtration systems for dry-cleaning, non-toxic alternative inks and generally enhanced recycling. General practices for disposal of such materials include off-loading to designed ports and in some

cases incineration [10]. No regulation on the matter is found on MARPOL 73/78. Instead, non-hazardous solid wastes include food leftovers, kitchen greases, packaging materials such as plastics, cardboards, paper, steel cans, glass, aluminum generated in all kind of activities present on board. According to estimations, for a 3000 passengers one-week cruise, about 50 tons of solid waste are generated [17]. Sliškovi´c et al. (2018) assessed the composition of the solid wastes by studying cruises docking to three of the main Croatian ports (Dubrovnik, Zadar, Split): their conclusion is that 62% of the total wastes are domestic wastes, 26% are plastics and 11% food wastes, where domestic wastes are the remaining non-hazardous wastes (paper, metals, cardboard...) [23]. According to MARPOL 73/78 Annex V, discharge in the sea of plastics and toxic incineration ashes is prohibited (toxicity in ashes must be assessed). For floating materials and dunnage, discharge is possible only if the ship is at least 25 nautical miles from the shore, while for paper, glass, cans discharge is possible, after shredding, if the distance is more than 12 nautical miles [19]. In case of accidental or unlawful discharges, the impact on the environment can be significant. Floating marine debris, depending on the type of materials and their dispersion properties, can accumulate on beaches, on the water and on the seabed. Potential impacts include ingestion of plastic by marine species or entanglements of birds, turtles, fish in packaging materials, alterations in the ecosystems by non-native species insertion, physical injuries to humans, aesthetic degradation of landscapes. As for hazardous materials, pushed by economic and environmental reasons, cruise lines are trying to reduce as much as possible the generation of wastes and the necessity to resort to incineration; for this reason, recycling programs are being enhanced and the purchase of reusable and/or biodegradable materials replacing plastics, are being encouraged [10].

### 2.7 Waste management systems and procedure

As it is clear, cruise ships must manage a considerable number of waste streams that differ in properties and potential harm to the environment and human health. The main convention regulating this issue at a global level is MARPOL 73/78, developed by IMO and ratified by 158 parties representing 98.95% of the total world tonnage. While MARPOL 73/78 is not a law per se, ratifying countries must comply by enacting domestic law to implement

the convention. One example is the APPS (Act To prevent Pollution from Ships), implemented by the US. MARPOL 73/78 is composed of six annexes, each tackling one issue related to marine pollution: annex I, IV and V were already mentioned when discussing the environmental impacts related to oily waters, sewage and solid wastes; Annex II, III and VI are concerned instead with pollution by noxious liquid substances, pollution by harmful substances in packaged form and air pollution [19]. It is important, before assessing the possibility of employing alternative and advanced technologies, to understand the state of art of waste management on vessels and how cruise ships comply with MARPOL 73/78 requisites. An inclusive and updated report on the matter is provided by CE Delft [24], and in the following sections these methods and technologies will be described.

### 2.7.1 Oily Bilge Waters management

Starting from oily bilge waters, as already mentioned, these cannot be discharged at sea without proper treatment. In fact, according to Annex I, all ships with 400 tons gross tonnage and above, which is the case for cruise ships, can discharge oily mixtures if the ship is not in a special area, proceeding en route and if the oil content does not exceed 15 ppm. Cruise ships must be provided with an oil tank for storage and pumps to recover oily waters collected in the bilge. Stored oily water can be accumulated and discharged at designed ports or can be treated on board for potential discharge or incineration. Indeed, many vessels are provided with OWS treatment systems (Oil Water Separator) to separate the oily fraction from water through absorption/adsorption methods, membranes or through density differences. While the clean water portion can be disposed of at sea, the remaining (65-85%) oily fraction is stored into a sludge tank. Subsequently, the oily residues can be retained and discharged at the ports or further treated. This treatment is usually comprised of evaporation to reduce water content and then incineration, which can reduce sludge volume even up to 1% of the initial value. Related to incinerators, the MEPC (Marine Environment Protective Committee) has released a resolution for the standardization and specification of design, manufacture, performance, operations of units up to 4000 kW. Cruise ships are often equipped with incinerator units for 1500kW or more of capacity, capable of treating oily residues, sewage sludge and solid wastes [25].

### 2.7.2 Black waters management

Black waters too, according to annex IV, cannot be discharged at sea without treatment. Cruise ships, and every ship producing sewage, must be equipped with a holding tank capable of holding enough sewage to allow correct functioning of the vessel and measurement instruments that display the level of filling of the tank. The amount of sewage produced depends on the type of toilet employed. In fact, vacuum toilets consume less water than standard toilets. After transportation, the accumulated blackwaters can then be comminuted and disinfected or treated into an on-board sewage treatment plant. Comminuting and disinfection are generally performed by type 1 MSDs (Marine Sanitation Device), while type 2 MSDs employ aerobic digestion to treat sewage [22]. Type 2 MSDs are the most common type of treatment plants: based on aerobic digestion by bacteria, these are generally divided in three main chambers: the first one is a septic tank in which the water fraction is separated by scum (top) and sludge (bottom), the second compartment is the aeration chamber where bacteria are assisted by air in breaking the remaining solid part and the third one is for disinfection of water by chlorination or UV light. The obtained clean water can be mixed with gray water and be discharged between 3 and 12 nautical miles from the shore [19], while the sludge is digested by aerobic bacteria and stockpiled until discharge at ports.

### 2.7.3 Solid waste management

Solid Wastes are a very heterogeneous type of waste and according to IMO can be generally divided into plastics, food wastes and domestic wastes. Cruise ships generate, and must therefore manage, all these kinds of garbage. Generally, these streams are separated, and the procedures followed as well as the machines involved, may be different. The number of plastic wastes generated on board depend on the number of passengers and the consumption of materials is linked to the standards of living [22]. Nevertheless, the CE delft report estimates a generation of 0.001 to 0.008 $m^3$ of plastics per day and per person. Plastics must be further classified in dirty and clean, and stored separately. The reason is because dirty plastics may have been in contact with spoiled food and therefore may carry hazardous pathogens. Collected plastics from bins are first separated and then can be treated in two different ways: compaction by crusher and discharge to destination port or else in-

cineration. The most common disposal method is discharge to port because in order to incinerate plastics, and in particular PVCs (Polyvinyl chloride), the incinerator must comply to MEPC.244(66) standards [25], however some types of plastics, such as PCBs (polychlorinated biphenyl), still cannot be incinerated; since separation and classification on board can be expensive and taxing, it is usually preferred to just compact, store and dispose at ports. Cruise ships generate a significant quantity of food wastes from galleys and restaurants: the estimates provided by the report are 0.001 to 0.003 $m^3$ of food waste per person per day. Often, soft organics like vegetables, meat, fruit are separated from hard organics like bones and disposed in different ways. MARPOL 73/78 annex V regulates the discharge at sea of food wastes: it is possible if the ship is at least 12 nautical miles away from the shore but it is also possible to discharge it closer (between 3 and 12 nautical miles) if the stream is treated beforehand. While the hard-organic fraction is generally released at ports, the soft part is shredded through on-board pulpers to minimize its volume and is subsequently flushed with water through the piping system to the galley waste tanks. From there, the ground soft-organic fraction can be discharged at sea together with gray waters. As an alternative, the waste stream can be dried and then incinerated, but this is not the most common practice. The remaining part of solid wastes, called domestic wastes, is particularly heterogeneous and is comprised of paper, cardboard, glass, metal cans, synthetic materials, fabrics, packaging, etc.... It represents the biggest fraction of solid wastes produced on board of cruise ships and the generation numbers estimated are 0.01 to 0.02 $m^3$ per person per cruise day [23]. While discharge at sea is not strictly prohibited, disposal at ports is the common practice, especially since some materials, like aluminum cans, hold some intrinsic value and can be recycled [22]. Nevertheless, the domestic waste collected from bins is sorted and then treated with compactors and glass crushers for volume reduction; in some cases, the paper and cardboard fraction is incinerated.

#### 2.7.4 Miscellaneous waste streams management

Cooking oils and operational wastes, which are generated during the correct functioning of the cruise ship (ropes, wood, ladders, fireworks, flares...), are other two types of waste streams to be managed on board. Both are generally collected and then discharged at ports or incinerated on board. Sometimes

cooking oils are mixed with sewage sludge, but this practice is unofficial and prohibited. Through incineration the volume of the waste is sharply reduced, and the remaining end-product must be treated. Incinerator ashes are the end-product of all the incineration processes on board, and are generally collected and stored in special bags, and eventually are discharged at ports for future landfilling.

The approaches and technologies described in this section allow to reach the standards provided by MARPOL 73/78 but nevertheless, there is a strong dependency on destination ports and the potentials of the waste streams are not fully exploited. Incineration is a diffuse practice employed on cruise ships that is not considered extremely environmentally friendly. In fact, incinerators contribute to the air emissions of cruise ships in the form of NOx, SOx, VOCs, particulate matter, potentially dioxins if the feedstock is not suitable and the combustion conditions are not adequate, therefore their operation on coastal areas is often restricted. Cruise ships incinerators are also generally bulky in dimensions and can occupy multiple decks in height, depending on the maximum quantity of waste that can be treated. As it was discussed, a lot of waste streams just cannot be fed to an incinerator and are either retained in storage, occupying useful space and needing in many cases forms of control and safety measures, or are discharged at sea, which is an approach that can have important consequences on the environment. From those crucial issues, it is thus clear that it could be beneficial to develop innovative, more flexible and environmentally friendly alternative systems for the volume minimization of wastes.

## 2.8 Chapter summary

In this chapter the main environmental issues linked to the operations of cruise ships were described, and particular focus was given to the impacts linked to the management of waste streams on board. The various waste streams were characterized, and data regarding their generation on cruise ships was also provided, as this kind of information is needed for the gasification unit modeling. Besides their characterization, the typical on board management techniques were also described and a regulatory framework, MARPOL 73/78, was referenced. From these considerations, it could be understood that incineration is one of the standard waste volume minimiza-

tion practices. In the next chapter, the different waste-to-energy approaches will be analyzed in further detail.

# 3 Waste-To-Energy solutions to the waste issue

As it is shown in the previous section, wastes come in different forms and compositions: solids, liquids, gaseous, and their chemical composition can differ greatly from material to material. Of particular interest are waste streams rich in carbon-based organic compounds, since they can be employed in a very large number of different processes and since they generally represent a big fraction of the wastes produced in municipalities and cruise ships. These are food wastes, paper, some types of fabric, sewage, human and animal wastes, leafage, wood, etc. Plastic wastes, while generally not considered strictly "organic" and often not biodegradable, are constituted by synthetic or semi-synthetic organic polymers, formed by long chains of carbon atoms with the addition of other elements such as hydrogen, sulfur, oxygen, nitrogen, chloride. For this reason, they will be included in the discussion. The interest in this category of wastes comes from the possibility of employing processes which allow to extract the chemical energy stored in the chemical bonds of their constituent atoms. In this approach, which is defined as Waste-To-Energy (WTE), the chemical energy is converted and recovered in thermal energy or electricity. The difference with respect to the standard landfilling, in which the bio-degradable organic waste undergoes slow aerobic decomposition producing methane ($CH_4$), is that unless the "landfill gas" is fully collected and exploited, potential recoverable energy is generally lost into the environment. There exist different waste-to-energy processes, based on the physical conditions and chemical reactions to which the waste stream considered is subjected: incineration was already mentioned, but there are also pyrolysis, torrefaction, gasification as thermal processes and biological processes such as anaerobic digestion, aerobic digestion, fermentation. It is important to note the difference between landfilling anaerobic digestion and WTE anaerobic digestion, in which the useful product of the process is recovered and put to use in specially designed systems. Another important point that must be clarified when discussing waste-to-energy systems is the generation of greenhouse gases (GHG) and, in particular, $CO_2$ emissions. It is true that most of thermal processes applied to organic waste streams generally yield as end-product carbon monoxide due to the oxidation of the carbon atoms, and this is definitely true for incineration but also for pyrol-

ysis, torrefaction and gasification, in which intermediate end-products are carbon and hydrogen based fuels that can be further oxidized to produce $CO_2$. However, the nature of the waste must also be taken into account. In fact, the issue with GHG emissions related to fossil fuels is linked to the exploitation of naturally confined sources of hydrocarbons which will generate a positive net contribution of GHGs to the atmosphere. In the case of natural biomasses derived for example from trees and plants, as long as the source of the waste is reinstated into the environment, the net contribution of GHGs to the atmosphere can be zero: it can be considered a renewable carbon source. For municipal solid waste (MSW) this is not entirely the case, since a significant portion of its composition is composed of fossil fuel derivatives, in particular plastics, which will produce a net positive contribution. For this reason and in these cases, the three Rs (reduction, reuse and recycling) approaches should be definitely prioritized with respect to conversion in waste-to-energy plants, but in those cases where the three Rs cannot be applied (dirty plastics) waste-to-energy approaches are generally prioritized and preferred compared to landfilling, since methane is characterized by an higher Global Warming Potential (GWP) with respect to carbon dioxide [26]. More in details, "waste hierarchies" were developed by regulatory organs such as the European commission, which emitted in 2008 the 2008/98/EC directive to lay down the basic principles of waste management [27]. Indeed, in the mentioned directive features the European Waste Hierarchy, schematized in Figure 1. According to the 5-steps European Waste Hierarchy, reduction, reuse and recycling practices should be prioritized with respect to waste-to-energy approaches. This is important and should be valid also on cruise ships, as dedicated screening of the waste should be performed to reduce to the minimum the needs to resort to energy recovery approaches. However cruise ships are also peculiar cases and the minimization of the waste volume is often a necessity. Having said that, in this study plastics will be considered as potential feedstock for the energy conversion processes anyway, and the focus will be given to a specific thermal process which is gasification, and more specifically plasma gasification.

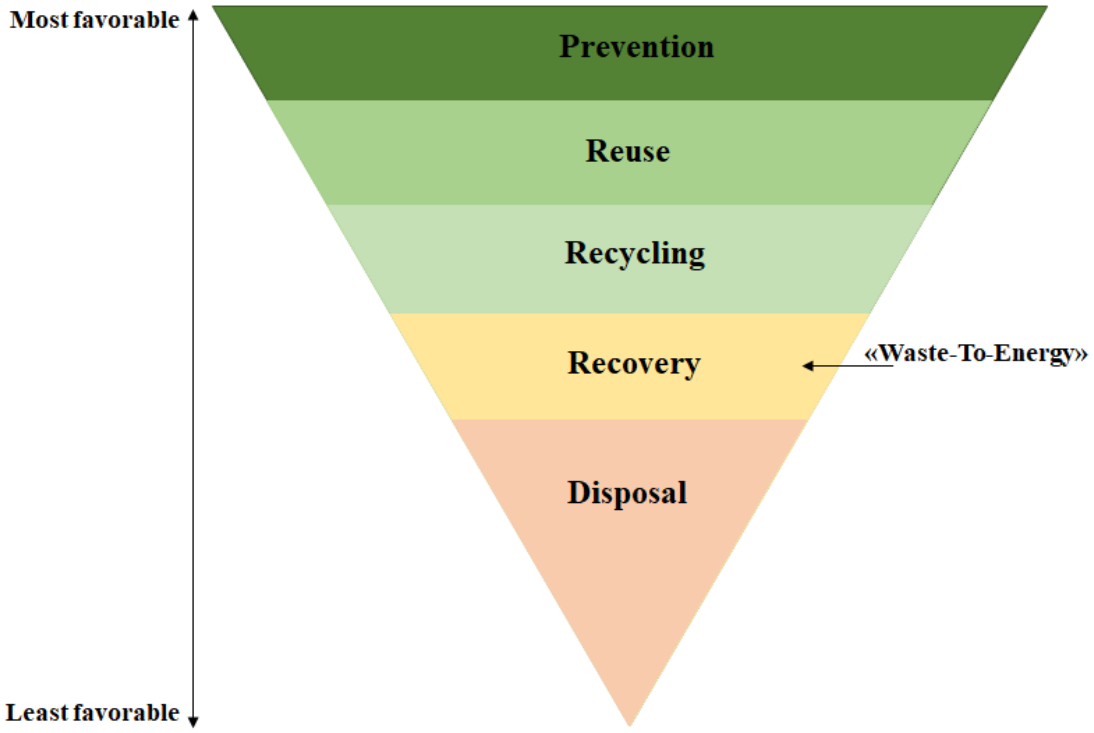


**Figure 1:** European 5-steps waste hierarchy. Waste-to-energy approaches should be preferred to landfilling.[27]

## 3.1 Incineration principles

Incineration is the process for the treatment of waste streams which involves combustion, generally in excess of oxygen, of the organic fraction. The inputs to the incinerators are the pre-treated wastes, which are mixed with the right quantity of air in the furnace where combustion reactions take place, and the main outputs are hot flue gases and ashes/metals, linked to the inorganic portion of the waste processed. Typical emissions of incinerators are particulate matter, $SOx$, $NOx$, $CO$, $HCl$, heavy metals and most importantly dioxins, which can form in the coldest spots of the furnace. While the main scope of the incinerator is to reduce the volume of the waste, the heat generated from the rapid exothermic combustion process can be recovered and used to produce steam for steam turbines or the heat that can be redirected for industrial processes or district heating. This is valid for incinerators serving municipalities but also for the smaller-size incinerators serving cruise ships.

## 3.2 Pyrolysis and gasification principles

Pyrolysis is a thermal decomposition process taking place in an oxygen-deficient environment and for temperatures ranging from 300 to 800 °C, depending on the composition of the feedstock [28]. During pyrolysis large hydrocarbon molecules break down in smaller compounds that can be in gaseous, solid and liquid phase: some of these are water, carbon monoxide, hydrogen, carbon dioxide, methane, benzene, tars and the remaining solid part which is denoted as char. A difference compared to incineration is the nature of the process, which is endothermic, as energy must be provided to break the chemical bounds of the large molecules. The yields of this process is strongly affected by parameters such as residence time, heating rate and temperature. Different applications may vary the parameters as function of the needed outcome: fast pyrolysis, which is characterized by low residence times and high heating rates is most suited for the production of bio-oils as most of the yield is in liquid form, while slow pyrolysis is generally used as pre-processing step for other thermal processes such as gasification. Gasification takes place in reactors named gasifiers, in which the feedstock is subjected to high temperatures and in an oxidant-starved environment. With respect to pyrolysis, in which no oxygen is provided, small quantities of oxidant are injected. Several reactions, including combustion, take place inside the chamber, but the combustion reactions are controlled to supply just the right amount of heat to allow the other endothermic gasification reactions to take place. If the heat for the endothermic reactions is provided by controlled combustion in the chamber we talk about autothermal gasification, if that is not the case we talk about allothermal gasification. Indeed, plasma gasification will fall in the latter definition. The main reactions of interest are summarized in Table 1, which is taken from reference [29]. The main gasification reaction is the water-gas reaction, which is strongly endothermic, and the heat needed is provided by the partial and full oxidation reactions, together with the methanation and hydrogasification reactions. The water-gas shift reaction is also important as it plays a role in the generation of hydrogen. As already mentioned, during the gasification process partial oxidation of the feedstock takes place, and the main gas product is the so-called synthetic gas or "syngas", which is a mixture of mainly hydrogen ($H_2$), carbon monoxide ($CO$), carbon dioxide ($CO_2$) and nitrogen ($N_2$), with traces of methane

($CH_4$), water ($H_2O$) and other contaminating species such as hydrochloric acid ($HCl$), hydrogen sulfide ($H_2S$), ammonia ($NH_3$), tars. The composition of the gas is crucial for the bottom applications, and depends strongly on the reaction conditions such as temperature, residence time, the chemistry of the gasifying gas, heating rates and on the feedstock composition. The interest in syngas resides in the fact that when properly cleaned it can be employed for a wide variety of applications, from simple combustion and heat production to electricity generation, to chemical processes for the production of methanol, ethanol, ammonia, pure hydrogen and many more. It is clearly a very flexible fuel that can be produced by a vast variety of biomasses, which is already an advantage per se. Some of the further advantages with respect to incineration are the following: while syngas must be cleaned before use, the reduction of gaseous volume, related to the reduced use of air, allows the use of smaller cleaning units, compared the flue gas cleaning units, and this could be a benefit from the point of view of space and costs, while also reducing the quantity of water streams needed by the plant. Furthermore, the employment of an oxygen-starved environment can hinder the mechanisms of formation of the dioxins which are dependent on the concentrations of oxygen [30], important consequence which may reduce the environmental impact of the system. If syngas is used as fuel the bottom combustion process is cleaner, since syngas is generally washed and treated as it leaves the gasifier. On the other hand, the main disadvantage of conventional gasification is the generation of tars, a crucial aspect that will be discussed in the future when describing the design of the syngas cleaning unit. In the next section, the differences between conventional gasification and plasma gasification will be discussed.

### 3.3 Plasma gasification principles

Plasma arc gasification is an allothermal gasification process in which the heat needed by the endothermic reactions, summarized in Table 1, is provided by an external heating source, which is commonly denoted as plasma torch or plasma generator. Plasma is a state of the matter in which the species constitutive of the medium are generally ionized or partially ionized. Electrons and ions are not bound together and long-range electro-magnetic interactions dominate over short-range interactions, that is particles are more influenced by the "average" background field than by their closer neighbors. For these

**Table 1:** Main gasification reactions and their reaction enthalpy at standard condition (T=298 K and P=1 atm) [29].

| No. | Reaction name | Chemical reaction | ΔH (kJ/mol) |
|---|---|---|---|
| (1) | Carbon Oxidation | $C + O_2 \rightarrow CO_2$ | -393.65 |
| (2) | Carbon Partial Oxidation | $C + 1/2O_2 \rightarrow CO$ | -119.56 |
| (3) | Water-Gas Reaction | $C + H_2O \leftrightarrow CO + H_2$ | +131.20 |
| (4) | Boudouard Reaction | $C + CO_2 \leftrightarrow 2CO$ | +175.52 |
| (5) | Hydrogasification | $C + 2H_2 \leftrightarrow CH_4$ | -74.87 |
| (6) | Carbon Monoxide Oxidation | $CO + 1/2O_2 \rightarrow CO_2$ | -283.01 |
| (7) | Hydrogen Oxidation | $H_2 + 1/2O_2 \rightarrow H_2O$ | -241.09 |
| (8) | Water-Gas shift reaction | $CO + H_2O \leftrightarrow CO_2 + H_2$ | -41.18 |
| (9) | Methanation | $CO + 3H_2 \rightarrow CH_4 + H_2O$ | -206.23 |

reasons, plasmas are generally extremely good electric conductors. There exist various types of plasmas as function of their properties and conditions, and while plasma generators produce fairly high temperature plasmas (4000 to 20000 K) they are nothing compared to "hot plasmas" produced during fusion experiments (around $10^8$ K). These "low temperature" plasmas are further classified in thermal, warm or cold plasma, according to the classification made by B. Ruj and S. Ghosh, in particular thermal plasmas are characterized by thermal equilibrium, while cold and warm are non-equilibrium plasmas [31]. With thermal equilibrium it is identified that condition in which all the species constituting the plasma remain at the same temperature, that is when the energy transfer from electrons to the gas is generally very fast and thus electron temperature and gas temperature are equalized. For that to happen temperatures must be high enough, higher than 10000 K. For their high temperatures, thermal plasmas have been used in the process industry since the 19th century and still nowadays many applications make use of plasma torches, such as plasma coating for metallurgy. The application of plasma torches to the treatment of municipal solid wastes is a relatively new concept, although some operating facilities do already exist in China, Japan, India and Taiwan. The advantage of using an external heating source is that by this configuration the concentration of oxygen and the heat needed can be decoupled, since the oxidation reactions are not the primary heat sources in this case. This is advantageous, and may allow for more flexibility of

operations and increases the ease of control of the gasification process. Flexibility is also reflected in the possibility of employing different plasma gases as oxidant, such as simple air, carbon dioxide, steam, pure oxygen or mixture of those, although this is true in general for conventional gasification too. Other advantages are linked to the higher temperatures that can be reached in the gasifier chamber, as higher temperatures enhance the decomposition of the chemicals constituting the waste and increase the presence of reactive species, speeding up normally slower reactions. The presence of ionized species is also a beneficial factor from this point of view. Some studies, such as the one produced by M. Hilna et al (2014), show that thermal plasma gasification could be advantageous from the point of view of tars production, as the enhanced decomposition of the carbonaceous feedstock my hinder their generation, an aspect that has to be evaluated experimentally but that could be extraordinary crucial for the developing of this technology [32]. Another aspect is that the inorganic portion of the waste stream, due to the higher temperatures, is melted forming molten ashes the can be removed from the chamber, quenched and finally produce a non-leachable vitrified slag. This slag is potentially an useful product, as the consensus in literature is that the toxicity of the material could comply with environmental standards, as shown in the book by Gary C. Young, "Municipal solid waste to energy conversion processes". it could even be employed as construction material for roads, instead of being landfilled, which is the typical fate of incineration bottom ashes [33]. Of course, the disadvantages should also be discussed, and these are in particular linked to the plasma torches as components, since they generally tend to increase the costs of the plant and to impose necessary and frequent maintenance operations, depending on the type of torch technology adopted. Furthermore, for the correct operation of the equipment, high electricity requirements are to be satisfied.

### 3.4 Plasma generators

As already mentioned, there are several plasma generators technologies being studied, developed and designed, each with their operating conditions, advantages and disadvantages. The general principle of functioning of a plasma generator is the following: a sufficient quantity of electric energy is provided to the flowing plasma gas, which is excited and its constituent atoms ionized.

The freed electrons produce subsequent ionization by collisions, and the process may be self-sustaining if the source of energy is constant and carefully controlled [31]. The way the energy is provided and the technical approach may vary, but two are the main methods considered in this discussion: plasmas generated by direct current (DC) and plasmas generated by Inductively Coupled Radio Frequency torches (RF). Other alternatives comprehend Alternate Current discharges (AC) and Microwave plasmas (MW). DC plasma generators work by applying a difference of potential between two electrodes, creating therefore huge currents in the gas and starting an electrical breakdown. The ionized gas flows out from an opening and is generally stabilized by varying the flow rate or by applying magnetic fields. DC torches are often classified in transferred or non-transferred torches, depending on the configuration of the cathode and anode. In a non-transferred torch, the cathode and the anode are both included in the component, usually the anode being the external electrode and the cathode the inner one. On the other hand, transferred torches are characterized by a separation of the two electrodes, having the cathode still inside the generator while the anode is placed outside as plate. Inductively Coupled Plasma torches work in a different way; in particular, for a cylindrical generator, an external coil act as electrode and an alternative current in the radio-frequency domain is driven in it. This current generates a time-varying vertical magnetic flux through the torch where the plasma gases are flowing, inducing, according to the Faraday-Lentz law, an electromotive force and an induced current, which will produce the discharge, once a spark is provided. The eddy current produced will heat the gas, in turn generating high temperatures. Both methods have their pro and cons: the main issue with DC transferred torches is the observed erosion phenomena at the electrodes, which calls for frequent maintenance and component substitution, impacting negatively on expenditures and availability of the system. Also, according to the literature, power deposition in plasma is not very efficient and a lot of heat produced must be removed by electrode cooling; on the other hand, ignition by this approach is relatively simple and the temperatures that can be reached are quite high (12000-20000K) [31]. RF torches do not incur in electrode erosion, as the excitation coil is placed outside the tube containing the flowing gas, reducing the impact on maintenance and expenses; power is deposited more efficiently in the gas region, however ignition is more complex and temperatures reached are lower (3000-8000K)

[31]. In this study and in the design of the small-scale plasma gasification system, RF plasma torches will be considered. The reason being that the laboratory where this research has been conducted is mainly focused on researching the RF technology, but the system could be extended for MW or DC plasma generators too.

## 3.5 Chapter summary

In this chapter the Waste-To-Energy approach to waste management was defined, as different existing techniques were described. The basic principles of incineration, pyrolisis, conventional gasification and plasma gasification were outlined, and the corresponding advantages and disadvantages were discussed. Particular attention was given to the plasma gasification process, it being the technology of interest of this work. A brief description of the existing plasma generator technologies was also given, as next chapter will deal with the modeling of the RF plasma torches that will operate in the gasification system.

# 4 Plasma generators modeling

Plasma generators are the key components of the system, as their function is to both provide the adequate amount of oxygen for the gasification process and the heat to enhance the gasification reactions. While in the next section the overall waste treatment model will be analyzed, in this chapter the attention will be focused on the plasma torches modeling. This is important, as the results from the simulations on these components will be part of the input to the waste treatment model, which are in particular the temperature of the plasma gas, the mass flow rate and the electrical consumption of the torch. As already mentioned, in this study radio-frequency (RF) inductively coupled torches will be investigated. According to these considerations, the chapter was structured in the following way: first of all, the COMSOL model developed was described, including discussions on the geometry definition, the materials, the mathematical formulations employed, the boundary and initial conditions, the meshing. Then, the inputs and the assumptions to the simulation were described, and the results were presented.

## 4.1 Model description

As already mentioned, the software COMSOL was used for the modeling phase. COMSOL is a simulation software that allows to model a wide range of physical processes and even to couple different phenomena together. This is important, as RF plasma generators inherently require a multi-physics approach. In particular, there is a coupling between the electro-magnetic phenomena, which are linked to the electrical excitation of the coils and the subsequent induced currents and time-varying magnetic fields in the plasma region, the heat transfer phenomena, taking place in both the fluid region and in the solid components, and fluid dynamics, since the gas is of course not still, but flowing from the inlet to the outlet of the torch, producing velocity and pressure fields inside the component. Other physical phenomena, like thermo-mechanics or erosion, were not modeled. COMSOL can be customized with different specific modules to expand the capability of the software to model disparate physical phenomena. Regarding this work, the modules of interest are the "Electromagnetics" Modules and the "Fluid Flow & Heat Transfer"

Modules. Furthermore, modules provide several physical interfaces to better suit modeling necessities. In particular, three were considered in this study: "magnetic fields (mf)", "heat transfer in fluids (ht)" and "laminar flow (spf)". These interfaces will be described, from a mathematical and physical point of view, in the next sections, together with their multi-physics couplings. The software built-in functionalities were employed for the geometry definition, and the material properties were also extracted from COMSOL's database. These modeling efforts were partially inspired by the research work of S. Xue et al. (2001), which developed a 2D model for an inductively coupled plasma using the code FLUENT [34].

#### 4.1.1 Geometry and materials

The model developed is characterized by a 2D axial-symmetric geometry. The plasma torch is constituted by concentric cylindrical tubes with the function of separating different fluid streams and constituting a barrier to the external environment. The cylinders are defined by the revolution of rectangles around the symmetry axis. The excitation coils, characterized by a full circular cross section, are normally helicoidal and twisting around the outermost cylindrical tube, forming a 3D object. Since a 2D axial-symmetric geometry was assumed, the coils were defined instead as parallel rings wrapping around the outer tube. This is an assumption that implies neglecting the axial component of the excitation current flowing in the coils. Based on these considerations, on the 2D axial-symmetric geometry the coils are represented by parallel circles. The external domain is defined similarly to the gas region as a rectangular area revolving around the axis. The inner region of the outer tube is where the plasma gas is flowing, and it must be noted that this configuration with three concentric tubes is normally employed for RF plasma torches as this way it is possible to separate the main gas feed in three streams: a carrier gas stream, a central gas stream and a sheath gas stream, which will be better defined in the laminar flow interface description. The parameters for the geometry are summarized in Table 2, while Figure 2 displays the 2D simulation domain defined according to these parameters. Regarding the materials, quartz ($SiO_2$) is normally used for the cylindrical concentric tubes, as it is a dielectric material that prevents arc discharges, it is capable of withstanding temperatures up to its melting temperature $\sim$ 1700 °C, moreover it is transparent and inert to most chemical

compounds. Quartz glass has a low thermal expansion coefficient, making it less susceptible to thermal shocks, however it is also fragile and therefore vulnerable to mechanical stresses. The coils were modeled with copper, given its good electrical conductivity, ductility and ease of manufacturing, as well as good thermal conductivity. The excitation coils are a critical part of the component, therefore their integrity must be guaranteed. The coils will be subjected to high temperatures due to Joule heating, which can affect its properties by degrading the material integrity, therefore in future modeling studies efforts should be devoted to investigate means of coil cooling. The external domain and the inner region of the torch are constituted by air. Air was indeed chosen as plasma gas with the double function of providing heat and oxidant for the gasification reactions, and it was chosen especially for its availability in the environment. As already mentioned, all the properties needed by the model were obtained from the software database, except for the total volumetric emission coefficient for air, extrapolated from reference [35].

**Table 2:** Geometrical parameters employed in the model.

| **Geometrical Parameter** | **Description** | **Dimensions (mm)** |
|---|---|---|
| $L_1$ | Central and carrier tube height | 50.00 |
| $L_2$ | Sheath tube height | 220.00 |
| $L_3$ | Lower coil height | 56.70 |
| $D_1$ | Carrier tube radius | 5.92 |
| $D_2$ | Central tube semi-width | 22.16 |
| $D_3$ | Sheath tube semi-width | 7.47 |
| $D_4$ | External domain semi-width | 85.25 |
| $D_5$ | Sheath tube radius | 39.75 |
| $T_1$ | Sheath tube thickness | 3.50 |
| $T_2$ | Central tube thickness | 2.20 |
| $T_3$ | Carrier tube thickness | 2.00 |
| $D_c$ | Coil diameter | 6.00 |
| $P_T$ | Transversal pitch | 6.75 |
| $P_L$ | Longitudinal pitch | 4.75 |

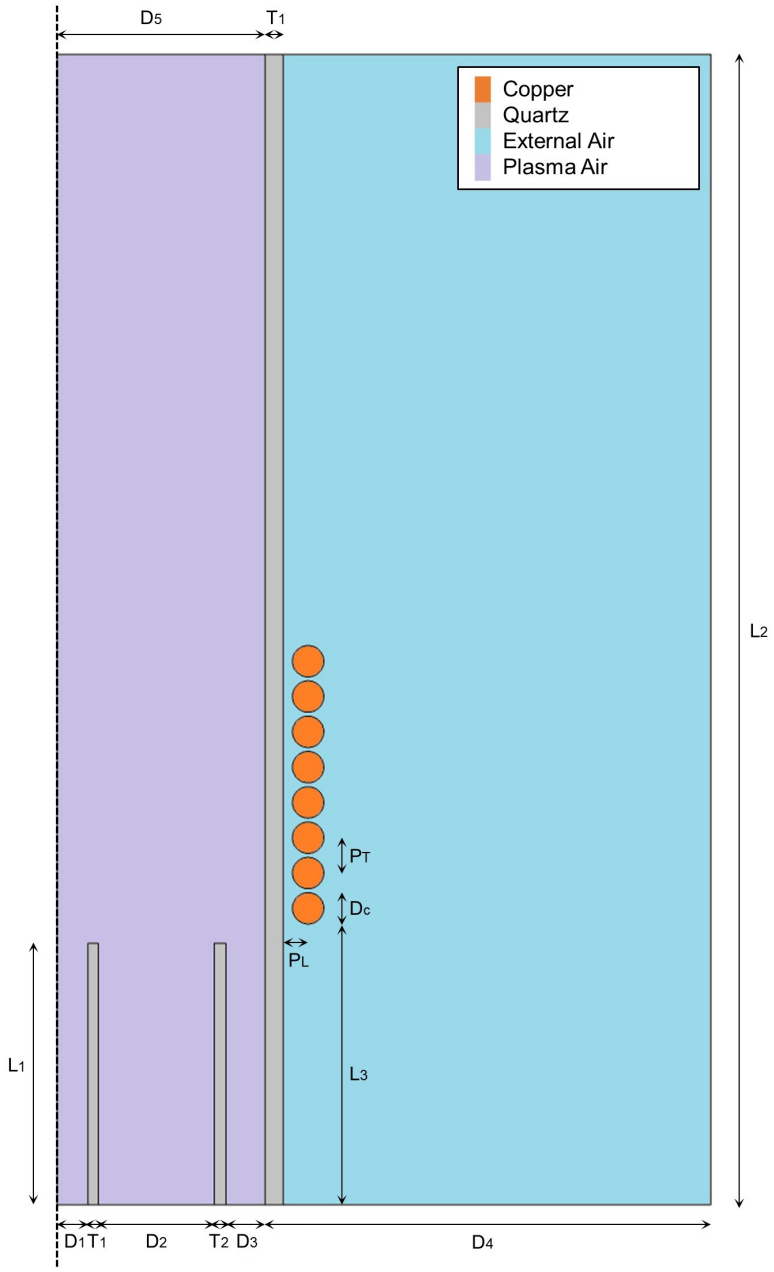


**Figure 2:** Axial symmetrical geometry employed in the model.

### 4.1.2 Physics description

In this section the physic interfaces employed are described, to present the mathematical formulations used in the model. As already mentioned, electromagnetism, heat transfer and fluid dynamics phenomena are modeled, which are also coupled between themselves. The general assumptions of the model are summarized:

- 2D axial-symmetric geometry;
- Parallel coils, therefore neglecting the axial component of the coil excitation current;
- Electromagnetism and heat transfer side, frequency-transient studies are performed; Stationary studies are performed fluid flow side;

The excitation current flowing in the coils is characterized by a frequency, which is necessary to produce the time-varying magnetic field responsible of the induced current in the plasma gas. Therefore, it is expected for the magnetic and heat transfer phenomena to be investigated in a frequency domain. The frequency is a fixed parameter which is equal to 13.6 MHz in this study, in accordance with ISM radio bands. The following physical models are extrapolated from the COMSOL guides, as these are the equations that are computationally solved by the software [36, 37, 38].

**Magnetic fields**

The magnetic fields interface (mf) is based on Maxwell's equations and more specifically on Ampère's Law, which is described in a general case as:

$$\nabla \times \mathbf{H} = \mathbf{J}$$

Where $\mathbf{H}$ represents the magnetizing field in $[A/m]$ and $\mathbf{J}$ the total current density in $[A/m^2]$. More in details, the total current density is also generally defined as:

$$\mathbf{J} = \sigma\mathbf{E} + \frac{\partial \mathbf{D}}{\partial t} + \sigma\mathbf{u} \times \mathbf{B} + \mathbf{J_e}$$

Where the first term represents the free current density, which is linked to the movement of free charges, the second one is the displacement current linked to the variations in time of the electric field, the third one is the Lorentz term, depending on the velocity of the conductor, and the forth one is a generic externally generated current density. $\sigma$ indicates the electrical conductivity of the medium $[S/m]$, the vector $\mathbf{u}$ the conductor velocity $[m/s]$. The quantities $\mathbf{D}$ and $\mathbf{B}$, which are respectively the electric displacement field

$[C/m^2]$ and the magnetic field $[T]$, are defined as follows as function of the electric field $\mathbf{E}$ $[V/m]$ and magnetizing field $\mathbf{H}$:

$$\mathbf{D} = \varepsilon_0 \varepsilon_\mathrm{r} \mathbf{E}$$

$$\mathbf{B} = \mu_0 \mu_\mathrm{r} \mathbf{H}$$

The last relation is true for diamagnets and paramagnets in which $\mathbf{H}$ and $\mathbf{M}$, where $\mathbf{M}$ is the Magnetization $[A/m]$, are linked by a linear relation of the type $\mathbf{M} = \varkappa \mathbf{H}$. $\mu_0$ is the vacuum permeability $[4\pi \times 10^{-7} N/A^2]$, $\mu_\mathrm{r}$ is the relative permeability [-], $\varkappa$ is the magnetic susceptibility ($\varkappa = \mu_\mathrm{r} - 1$) [-], $\varepsilon_0$ is the vacuum permittivity $[8.854 \times 10^{-12} F/m]$ and $\varepsilon_\mathrm{r}$ is the relative permittivity [-]. However, the dependent variable of the system is neither $\mathbf{H}$ or $\mathbf{B}$, but $\mathbf{A}$, which represents the Magnetic Vector Potential, defined by the following relations:

$$\nabla \times \mathbf{A} = \mathbf{B}$$

$$\mathbf{E} = -\nabla \phi - \frac{\partial \mathbf{A}}{\partial t}$$

Where $\nabla \phi$ is the Electro Scalar Potential $[V]$. Fourier transforms can be used to elaborate the terms containing partial derivatives in time, using the following relation:

$$F[\frac{dx(t)}{dt}] = i\omega X(iw)$$

By making use of all the previous considerations, the Ampère's Law can be written as:

$$(i\sigma\omega - \omega^2 \varepsilon_0 \varepsilon_\mathrm{r}) \mathbf{A} + \frac{\nabla \times \nabla \times \mathbf{A}}{\mu_0 \mu_\mathrm{r}} - \sigma \mathbf{u} \times (\nabla \times \mathbf{A}) = \mathbf{J_e}$$

which is solved for $\mathbf{A}$. The software will discretize the equation and solve it at every node of the domain mesh. Regarding the coil domain, power excitation is chosen as excitation method, which in the frequency domain

(cycle average) can be modeled using the following constraints to the coil current and coil voltage:

$$P_{\text{coil}} = \frac{1}{2} real(V_{\text{coil}} {I_{\text{coil}}}^*)$$

$$J_{\text{e}} = \frac{\sigma V}{L}$$

Where V is an unknown voltage obtained according to $I_{\text{coil}}$, L is the length of the coil. The problem is non-linear. As initial condition, the magnetic potential is simply assumed 0 everywhere. For what concerns the boundary conditions, beside the symmetry condition at the symmetry axis, magnetic insulation was assumed at all the external boundaries of the domain, which is equal to assume 0 the tangential component of the magnetic potential A:

$$\mathbf{n} \times \mathbf{A} = 0$$

As initial condition, the magnetic potential is simply assumed 0 everywhere.

**Heat transfer in fluids**

The heat transfer in fluids interface (ht) is based on a heat balance equation, which is in a general case defined as:

$$\rho C_{\text{p}}(\frac{\partial T}{\partial t} + \mathbf{u} \cdot \nabla T) + \nabla \cdot \mathbf{q} = Q + Q_{\text{p}} + Q_{\text{vd}}$$

Where, on the left-hand side, the first term is linked to the time variations of the temperature, the second term is linked to convection phenomena and the third term is related to heat transfer by conduction. On the right side, Q identifies generic heat sources, $Q_{\text{p}}$ the work by pressure changes and $Q_{\text{vd}}$ the viscous dissipation in the fluid, and all the terms are in $[W/m^3]$. T $[K]$, which of course represents the temperature, is the dependent variable, while $\rho$ and $C_{\text{p}}$ are thermal properties of the materials, respectively the density $[kg/m^3]$ and the specific heat capacity at constant pressure $[J/kg/K]$. Some terms can be further expanded:

$$\mathbf{q} = -k\nabla T$$

$$Q_{\mathrm{p}} = \alpha_{\mathrm{p}} T(\frac{\partial P}{\partial t} + \mathbf{u} \cdot \nabla P)$$

$$Q_{\mathrm{vd}} = \tau : \nabla \mathbf{u}$$

The first one is the Fourier's law for heat conduction, and k represents the thermal conductivity $[W/m/k]$. The second one, the work by pressure changes, is generally small for low mach numbers, which is the case for this model. The third one is the viscous dissipation in the fluid and $\tau$ represents the viscous stress tensor $[Pa]$. The Q term will be described in the multiphysics couplings section, as the heat sinks and sources related to electromagnetic phenomena will be discussed. For what concerns heat transfer in solids instead, the relation is similar to the one for the fluids, with some changes to the right-hand side:

$$\rho C_{\mathrm{p}}(\frac{\partial T}{\partial t} + \mathbf{u}_{\mathrm{trans}} \cdot \nabla T) + \nabla \cdot \mathbf{q} = Q - \alpha T : \frac{dS}{dt}$$

$\mathbf{u}_{\mathrm{trans}}$ in this case represents the velocity vector of translation motion $[m/s]$, while the last term on the right-hand side identifies the thermoelastic damping, where $\alpha$ is the coefficient of thermal expansion $[1/K]$ and S is the second Piola-Kirchhoff stress tensor $[Pa]$. Indeed, this equation will be used for solid domains, in particular the quartz tubes, while the previous one will be used to describe the fluid region occupied by the plasma gas. Regarding the boundary conditions, besides axial symmetry, the following constrains were imposed:

- $T = T_0$, Dirichlet boundary condition;
- $-\mathbf{n} \cdot \mathbf{q} = 0$, thermal insulation condition;
- $-\mathbf{n} \cdot \mathbf{q} = 0$, outflow condition.

The Dirichlet boundary condition was imposed at the gas inlet and quartz tube outer wall, with a $T_0$ equal to 300 K. The outflow condition was used for the gas outlet, while the thermal insulation condition modeled the remaining

boundaries. These last two conditions imply that the temperature gradient across the boundary is equal to zero. Concerning the initial condition, the temperature was assumed equal to $T_0$.

**Laminar flow**

The laminar flow interface (spf) was used to model the single-fluid dynamics of the plasma gas to obtain the steady state velocity and pressure fields. The interface, which is valid for reasonably low Reynolds number and no turbulence phenomena, solves the Navier-Stokes equation on the discretized fluid domain:

$$\frac{\partial \rho}{\partial t} + \nabla \cdot (\rho \mathbf{u}) = 0$$

$$\frac{\partial \rho \mathbf{u}}{\partial t} + \rho(\mathbf{u} \cdot \nabla)\mathbf{u} = \nabla \cdot [-P\mathbf{I} + \tau] + \mathbf{F}$$

In particular, the first one is the continuity equation, which describes the transport of the quantities and mass conservation, while the second one is the weakly compressible momentum conservation. The time dependent terms will be neglected since we are dealing with a stationary study, while the weakly compressible assumption was made to take into account the strong variations of density with temperature. This assumption is valid if the Mach number (Ma) is lower than 0.3, which will be the case for this study. The second term on the left side in the momentum conservation is the convective acceleration, which is time-independent. On the right side, the term containing the pressure P $[Pa]$ describes hydrostatic effects, the last term takes into account body forces such as gravity, while the second one contains $\tau$ which denotes the viscous stress tensor $[Pa]$. This last term can be expanded in the following way:

$$\tau = \mu(\nabla \mathbf{u} + (\nabla \mathbf{u})^{\mathrm{T}}) - \frac{2}{3}\mu(\nabla \cdot \mathbf{u})\mathbf{I}$$

Where the first term represents the strain-rate tensor and $\mu$ indicates the dynamic viscosity $[Pa \cdot s]$. Similarly to the magnetic fields and heat

transfer interfaces, boundary conditions need to be specified, beside the axial symmetry condition:

- $\mathbf{u} = 0$ at walls, no-slip condition;
- $P_{outlet} = P_0$, outlet specified pressure condition;
- $u_{inlet,1} = v_1$, $u_{inlet,2} = v_2$, $u_{inlet,3} = v_3$, inlet specified velocity conditions.

Indeed, as already anticipated, in typical RF torches the plasma gas mass flow is split into three different streams, which perform different functions. The innermost and smaller tube is normally used to inject nano-powders for metallurgical applications, therefore the stream is denoted as carrier gas stream. It is generally characterized by the smallest mass flow rate between the three, and for waste treatment applications it carries no specific function other than injecting a portion of air in the component. The second tube carries the central gas which is the main plasma forming stream, although the biggest mass flow rate is generally provided by the sheath gas, which is injected by the outermost tube with the function of cooling and protecting the quartz external tube from the high temperatures. This model adopts a simplified version of an RF torch since all the three streams are fed axially, but normally, to increase flame plume stability and cooling capabilities, central gas and sheath gas can be injected tangentially achieving beneficial effects [39]. Regarding the initial conditions, $\mathbf{u}$ was assumed equal to 0 everywhere, and the absolute pressure equal to $P_0$, which is assumed as 1 bar. The boundary conditions for the three interfaces described are summarized in Figure 3.

**Couplings**

As anticipated, the three physical models described are not decoupled, as some of the quantities described in the interfaces are actually dependent on the results of the other interfaces. In particular, it was already implied with the weakly compressible condition that the density is strongly affected by the temperature which is the solution of the heat transfer model. In addition, it was already shown that viscous dissipation acts as heat source which depends on the velocity field, solution of the laminar flow interface. The dependence of the density on the temperature is provided by COMSOL's properties database, not explicitly shown here.

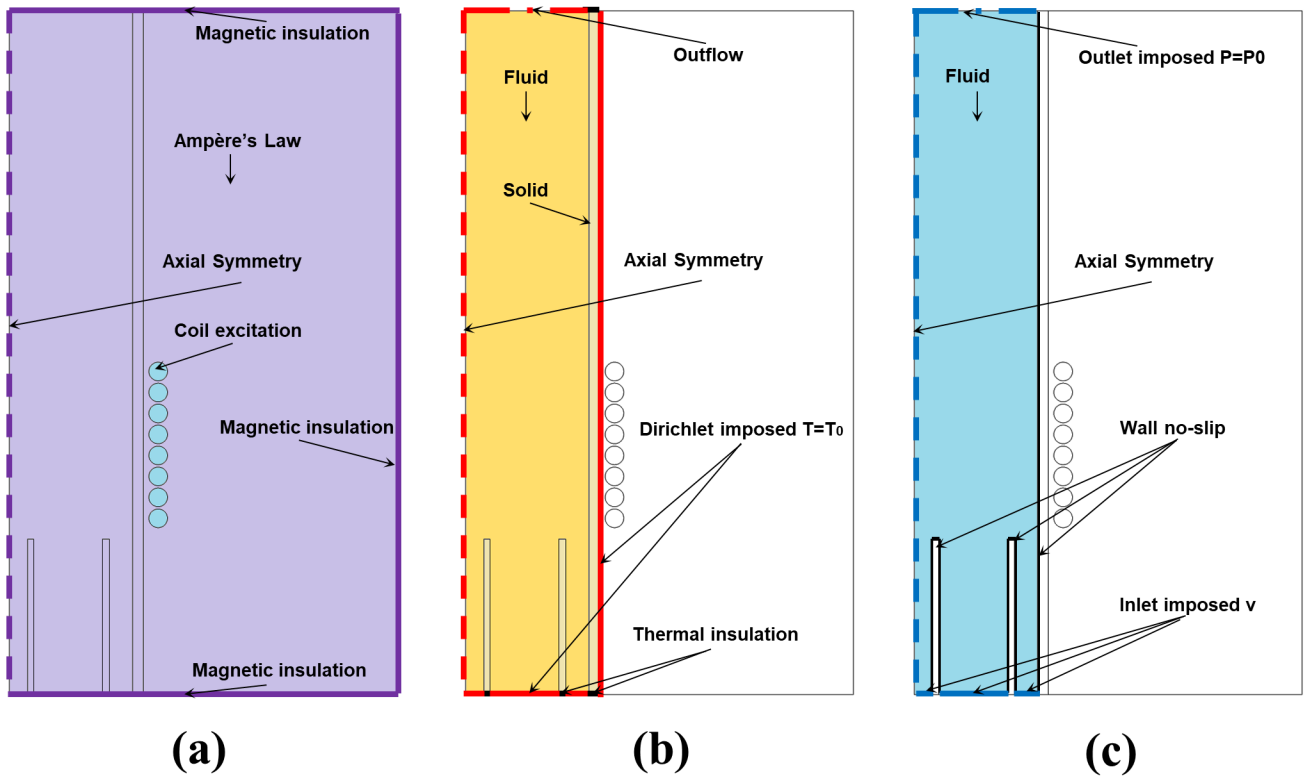


**Figure 3:** (a) Magnetic fields interface boundary conditions; (b) Heat transfer in fluids interface boundary conditions; (c) Laminar flow interface boundary conditions.

$$\rho = \rho(P_0, T)$$

$$Q_{\mathrm{vd}} = \tau : \nabla \mathbf{u}$$

Similarly, the magnetic field interface affects the heat generation in the plasma, as we can expand the generic Q term found in the heat transfer equation in three contributions:

$$Q = \mathbf{E} \cdot \mathbf{J} + Q_{\mathrm{rad}} + \frac{\partial}{\partial T}(\frac{5k_{\mathrm{b}}T}{2q})(\nabla T \cdot \mathbf{J})$$

The first term represents heat produced by resistive heating (Joule effect), related to the passage of a current through a conductor characterized by a certain resistance. The second one is linked to the volumetric net radiation loss $[W/m^3]$, evaluated using the plasma air volumetric emission coefficient.

The third one is the energy transported by the electric current. Finally, the last coupling relates the magnetic field and the laminar flow models through the Lorentz force, which is included in the **F** term of the momentum conservation as cycle-averaged:

$$\mathbf{F} = \frac{1}{2} Re(\mathbf{J} \times \mathbf{B}^*)$$

## 4.2 Simulation description and meshing

The physical model described is used to solve a frequency transient study for the electromagnetism and heat transfer part and a stationary study for the laminar flow. Since heat transfer and magnetic field phenomena are described with different time scales, a frequency-transient study was used, given that the electromagnetic loads are sinusoidally varying with a fixed frequency and solving the interface with a time dependent study would be too computationally intensive. The temperature fields are calculated as time dependent, while electromagnetic fields are solved in the frequency domain considering cycle-averaged loads. The excitation power to the coil is fixed and it is one of the inputs to the simulation. Current and voltage in the coil vary until steady state is reached and the coil current stabilizes to its nominal value. Other fundamental inputs are the mass flow rates in the three channels, used to evaluate the inlet velocities imposed as boundary conditions in the laminar flow interface, as shown by the following relations:

$$A_{\text{flow}} = \pi({r_{\text{o}}}^2 - {r_{\text{i}}}^2)$$

$$v = \frac{\dot{m}}{\rho_0 A_{\text{flow}}}$$

Once the geometry has been defined, the first expression can be used to evaluate the cross sectional area of the channel (annular in this case, circular for the innermost one), which is in turn used to evaluate the velocity. $\dot{m}$ represents the mass flow rate to the channel $[kg/s]$, while $\rho_0$ is the density at $T_0$ and $P_0$. The basic meshing layout was generated according to the physics by the software, and it was then slightly adjusted manually. In particular,

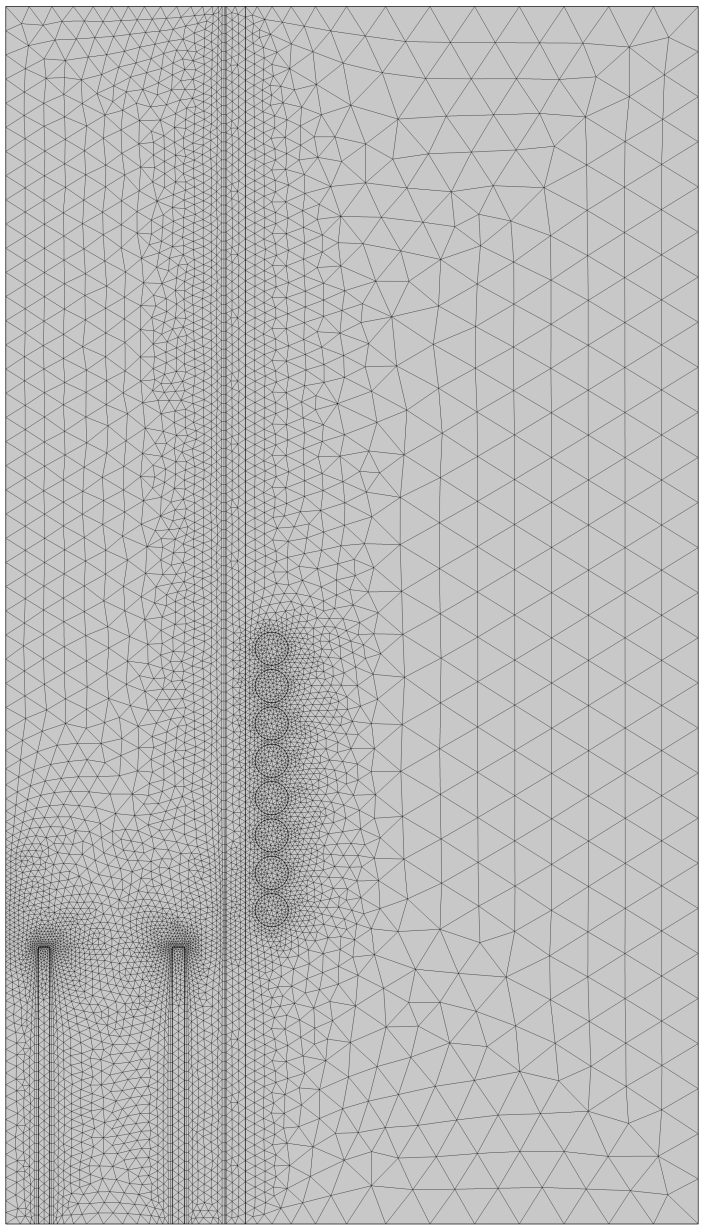

**Figure 4:** Meshing of the computational domain, thicker areas can be noticed close to the walls and the coils.

the nodes are more thickly clustered around the copper coils, where we have the biggest variations of magnetic flux, and at the edges of the quartz tubes, in particular at the end tips of the two inner quartz walls, where the velocity fields are more likely to be perturbed. This was done using the corner refinement function, which decreases the elements size at sharp corners. Along the internal walls a thin boundary layer mesh with a dense distribution in the

normal direction was defined to better resolve the no-slip boundaries. On the other hand, the mesh is sparser on the external air domain, where no strong variations of the quantities are expected. The mesh is mostly composed of triangular elements varying in size. The maximum element size is 10.6 mm, while the minimum is 0.05 mm. The meshing performed can be seen in Figure 4, while the main inputs to the simulation are synthesized in Table 3.

**Table 3:** Input parameters employed in the model.

| **Input Parameter** | **Description** | **Unit** | **Quantity** |
|---|---|---|---|
| $P_{el}$ | Excitation power | kWel | 75.00 |
| $v_1$ | Carrier gas inlet velocity | m/s | 0.21 |
| $v_2$ | Central gas velocity | m/s | 0.09 |
| $v_3$ | Sheath gas velocity | m/s | 7.11 |
| $m_{air}$ | Total air mass flow rate | kg/h | 54.10 |
| $freq$ | Radiofrequency | MHz | 13.60 |
| $T_0$ | Reference temperature | K | 300.00 |
| $P_0$ | Reference pressure | bar | 1.00 |

## 4.3 Simulation results

The results of the simulation are shown in this section. The solutions are shown as 2D plots (apart from the last one), according to the axial symmetry. The temperature of the plasma gas is one of the quantities of most interest, as in the gasification model we will need to choose a temperature for the stream of air introduced in the gasifier. It will not be possible to introduce a temperature profile, since the gasification model will be 0D, so an average value based on the results of this model will be chosen. All the 2D plots display the steady state solutions, which are reached after 0.3s, starting from 0s. The time step chosen is 0.015s.

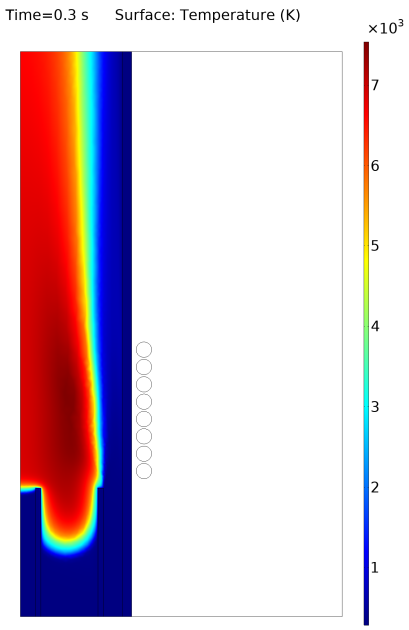


**Figure 5:** 2D temperature field in the domain.

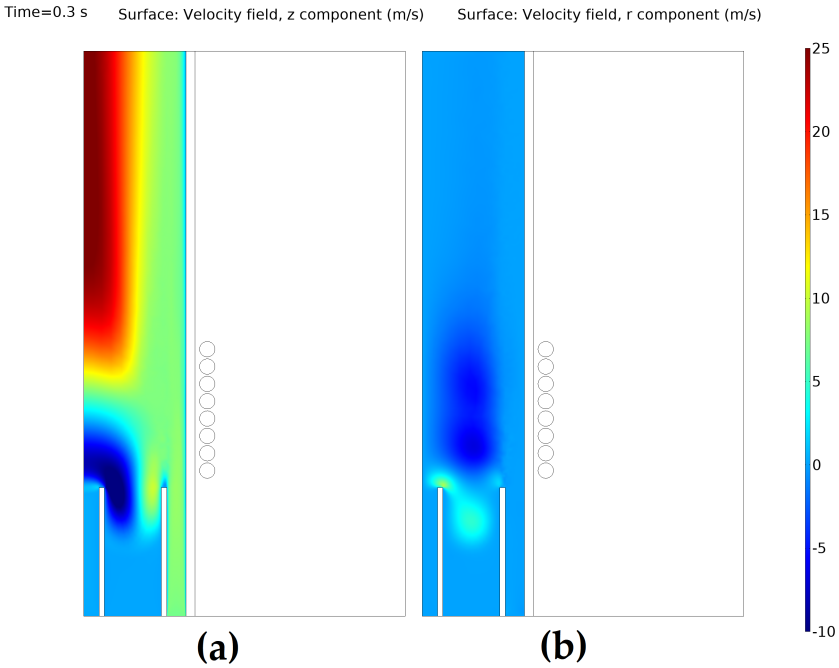


**Figure 6:** 2D velocity field (a) axial and (b) radial components

## 4.4 Discussion

Figure 5 shows the 2D steady state temperature field in the torch, after ignition. As expected, the temperatures are very high and the maximum

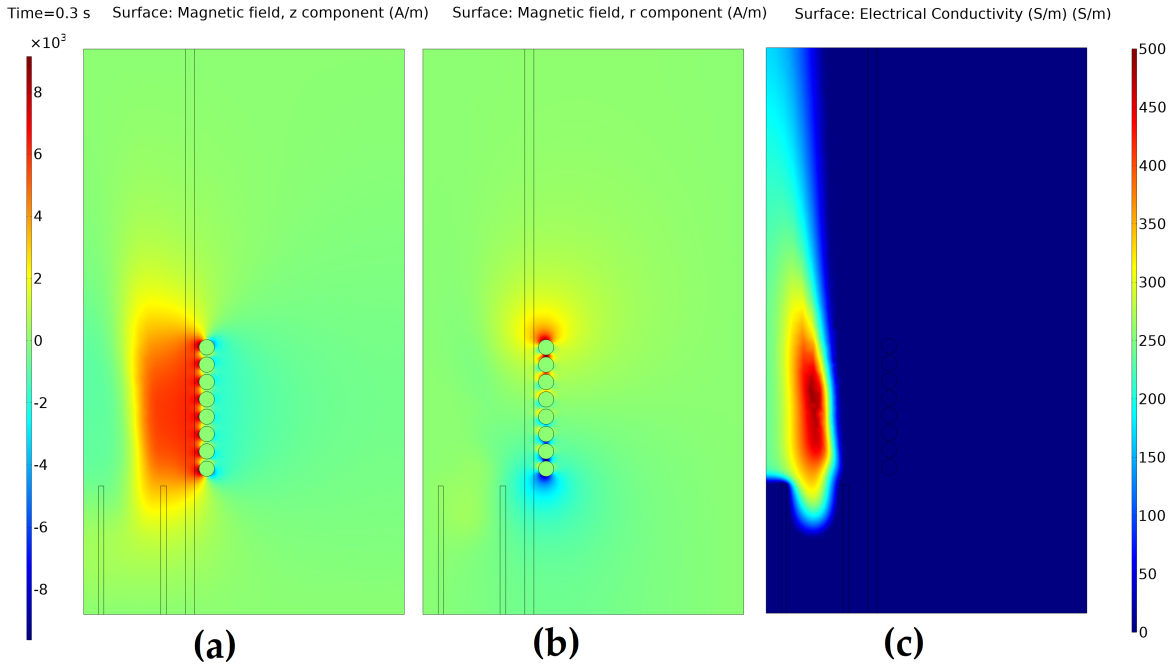


**Figure 7:** 2D magnetic field (a) axial and (b) radial components and (c) plasma electrical conductivity.

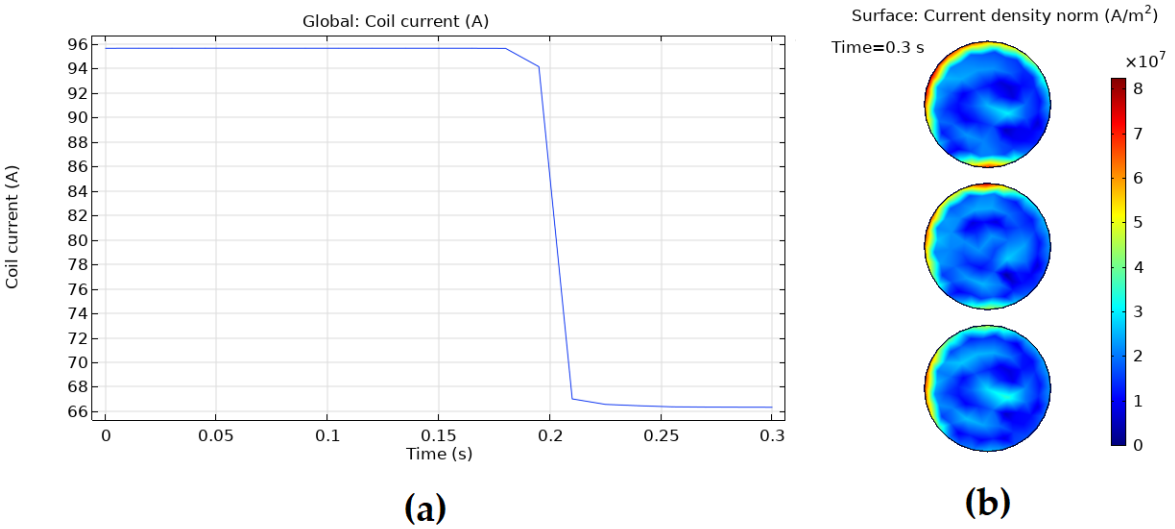


**Figure 8:** (a) Total current in the copper coils; (b) Skin effect on the upper copper coils.

temperature obtained is 7535 K, in the central region of the plasma plume, closer to the excitation coils. Very strong temperature gradients are observed closer to the outer quartz wall, consequence of the sheath mass flow: this is essential to protect the glass from the high temperatures. In the real world, the low temperatures on the external wall and in the coils should be main-

tained by a dedicated cooling system, as the copper coils will tend to heat very fast due to Joule heating. At the outlet the maximum temperature is still very high, 6634 K, while the minimum temperature is $T_0 = 300K$ at the inlet. These values of temperature are high enough for plasma gasification processes, considering also the possibility of adjusting the enthalpy provided to the feedstock by tweaking the mass flow rate provided by the five envisioned torches. Figures 6 (a) and (b) show two of the components of the velocity field at steady state, as the velocity field is crucial for the torch ignition. Indeed, the inlet velocity should be kept constant to maintain the plasma plume stable, which is a sensible matter and a potential issue if adequate control of the flow is not provided. In fact, strong changes to the velocity field could lead to the extinguishment of the plasma and potential damages to the coils. The model does not take into account turbulences, and the maximum axial velocity is reached on the symmetry axis, while negative axial velocities are observed at the outlet of the carrier and central tube, producing reintroduction of the flow inside the tubes. This effect is also visible in the temperature field, as the temperature inside the central tube is increased. This may be an undesirable effect that should to be investigated by an experimental apparatus, as it could potentially lead to a loss of integrity of the two inner tubes. Small negative radial velocities are observed in the same region, which are linked to the circular motion just described. Besides that, no other radial velocity gradients are noticeable in the remaining domain. The tangential component in this model is equal to zero everywhere, in real applications instead the sheath gas is injected tangentially for increased plasma stability, therefore tangential components are normally present and beneficial. In Figures 7 (a) and (b) the components of the magnetic field are displayed. The shape of the field is the classic one produced by a solenoid, in this case the excitation coils, with a positive axial component inside the coils and a negative axial component in the external domain. As expected, the radial component is positive on the top of the coil bundle and negative in the lower part. It can be observed how following plasma ignition the magnetic field produced by the coils is not completely able to penetrate the plasma jet, as after ignition the electric conductivity of the plasma is increased significantly, and the field lines are pushed away. This is also shown in Figure 7 (c), which displays the 2D electrical conductivity in the plasma at steady state. Regarding the excitation coils, Figure 8 (a) shows the time-dependent

behavior of the total current in the coils, which has a drop once the plasma is ignited at 0.185s and then stabilizes at steady state. A known consequence linked to the use of alternate currents is the skin effect, which is noticeable in Figure 8 (b), as the coils clearly show higher current densities at the edges of the three upper copper coils. As consequence, the conductor will have an higher electric resistance and a more significant electric dissipation. This is another reason why the copper coils will most likely need efficient cooling in the actual design of the torch to maintain their integrity and electrical properties. Finally, Figure 9 displays again the temperature in the volume domain, as an example of the whole 3D geometry generated by the rotation of the 2D axial-symmetric geometry around he symmetry axis. The same Figure is used to also show how the magnetic flux density [T] and electric field [V/m] streamlines propagate in the external domain. As expected the electric field is only azimuthal.

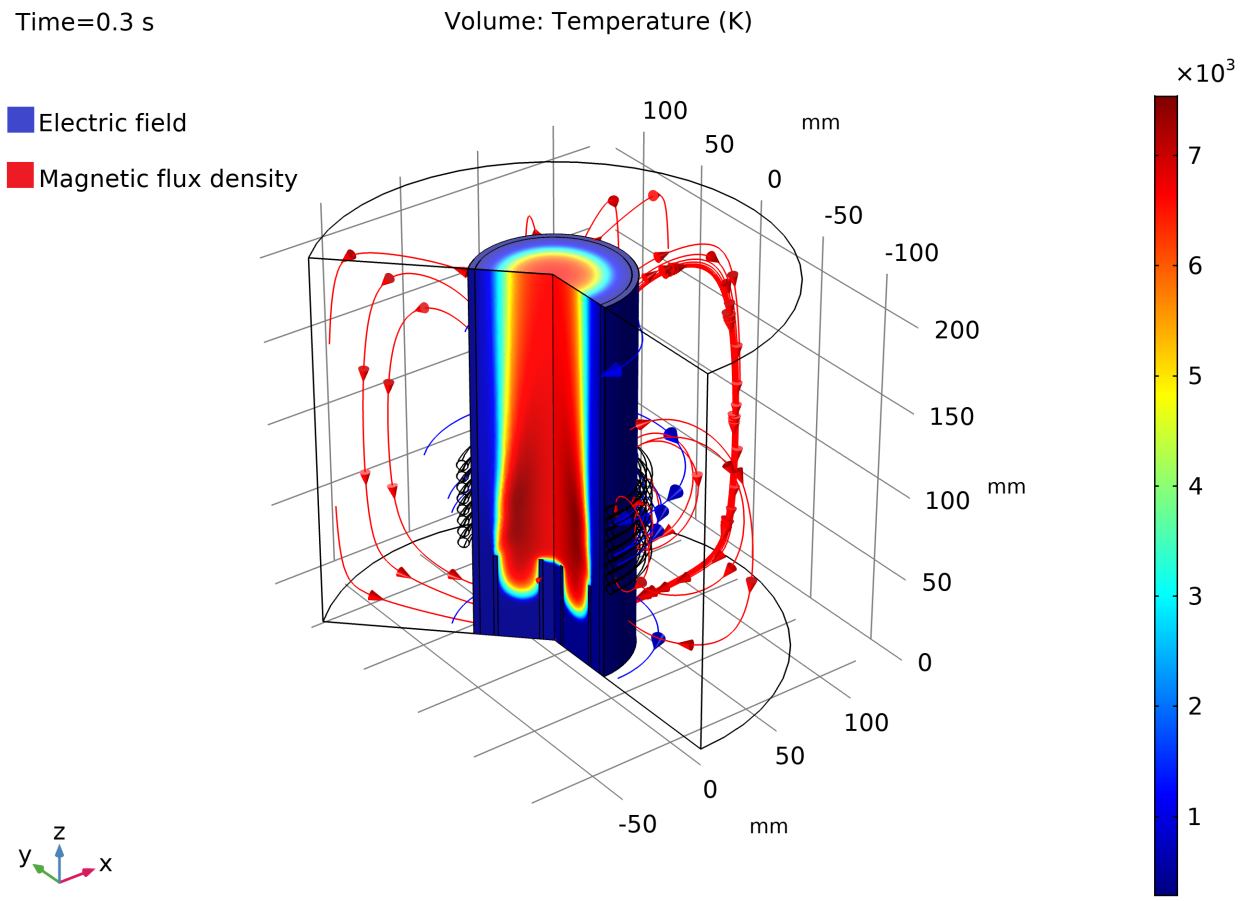


**Figure 9:** 3D Temperature in the domain and magnetic flux density and electric field streamlines.

## 4.5 Chapter Summary

In this chapter, the modeling of an air RF plasma generator was performed using the modeling software COMSOL. The geometry, which was assumed 2D axial symmetric, was defined using the inbuilt functionalities while the material properties for the quartz tubes, the copper coils and the air were taken from COMSOL database. Being the nature of Inductively Coupled Plasma torches multi-physical, different specific and coupled interfaced were employed: the magnetic fields (mf) interface, the heat transfer in fluids (ht) interface and the fluid flow (spf) interface. As multiphysical links, Lorentz forces and equilibrium discharges heat sources presence, as well as the dependence of the fluid properties on the temperature, were considered. The mathematical formulations of the interfaces were described, as to define the dependent variables the models are solved for. In particular, the main quantities of interest for this study are the fluid temperature profile, the electrical power consumed and the fluid mass flow rates. In fact, the results of this model are direct inputs to the gasification unit system model which will be described in the next section: the air flow mass flow rate and its temperature will be used to characterize the gasification reactions, while the electrical power consumed is used for system energy balance assessments. The results of the simulation were shown, and in particular high temperatures, with maximum values around 7353 K, were observed for 54 kg/hr of air and an electrical power coil excitation equal to 75 kWel at 13.6 MHz. The temperature values found are within the typical ranges for RF torches, and the behaviors of the magnetic fields and the total current in the coils appeared as expected.

# 5 Waste-To-Energy plasma gasification unit modeling

In the present chapter, the preliminary development of a WTE plant model based on plasma gasification was conducted. The subsequent logical steps were followed. First, a possible and suitable case study was identified; in particular, a vessel was chosen based on passenger capacity. Then, based on these information and the data on waste found in literature, a feedstock investigation was performed in terms of proximate and ultimate analysis and average mass flow rates to be treated. After that, a model of the various processes involved was developed using the software Aspen Plus. The waste streams defined in the previous step were used as input. It must be noted that the model is composed of different sub-sections which will be described in further detail in the next sections. Once the base model was structured, optimization of the streams and analysis of different scenarios were performed, in order to investigate the best conditions of operation of the system and to extract some preliminary results on feasibility of such systems.

## 5.1 Case study description

All over the world, in 2019, about 272 cruise ships and 55 cruise lines were operational, the Caribbeans being the most visited region, directly followed by the Mediterranean region. However, the actual number and variety of destinations is increasing every year, and new destinations are becoming more and more popular [1]. This is, as an example, the case for the arctic region which has seen a strong surge in the number of passengers in the last decades. Given the large number of cruise lines and vessels, and given the large number of destination ports, a large variety in terms of ship dimensions and passengers capacity is expected: for ocean liners, the average number of passengers is around 3000 guests, but some ships can host more than 5000 passengers, while some cannot host more than 1000 [6]. Naturally, the dimension of the ship in terms of gross tonnage (GT) affects the transportable number of passengers but also the itinerary, since ports must be adequately equipped to accept ships of increasing size. Destination ports provide temporary space for cruise ships and essential utilities that allow the continuation of the trip, such as waste handling, refueling, cargo restocking (food, commodities and various goods).

For this study, it was deemed convenient to take as reference an average-sized ship, following a fairly common itinerary. Nevertheless, bigger or smaller ships could have been also considered. For these reasons, the vessel "Carnival Freedom" was chosen. The Carnival Freedom is a cruise ship whose volume amounts to 110320 GT, it is long 298.8 meters and designed to transport a maximum of 4914 people (crew included). The ship follows two different main itineraries: during the winter period it travels in the Caribbean region, while in the summer period it travels in the Alaskan region. It is provided with 6 diesel engines Wärtsilä (6 x 12600 kW) for electrical power production, and two electrical motors Alstom (2 x 20000 kW) for propulsion. No more technical details are given in its technical sheets [40]. For this reason, it is expected that standard waste management techniques are employed on board, such as storage and off-loading, sea discharge and on-board incineration.

## 5.2 Feedstock analysis

Once the general context and case study have been defined, the first essential step is to define the feedstock streams to be investigated from the point of view of their composition and mass flows. Indeed, we are interested in identifying, for each waste stream, the composition in terms of moisture content, volatile matter, fixed carbon and ashes, which is called proximate analysis, and their composition in terms of weight percentage of C, H, O, N, Cl, S and ashes, which is called ultimate analysis. The knowledge of these parameters is fundamental for the simulation of the gasification reactions in the gasifier. It should be noted that it is extremely complex to define an absolute and precise waste composition, since biomasses tend to be extremely variegated. This is caused by different issues: first, on a bigger scale, every cruise ship system is different from the other in terms of the type of materials employed on board; as an example, one cruise ship could use more plastics of a certain type while another one could offset the use of plastics by employing more paper or glass, and this would naturally affect both the waste stream composition and the flow rate of waste that can be treated. Furthermore, even on the same ship, the waste composition can vary in a significant way during the itinerary; this issue can be understood when food waste is considered: different types of food are characterized by different chemical compositions, as an example bones contain much more "ashes" (when speaking about ul-

timate analysis) than fruit and nuts [41]. In the same way, the other types of wastes could also have a non-constant composition, affecting overall waste properties. This second issue can be partially solved by employing storage systems for the different waste streams and homogenization of the biomass, allowing at the same time reduction to composition variability and increased versatility of the system. For this study, an average composition of the waste stream was assumed, based on the data retrieved from the literature. In particular, for what concerns the solid waste stream removed of plastics, glass and metals, by elaborating the data obtained from [22, 23, 24] it was calculated that 75% of the stream is composed of domestic waste while 25% is food waste. Domestic waste and food waste typical distributions were assumed, since no specific data is available. In Table 4 some reference data is provided regarding the volumetric flow rates of different type of waste as function of people transported and the gross tonnage of the ship considered. These are the values which are used as main guideline for the study, obtained from the CE Delft report [24]. For domestic waste, it was assumed a distribution of 40% paper, 20% cardboard, 20% tissue paper and toilet paper, 10% cotton and 10% wood, while for food waste it was assumed a distribution of 30% vegetables, 20% fruit, 30% meat and bones, 10% nuts and 10% starch. The proximate and ultimate analysis of the basic components were then averaged, assuming perfect homogenization of the biomass. A way to increase the faithfulness of this model would be to sample the actual waste streams during a real one-week cruise. While solid wastes can be considered the main and most important source of feedstock, some alternatives can be integrated to reduce the burden of their handling and to minimize their volume. Indeed, sewage sludge and plastics will be integrated in the scenarios analyzed, but in general also oily sludges from the oily bilge waters and hazardous wastes could be investigated. The main difficulty is that, while proximate and ultimate analysis for solid waste and sewage sludge can be found in literature, for what concerns oily sludges and hazardous wastes data is lacking, probably due to their extremely high degree of variability. Proximate and ultimate analysis for domestic wastes and food wastes were retrieved from [41], while for sewage sludge they were obtained from [42] and for non-chlorinated plastics from [43]. Unfortunately, the data for sewage sludge does not contain any information on Chlorine weight percentage and was therefore assumed as 0, while moisture content was considered as 68%, assuming initial physi-

cal dewatering in a Marine Sanitation Device. Sewage Sludge composition is also affected by strong variability, so an average composition was considered. For plastics, only non-chlorinated plastics were considered, and regarding the composition, average values from the literature were used. It must be noted that a wide variety of different type of plastics exist with different compositions and different propensity to recycling (LDPE, HDPE, PET, PP, PS...), but for the sake of simplicity a single proximate and ultimate analysis is considered. In Table 5 the proximate and ultimate analysis of the various feedstock streams used in the simulations are shown. One of the main drawbacks of assuming this type of analysis is that some pollutants cannot be modeled; this is the case for heavy metals such as aluminum, lead, zinc, iron, copper, etc... however it is expected that the vast majority of those will remain collected in the produced vitrified slags, although this should be assessed experimentally through the analysis of samples and experimentally. On the other hand, knowing the weight percentages of S, N, and Cl in the feedstock allows to model the generation of common gasification pollutants, such as $H_2S$, $COS$, $HCl$ and $NH_3$, which will be important for the Syngas Cleaning Block modeling.

**Table 4:** The waste generation rates of different waste streams and their drivers [24].

| **Waste stream** | **Generation rate** | **Unit** | **Drivers** |
|---|---|---|---|
| Domestic waste | 0.001 - 0.02 | $m^3/person/day$ | Number of people and type of products used |
| Operational waste | 0.001 - 0.1 | $m^3/person/day$ | Number of people and size of the ship |
| Plastic waste | 0.001 - 0.008 | $m^3/person/day$ | Number of people and type of products used |
| Food waste | 0.001 - 0.003 | $m^3/person/day$ | Number of people and type of provisions |
| Sewage | 0.01 - 0.06 | $m^3/person/day$ | Number of people and type of toilets |
| Oily bilge waters | 0.01 - 0.13 | $m^3/person/GT$ | Size of the ship |

**Table 5:** Averaged proximate (dry basis) and ultimate (dry ash-free basis) analysis for the investigated streams of solid wastes, sewage sludge and plastic waste [41] [42] [43].

| **Waste stream** | **Solid waste** | **Sewage sludge** | **Plastic waste** |
|---|---|---|---|
| | **Proximate analysis (wt.%)** | | |
| Moisture | 20.00 | 68.00 | 0.13 |
| Ash | 6.81 | 26.10 | 0.48 |
| Fixed Carbon | 11.21 | 5.00 | 0.08 |
| Volatile matter | 81.98 | 68.90 | 99.4 |
| | **Ultimate analysis (wt.%)** | | |
| C | 46.90 | 44.24 | 86.22 |
| H | 6.22 | 6.12 | 12.97 |
| O | 45.44 | 40.39 | 0.73 |
| N | 0.99 | 7.06 | 0.08 |
| S | 0.24 | 2.19 | 0.05 |
| Cl | 0.21 | 0.00 | 0.00 |

## 5.3 Model introduction

As already mentioned, one of the objectives of the model is to show that the system modeled can operate without the need of external sources of electric energy, by exploiting the syngas produced to produce internally the power needed to maintain the plasma generators. It is not expected for the system to produce a big surplus of electric energy for the vessel. It would be relevant to show that a system of this kind could be able to alleviate cruise liners burdens in terms of waste management. This can be done in a preliminary way through simulations, by investigating some of the most relevant aspects related to the chemical and physical processes, such as emissions, syngas composition, contamination and characterization, energy balances, operational temperatures, streams mass flow rates. In order to model the various chemical and physical processes of interest, the software Aspen Plus V10 was used. The software is based on a blocks and streams approach, allowing the simulation of even complex processes by coupling multiple simpler blocks together in a modular way. The blocks are linked by directed material, work and heat streams, therefore allowing to determine energy and mass balances for the overall system and for each block. Some examples of blocks that can be employed are separators, heat exchangers, reactors, crushers, compressors and

turbines. For what concerns this study, the entire process will be separated into 5 different main sections:

- Waste pre-treatment unit;
- Gasification unit;
- Syngas cleaning unit;
- Syngas combustion and thermal energy conversion;
- Heat recovery units.

Each unit will carry out a specific function and will take as input the output of the previous section. The disposition of the units follows the logical development of the feed stream, developing from untreated coarse biomass, to raw and subsequently clean syngas, to finally flue gas. Th details of each unit will be described in the next sections, starting off from the waste pre-treatment unit. The general assumptions of the overall model are the followings:

- The model is 0D, no spatial dependency;
- Steady state conditions were considered;
- Tar and dioxins formations, and heavy metal transport were not modeled given the limitations of the software and the complexity of the processes involved;
- Some operational parameters, like drying and decomposition temperature, were fixed and based on literature;
- The effects of ionized species could also not be modeled, but it is expected to have a beneficial effect on the decomposition of the feedstock and tars [29] [44].

### 5.3.1 Waste pre-treatment unit

The waste pre-treatment unit is concerned with all those operations that are performed before the feed is sent to the gasifier, to enhance and optimize the devolatilization and gasification reactions and improve syngas quality. The three main feedstock streams considered are solid wastes, sewage sludge

and plastics, but the system could be expanded to integrate oily sludge and hazardous wastes. For the solid waste portion, a first screening process is necessary for the removal of undesirable materials such as glasses, metals and recyclable plastics. In fact, what can be reused or stored and recycled off board should be screened. The feedstock, which is composed of paper, cardboard, fabrics, food waste, wood, ropes and un-recyclable chlorine-free plastics is generally sent through a magnet to further remove undesirable inorganic small metallic. For the untreated solid waste, it was assumed a normal distribution characterized by a medium particle width (D50) of 20 cm with a standard deviation of 15 cm, so that a significant percentage of smaller and bigger objects are considered. Particle size reduction is performed in two steps: initially a primary and coarse reduction is obtained using a shredder, while for finer pulverization a mill is employed. The target normal particle distribution is chosen to have a medium particle width (D50) of 0.3 cm and a standard deviation of 0.05 cm [45]. Particle size reduction is important not only because smaller particles occupy less volume therefore impacting positively on the dimensions of the gasifier, decreasing costs and occupied space, but also because it is shown experimentally that a reduced particle size distribution influences in a positive way syngas yield by increasing the amount of H2 and CO produced and reducing the production of char and tar, which is a highly desirable effect [45]. For sewage sludge a similar process is employed but given the intrinsic high moisture content a drying step is necessary. The drying process is performed before the milling since the removal of water reduces significantly the mass flow rate of the biomass and the heat needed is provided by the heat recovery system. Sewage sludge and solid wastes should be mixed before milling for increased homogenization of the feed.

**Model details**

On Aspen plus, the feedstock streams are considered non-conventional solid streams with the prescribed proximate and ultimate analysis and the particle size distributions defined previously. The shredder and the mill are modeled using CRUSHER blocks in which the target PSD and HGI (Hardgrove Grindability Index) are defined, while for the drying process a DRYER block was used and characterized as contact dryer which receives heat from outside. The HGI is a dimensionless number generally used to measure the grindability of coal (a smaller HGI implies an harder to grind coal) but in

this study it was assumed applicable also for biomasses. The output of the waste pre-treatment system is a milled and homogenized feed with reduced moisture content that can be finally sent to the gasification unit. The model is shown in Figures 10. The assumptions for the model are the synthesized as follows:

- The feedstock introduced is at 25°C and 1bar (ambient conditions);
- Initial normal particles size distribution assumed with average particle width of 20cm and a standard deviation of 15 cm;
- Target normal particle size distribution assumed with average particle width of 0.3cm and a standard deviation of 0.05cm;
- Moisture is removed from sewage through a drying step (from 68% to 20%);
- The HGI for biomass was assumed in a conservative way as 20 (coal has a grindability index of 45 and more).

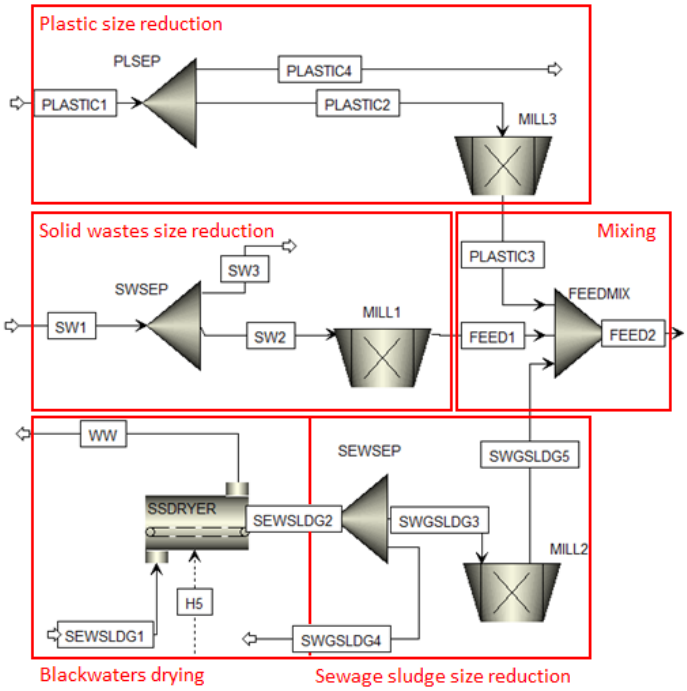


**Figure 10:** Waste pre-treatment unit.

### 5.3.2 Gasification unit

The gasification unit is the hearth of the whole system and its function is to convert the pre-treated feed stream into useful raw syngas. As it is known, syngas or synthetic gas is a gas mixture mainly composed of hydrogen, carbon monoxide, carbon dioxide, nitrogen and in some smaller quantities water and methane, produced by carbonaceous feedstocks through gasification reactions. In this study, gasification takes place at high temperatures due to the injection of oxidant through a system of plasma torches working with air as plasma gas. Air was chosen because it is the easiest gas obtainable in nature, thus reducing the complexity of the system, however pure oxygen, steam and even carbon dioxide could be used as oxidants as well. The model which will be described was inspired by the work of Janajreh, Shabbar and Valmundsson [46], as they developed a simulation on Aspen Plus for an updraft gasifier with plasma torches as heating source using a mixture of air and steam as plasma gas. For the present study, the main assumptions made are the following:

- The gasifier is split into two main zones, a Low Temperature Zone (top) and a High Temperature Zone (down), both zones are maintained in isothermal conditions and 1 bar of pressure;
- Residence times are sufficiently high to allow the use of models not based on reaction kinetics but minimization of Gibbs free energy instead;
- The air/fuel ratio is optimized to obtain the highest syngas LHV;
- The plasma torches are modeled as heat exchangers heating air to 4000°C, which is a 0D average value of the temperature obtained by lumping the results of the plasma generator model (the gasifier is a 0D object).

The gasifier is modeled following the operational scheme of an updraft gasifier without combustion zone, since heat is provided externally by the plasma torch: first, the milled feed falls from the top of the chamber into the low temperature zone where it is further dried thanks to the heat received by the leaving syngas. The feed, which is still heated by the hot syngas, starts to devolatilize and reaches the high temperature zone where the plasma torches and the plasma plumes are localized. The heat and oxidant provided by the torches sharply increase the temperature of the biomass, enhancing gasification reactions, therefore producing extremely hot syngas. The minimized

solid residue, composed mainly of molten ashes, is collected from the bottom and subsequently quenched to produce a non-leaching slag. The hot raw syngas rises from the bottom of the chamber providing heat to the new feed and reacting with the steam generated from the drying process. The syngas then leaves the gasifier and heads to the syngas cleaning unit.

**Model details**

This scheme is modeled on Aspen Plus by using reactor blocks, heat exchangers, separators and mixers. In particular, for the drying process, an RSTOIC reactor block, which is used when the stoichiometry of a reaction is known (full evaporation of water is assumed), coupled with a separator, were employed and the input feed temperature was increased using an heat exchanger (heat provided by the leaving hot syngas). The devolatization process was modeled by applying another heat exchanger and a RYIELD reactor block, which is used when the output yield distribution is known. This block is fundamental since it allows to decompose a non-conventional stream into basics components (H2, C, S, O2, Cl2, N2) according to proximate and ultimate analysis of the feedstock. The output yield composition in the RYIELD block is calculated through a CALCULATOR block (complete decomposition assumed). The decomposed stream and high temperature air provided by the plasma torches are sent to the first RGIBBS reactor, which operates by minimizing the Gibbs free energy of the compounds involved, for the gasification reactions to happen. The ashes are then separated using a new SEP block, while the syngas stream goes through the low temperature zone and reacts with the steam in a second RGIBBS reactor block. Heat exchangers and heat streams are used to maintain the overall energy balance in the system, in particular this is important for the RSTOIC and RYIELD blocks that are strongly endothermic and need the heat provided by the two RGIBBS reactors. The model is displayed in Figure 11 while some fixed operational parameters are listed in Table 6.

### 5.3.3 Syngas cleaning unit

Syngas departing from the gasifier is considered raw, since it is contaminated by a broad spectrum of pollutants. The solid feedstock may be characterized by significant percentages of Sulfur, Nitrogen, Chloride which will form, during gasification reactions, compounds such as $H_2S$, $COS$, $HCl$, $NH_3$. These,

**Table 6:** Fixed temperatures assumed in the gasifier. The temperature of the low-temperature zone changes slightly for each simulation, but always around 800°C. The pressure is 1 bar.

| Parameter | Description | Value [°C] |
|---|---|---|
| $T_{Dryer}$ | Dryer block temperature | 150 |
| $T_{Pyro}$ | Decomposition block temperature | 400 |
| $T_{HTZ}$ | High-Temperature zone temperature | 1500 |

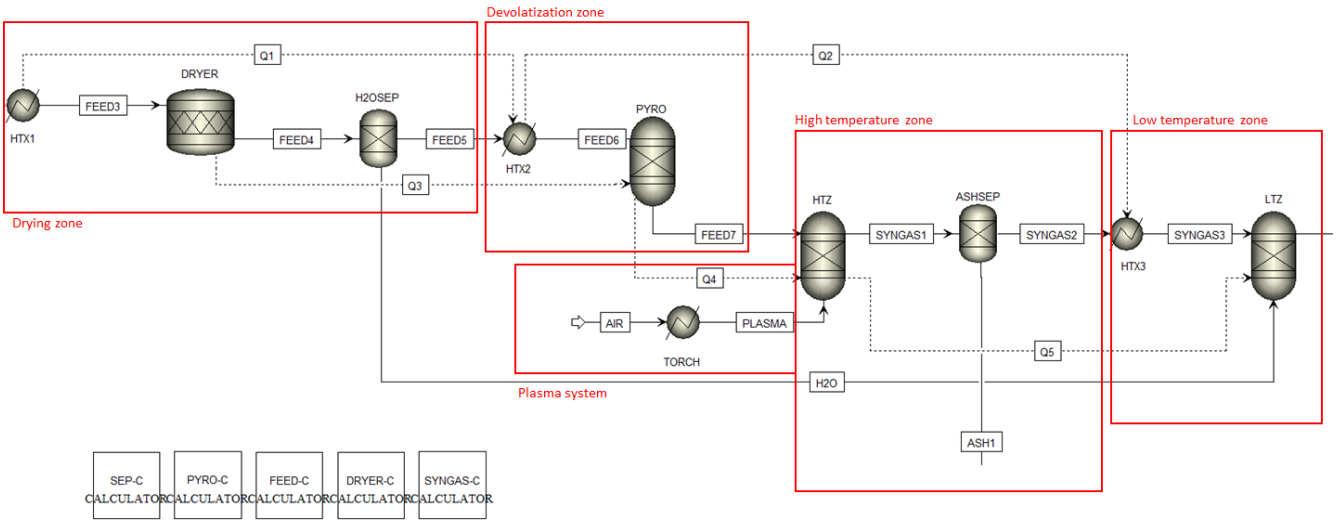


**Figure 11:** Plasma gasification unit.

along with Tars, heavy metals, solid dust particles and dioxins/furans are some of the most important species that need to be controlled during syngas production. Downstream applications often impose stringent requirements in terms of contaminant concentrations, in order to increase the lifetime of mechanical components, to reduce the environmental impacts and the risks associated to human health. It is important to understand the consequences of the presence of these pollutants in the main stream and it is important to control, through primary or secondary methods, their concentration.

**Tars**

Under the denomination "Tar" are considered all those organic compounds with a molecular weight greater than benzene, therefore engulfing a wide portion of organic compounds. Tars are extremely important in biomass gasification processes since, at reduced temperature, they tend to condensate,

therefore impacting components such as pipes, engines or turbines with fouling. It is not an easy task to simulate tar formation, due to the huge number of chemical species and the complex chemistry. For a better understanding on how Tars impact the system, a dedicated experimental apparatus will be needed in future works, but it is important to acknowledge that Tars may pose a significant risk for the system. On the other hand, studies on the effect of high temperature plasmas on the formation of Tars exist in literature, suggesting that this approach may improve their degradation and improve Syngas purity [29].

**S, Cl and N based contaminants**

$H_2S$ (Hydrogen Sulfide) is the main product of reactions involving Sulfur and, in presence of air and water, can produce sulfuric acid which is able to corrode metals and reduce the lifetime of metallic components. If not removed, an higher amount of $SOx$ (Sulfur Dioxide and Sulfur Trioxide) are produced during combustion. It is also dangerous for the human health, as high concentrations can lead to unconsciousness, coma and even death. $COS$ (Carbonyl Sulfide) too is produced in smaller quantities and, as $H_2S$, can have detrimental effects on human health by irritating eyes and skin and by having narcotic effects at high concentrations. $HCl$ (Hydrogen Chloride) is the main product of chloride reactions. It is a strong acid, highly corrosive and also a poison for certain Figure, such as Ni-based catalysts [47]. It is also dangerous for human health, as acute oral exposure may cause corrosion of mucous membranes and subsequent nausea, vomit, diarrhea and skin contact can produce burns. In aqueous environment pH shifts induced by $HCl$ can have strong effects on flora and fauna. $NH_3$ (Ammonia) is generated by nitrogen reactions and as pollutant it is often linked to environmental impacts such as eutrophication. When syngas is burned, $NH_3$ is readily converted into NOx (Nitrogen Oxide and Nitrogen Dioxide), which are notoriously linked to deleterious effects on human health (like inflammation of the airways) and the environment (leaf damage and reduced growth in vegetation, for example). Strong requirements are imposed on $NOx$ emissions in internal combustion engines and gas turbines.

**Dioxins**

Dioxins are often produced during incineration processes of municipal solid

wastes, plastics, tires but also during the production of some pesticides and herbicides, smelting and chlorine bleaching. The term dioxin does not stand for a single specific compound but for a very large group of compounds sharing similar chemical structures and characteristics, such as the presence of chlorine atoms. The most notorious and dangerous dioxin is called 2,3,7,8-Tetrachlorodibenzo-p-dioxin (TCDD). These compounds tend to collect in the soil and sediments until they are absorbed by plants and animals which function as bio-accumulators. Dioxins are mainly assumed through the ingestion of food such as fish and meat and, since these are very stable chemicals, they can reside in the human body for a long time as well as persist in the environment (POPs). The health effects are linked to their toxicity and exposure can lead to skin disorders, liver damage and in case of long exposures to impairment of the immune system, nervous system, endocrine system and reproductive system. Some dioxins, like TCDD, are also known human carcinogens [48]. One of the main advantages of using a plasma gasification chamber instead of an incinerator is the possibility of reducing the formation of dioxins. In fact, as detailed by Lopes, Okamura and Yamamoto (2014) [30], there exist two main hypothesis that try to describe dioxins formation during combustion: one is "De novo" synthesis, related to the breakdown of macromolecular carbon structures leading to the formation of dioxins precursors, the other is generation by thermal breakdown and rearrangement of aromatic precursors that formed in the main stream by incomplete combustion processes. Both reactions most likely happen in the post oxidation zone, where temperatures are dropping in the range 200 – 450 °C and are enhanced by the presence of solid surfaces such as fly ashes and catalyzed by transition metals such as Copper [49]. Both mechanisms are significant in gasification processes with low oxidant content, while for combustion processes rich in oxidant de novo synthesis is dominant. The higher temperatures obtained through the plasma torches as heating source, the removal of chlorinated plastics from the feedstock and the oxygen-starved environment typical of the gasification processes [30] should ideally reduce the generation of dioxins in the raw syngas stream, but it must be noted that a high content of HCl, which is the main source of Cl in the syngas stream, could lead to the formation of dioxins in the bottom complete combustion processes. It could be therefore important to remove HCl from syngas also for this reason, and indeed this will be one of the main objectives of the syngas cleaning unit. In this study it will not

be possible to simulate the generation of dioxins given the complexity of the phenomena involved and the huge quantity of dioxin-like compounds that could be formed. As for Tars formation, it will be necessary to investigate dioxins formation though an experimental setup in future works.

**Particulate matter and ashes**

As it is evident, gasification is not an emission free process, and numerous different pollutants are generated, like the ones already described and particulate matter. Particulate matter (PM) are microscopic particles of solids or liquids that are often produced by natural and anthropogenic sources, like volcano eruptions, fires, storms and generally by fossil fuel combustion in power plants and vehicles. Particulate matter are classified based on the dimensions of the particles and their capability to penetrate deeper in the human respiratory system. In fact, these particles are often divided in coarse (dimensions between 10 and 2.5 µm, PM10 – PM2.5), fine (smaller than 2.5 µm, PM2.5) and ultrafine (smaller than 0.1 µm). Coarse particles can penetrate In the lungs while fine and ultrafine particles can even enter the blood system. Strong health effects are produced by exposure to particulate matter such as developing of cardiovascular and respiratory diseases and even lung cancer. As dioxins, in this study it was not possible to simulate the generation of particulate matter but systems such as spray towers or venturi scrubbers are envisioned and included in the model. As already mentioned, heavy metals such as aluminum, lead, zinc, iron, copper and mercury will also not be considered in the simulation and it will be assumed that they are completely retained into the molten ashes. In a real operating system of this kind, it would also be important to check the toxicity of the resulting ashes slags, as they could potentially be used as construction materials instead of being landfilled, if deemed secure enough [33].

**Model details**

Syngas cleaning can be performed at low temperatures (cold cleaning) or high temperatures (hot cleaning). Cold gas cleaning, carried out at temperatures lower than room temperature, is the most widespread technique due to its reliability and high removal efficiency, but suffers some disadvantages in terms of reduction of overall efficiency of the plant due to cooling and the presence of numerous contaminated water streams that must be treated

before discharge, making it unappealing for small-scale process plants [52]. High temperature syngas cleaning methods, which operate at temperatures higher than 300 °C, address the issues described and could be better suited for smaller applications such as the one it is being developed in this study. These methods are based on the employment of reagents which may represent a disadvantage from the economical point of view, as generally chemical reagents can be expensive and need to be replaced when consumed. In this study, the hot syngas cleanup approach was preferred, as the reduction of wastewater streams produced and the increased efficiency were deemed valuable. The syngas cleaning unit in this model is divided in three components: a water spray tower and two catalytic removers for $HCl$ and $H_2S$. The water spray tower operates as partial quench and solid particles remover, and could also potentially remove small percentages of $NH_3$ and Tars. The only wastewater stream expected as output from the syngas cleaning unit comes from the tower, as its objective is also to cool the stream to a target temperature for the subsequent catalytic removers. In fact, the two removers are based on chemical reactions between the target pollutant and the sorbent and temperatures must therefore be optimized to reduce as much as possible costs and occupied space by the component. $HCl$ is removed first, as $HCl$ could be source for the formation of dioxins, through the employment of $Na_2CO_3$ (Sodium carbonate) as sorbent according to the following reaction:

$$Na_2CO_3(s) + 2HCl(g) \rightarrow 2NaCl(s) + H_2O(g) + CO_2(g)$$

Sodium carbonate was chosen for reactivity with HCl and effectiveness in removing the pollutant, but it must be noted that it is also generally expensive, three times more than limestone, which could represent an alternative [50, 51]. As it can be seen, the products of the reaction are harmless, although this system increases the concentration of CO2 in the gas stream. After HCl removal, a system based on ZnO sorbent is used for H2S removal, according to the following reaction:

$$ZnO(s) + H_2S(g) \rightarrow ZnS(s) + H_2O(g)$$

ZnO has been chosen since it is regarded as one of the most efficient sorbents for H2S removal, often incorporated with iron oxide and titanium oxide [52]. ZnO is affected by metal Zn volatility at temperatures higher than 700°C, therefore this will need to be taken into account when considering the operating temperature of the component [51]. On Aspen plus, the cleaning system was modeled based on the considerations made in the previous sections. In particular, each component was modeled using different blocks, starting from the spray tower, which receives the raw syngas stream. The spray tower was modeled using a FLASH2 separator block, in which water and syngas are mixed and the solid-liquid fraction is removed. In this way the syngas is both cooled by the water and the solid particles retained following the gasification process are removed. The following two sorbent-based pollutant removers are modeled in the identical way, subsequently: the pollutants of interest and the chemicals involved in the reactions are virtually separated from the mainstream using a SEP block and are made react in a RGIBBS reactor block. After that, the product stream is re-mixed with the virtually separated part of the syngas, while the pure sorbent and the consumed sorbent are considered as streams, although in real life the components will contain the sorbent which will be changed only after a certain period of time. In this way, the raw syngas is cleaned of solid particles, $HCl$ and $H_2S$, and the possibility of formation of dioxins during the combustion process, which is the main focus of the following section, is severely hindered. The model is shown in Figure 12, while the operational parameters of the model are synthesized in Table 7.

**Table 7:** Temperatures assumed in the hot syngas cleaning unit.

| **Parameter** | **Description** | **Value [°C]** |
|---|---|---|
| $T_{HCl}$ | $HCl$ removal system inlet temperature | 450 |
| $T_{H_2S}$ | $H_2S$ removal system inlet temperature | 400 |

### 5.3.4 Syngas combustion and thermal energy conversion unit

The syngas stream departing from the cleaning unit can now be employed as fuel, as it is necessary to convert its chemical energy first in thermal energy by combustion, then in mechanical energy by exploiting the expansion of the

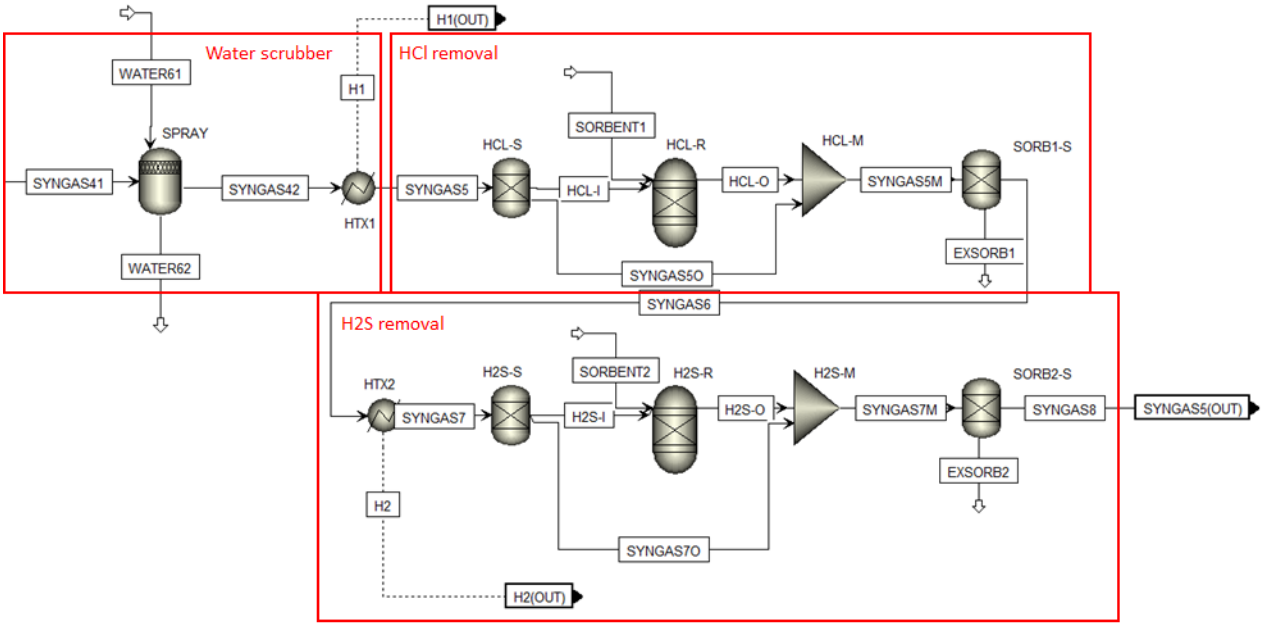


**Figure 12:** Syngas Cleaning unit.

hot gas and finally in electric energy through a generator. The electric energy extracted from this process can be used to run those pieces of equipment that require power, most importantly the plasma torches, which are crucial for the whole gasification process, but possibly also auxiliaries such as pumps, crushers, mills, conveyor belts. It is therefore necessary to devolve this function to a specific unit, which will be the combustion and energy conversion unit. The two main technologies considered for the energy conversion were gas turbines and internal combustion engines. As it is known, gas turbines are particular types of combustion engines (with continuous combustion) that are, in the simplest configuration, composed by a gas compressor, a combustion chamber, a gas turbine and an electric generator. The fuel, which is injected into the combustion chamber together with compressed air, is burnt to generate an high temperature flow of combusted gases which will spin the gas turbine, effectively converting their thermal energy in mechanical energy at the shaft that connects turbine, compressor and generator. The thermodynamic cycle followed by a gas turbine is generally the Brayton cycle. Gas turbines are akin to internal combustion engines, but the latter refers to those engines characterized by intermittent combustion (not continuous) in which the force produced by the combusted expanding hot gas is applied to the surface of pistons in the so-called four-stroke or two-stroke piston engines.

These types of engines generally follow the Otto thermodynamic cycle or the Diesel cycle. In order to make a choice between the two technologies, several factors were taken into account: first of all, cruise ships are generally already equipped with big internal combustion engines for propulsion and electrical power generation, therefore the installation of an already experienced technology could be beneficial for the crew from the point of view of maintenance and operability. Furthermore, internal combustion engines are characterized by significant fuel flexibility and rapid startup, with a very large market of unit sizes and higher overall efficiencies. Micro gas turbines, while being much more compact and with lower potential emissions, are generally more expensive and with lower overall efficiencies, although it must be noted that their lower maintenance expenses could offset the higher investment cost [53]. The proved aspect of the internal combustion engines, their readiness and the fact that a much wider number of technical sheets for commercial engines were found in literature were crucial in the choice-making. In particular, as example for the modeling on Aspen plus, the SGE-S series of Siemens gas engines were considered as guidelines, especially the model SGE-36SL (1800 rpm) [54]. Of course, it is expected that the numbers on the technical sheets and the results of the simulation are not totally the same, moreover because the one on the sheets are related to operations with Natural gas, which is very different compared to syngas. In any case, since the engine considered is stated to be compatible with syngas, it will be considered as guideline for the modeling of the energy extraction unit.

**Model details**

The model SGE-36SL (1800 rpm), when using natural gas as fuel, is characterized by a nominal electrical power of 485 kW and a compression ratio of 11.6:1. Structurally it is a V12 engine with two banks of six cylinders with a double intercooler stage, a total volume of approximately 10 $m^3$ and a total dry weight of 4.2 tons. According to the model, a solution could be of considering two SGE-36SL (1800 rpm) in parallel, therefore on Aspen Plus the main clean syngas stream was split into two identical streams. The compression phase is modeled as COMPRESSOR blocks and the expansion phase as TURBINE blocks. The intercoolers are modeled as heat exchangers, working with water, while the combustor is modeled using an RGIBBS block with specified pressure and heat losses. Heat exchangers are also used to extract

heat from the flue gases, which are finally exhausted in the environment. While the technical sheet of the engine guarantees low levels of NOx (<1.35 g/kWh) and CO (<2.41 g/kWh), it must be noted that those values are just references and based on operations with natural gas. The model is displayed in Figure 13, while some fixed operational parameters are shown in Table 8 .

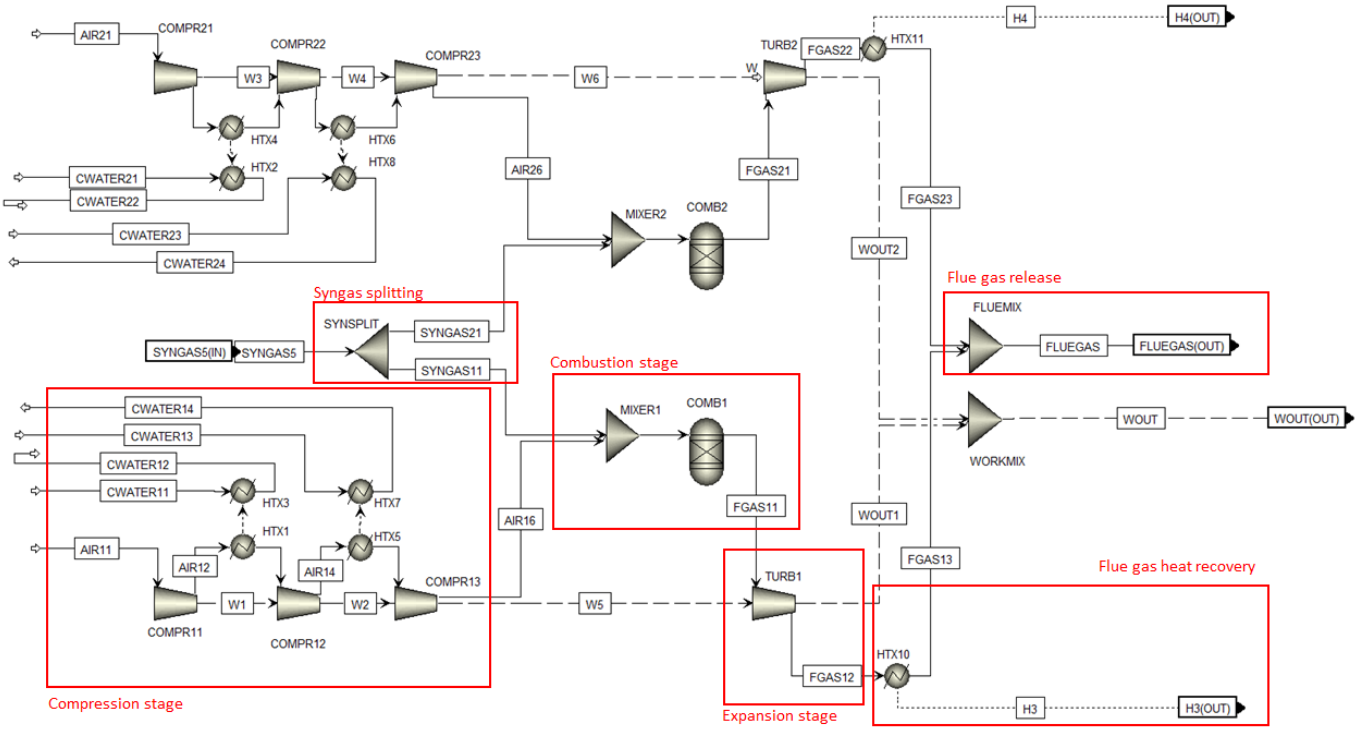


**Figure 13:** Energy conversion unit.

**Table 8:** Temperatures assumed in the gas engines. The combustion temperature changes slightly according to the equivalence ratio and the LHV of the syngas burned.

| Parameter | Description | Value [°C] |
|---|---|---|
| $T_{Flue}$ | Flue gas temperature | 150 |
| $T_{Comb}$ | Average combustion temperature | 1590 |
| $T_{water}$ | Temperature of inlet intercooling water | 25 |

### 5.3.5 Heat recovery unit

The last unit of the system is the one which is responsible for the extraction of waste heat from the various processes considered, in order to produce hot

water and/or steam stream. These can be integrated into the on-board hot sanitary water system used by the crew and the passengers or the fuel heating system, which is fundamental for the correct operations of the main diesel engines. In fact, when heavy fuel oils are employed, pre-heating is necessary to reduce its viscosity and to do so, high temperature steam streams are used. Cruise ships satisfy most of their heat needs by recovering waste heat from auxiliary and main engines, from the cooling of their components and from the hot flue gases. When heat demand is higher than the recoverable heat available, which generally happens when a ship is docked at a destination port with engines shut down, auxiliary boilers are used. The quantity of heat recovered from this system is expected to be very small compared to the actual demand of the ships systems, which will be mainly aided by the various HRSG and HRHT (Heat Recovery Steam Generator and Heat Recovery from High Temperature systems) generally present on cruise ships. Nevertheless, this system can be fired-up when the ship is docked at ports, potentially reducing the fossil fuel consumption linked to the use of auxiliary boilers. This could be especially significant during winter, when heat demand is generally increased. During summer the heat recovered could still be valuable if the ship is provided with absorption chillers serving the HVAC system of the vessel (Heat, Ventilation and Air Conditioning). Absorption chillers are, in fact, systems that employ different fluids which are in affinity (like ammonia and water or water and lithium bromide) and exploit the different boiling points of the substances in order to allow the use of an heating source to drive a cooling process without the need of compressors.

**Model details**

In this study different sources of heat are considered: heat from the quenching of the molten ashes, heat from the wastewaters of the syngas spray tower, heat from the syngas cleaning processes, heat from the inter-cooler stages of the internal combustion engine, heat losses from the combustion chamber, exhaust heat from the flue gases. On Aspen Plus the heat produced by these systems is recovered using Heat Exchanger blocks and provided to water streams. Based on necessities of the vessel, these water streams can be tweaked to produce more steam or more hot water. When sewage sludge is considered, part of the heat recovered is driven to the sewage drying unit, effectively reducing the availability of heat from the system. The

model is shown in Figures 14.

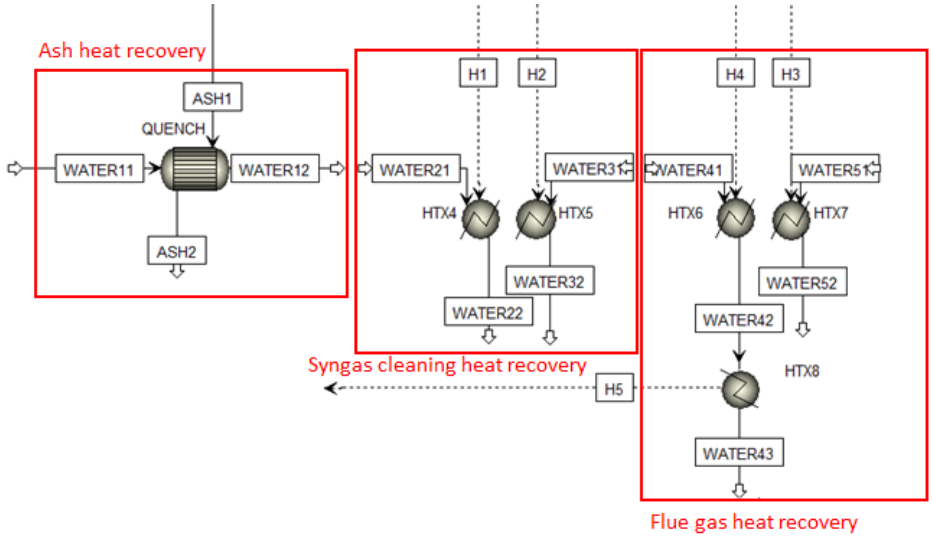


**Figure 14:** Heat recovery unit.

## 5.4 Results analysis

In this section the variables are identified and some important quantities are defined. In fact, some operational conditions were fixed beforehand based on the knowledge obtained from the literature, while some were varied and provided as input according to the scenarios analyzed. The remaining parameters are obtained as outputs at the end of the simulation. The main inputs to the simulation are:

- The feedstock mass flowrate and composition in terms of the various waste streams considered (solid wastes, sewage sludge, plastic);
- The gasification air mass flowrate and thus the gasification Equivalence Ratio, from the plasma torch simulation;
- The plasma air temperature, from plasma torch simulation;
- The combustion air mass flowrate and thus the combustion Equivalence Ratio;
- The sorbent mass flows interacting with the raw syngas.

These parameters affect the syngas yield and composition, which in turn affect the operating conditions of all the bottom components and the therefore generation of heat and mechanical/electrical power. On the other hand, the main outputs of the simulations are:

- The syngas molar and mass composition;
- The mechanical/electrical power produced;
- The heat recovered;
- The combustion temperature, syngas outlet temperature, flue gas outlet temperature;
- The ash mass flow rate;
- $NOx$, $SOx$ and $CO$ emissions;
- The cold gas efficiency of the gasification process.

The already mentioned Equivalence Ratio is one of the key parameters that must be considered during the study of a gasification/combustion process. It is defined as follows:

$$ER = \frac{A/F}{(A/F)_{st}}$$

Where $A/F$ identifies the air-to-fuel ratio in the actual conditions, while $(A/F)_{st}$ represents the air-to-fuel ratio in stoichiometric conditions, which is constant for a given reaction. The main advantage of considering the Equivalence Ratio instead of the simpler Air-To-Fuel ratio is that it does not change when considering either molar quantities or mass quantities:

$$ER = \frac{m_{air}/m_{fuel}}{(m_{air}/m_{fuel})_{st}} = \frac{n_{air}/n_{fuel}}{(n_{air}/n_{fuel})_{st}}$$

Where $m$ and $n$ represent the mass quantity and molar quantity of a substance. The Equivalence ratio can be employed for both oxidant-starved and oxidant-rich processes, and it is particularly useful since $ER < 1$ always

identifies a process in deficit of air, while $ER > 1$ identifies a process rich in air. $ER = 1$ implies an oxidation reaction in stoichiometric conditions. In this model two different ER will be considered: a gasification one, for the gasification process and a combustion one, for the syngas combustion. While the actual $A/F$ ratios varies depending on the input values of the feedstock mass flow rate and the air mass flow rates and can be easily estimated, the stoichiometric $A/F$ ratios are less direct to compute. The waste streams are characterized in terms of proximate and ultimate analysis, and thus it is not easy to identify a simple reaction over which evaluate the stoichiometric air needed. For syngas burning we have the same issue, as syngas is a mixture of different compounds in varying compositions. The $(A/F)_{st}$ were calculated as follows:
When considering the waste stream input to the gasification process:

$$(A/F)_{stoic} = m_{O_2} + m_{O_2}\frac{X_{N_2}M_{N_2}}{X_{O_2}M_{O_2}}$$

Where $m_{O_2}$ is the mass of oxygen needed, $X_{N_2}$ and $X_{O_2}$ are the volume fractions of $N_2$ and $O_2$ in air and $M_{N_2}$ and $M_{O_2}$ are the molecular weight of the compounds. The second term appears because we are using air and not pure oxygen. $m_{O_2}$ is calculated as follows, according to [55]:

$$m_{O_2} = Y_C\frac{M_{O_2}}{M_C} + Y_H\frac{M_{O_2}}{M_H} + Y_S\frac{M_{O_2}}{M_S} - Y_O$$

$Y_C$, $Y_H$, $Y_S$ and $Y_O$ are the mass fractions of C, H, S and O constituting the feedstock according to the ultimate analysis. It is evident how by varying the feedstock composition (in terms of solid waste, sweage sludge, plastic percentage) this ratio will vary accordingly. To take this into account, the following relation was used according to the scenario of interest:

$$(A/F)_{stoic,feed} = (A/F)_{stoic,SW}X_{SW} + (A/F)_{stoic,SWG}X_{SWG} + (A/F)_{stoic,PLS}X_{PLS}$$

Where $X_{SW}$, $X_{SWG}$ and $X_{PLS}$ indicate the mass fractions of Solid Wastes, Sewage Sludge and Plastics. For what concerns the combustion stage, a different approach was employed. Knowing the cleaned syngas composition the ratio was calculated as follows:

$$(A/F)_{stoic} = \frac{(\dot{m}_{H_2} * 8 + \dot{m}_{CO_2} * 0.571 + \dot{m}_{CH_4} * 4) * 4.31}{\dot{m}_{syngas}}$$

Where $\dot{m}_i$ is the mass flow rate of the i-th syngas component, and in this case only $H_2$, $CO$ and $CH_4$ were considered. The numerical values found at the numerator represent the kg of oxygen needed to have stoichiometric combustion with 1kg of fuel considered (8 for $H_2$, 0.571 for $CO$ and 4 for $CH_4$), while 4.31 are the kg of air per kg of $O_2$. $\dot{m}_{syngas}$ is the overall syngas mass flow rate at the combustor. Implicitly, it was assumed that only $H_2$, $CO$ and $CH_4$ do react with the air oxygen according to the following reactions, which is not entirely correct as several other oxidation reactions may take place. It is anyway an acceptable approximation as these are the most abundant oxidizable compounds in syngas.

$$CO(g) + 1/2O_2(g) \rightarrow CO_2(g)$$
$$H_2(g) + 1/2O_2(g) \rightarrow H_2O(g)$$
$$CH_4(g) + O_2(g) \rightarrow CO_2(g) + H_2O(g)$$

Another key parameter calculated on the basis of the results of the simulations is the Cold Gas Efficiency, which is the ratio of the syngas chemical energy and the biomass chemical energy plus any additional sensible heat provided to the gasification process. It gives an indication of the energy lost during the process, as the Low Heating Value (LHV) of the synthetic gas is lower compared to the treated biomass one. It is defined in the following way:

$$\eta_{cg} = \frac{LHV_{syngas}\dot{m}_{syngas}}{LHV_{biomass}\dot{m}_{biomass} + \dot{W}_{el}/\eta_{el}}$$

The electrical power consumed by the plasma torches is converted into heat by dividing for an average electrical power plant efficiency (fossil fuel-fired), $\eta_{el}$ [46].

The LHV of the syngas and the LHV of the feedstock are evaluated in the model in the following way: as for the syngas, it is simply calculated by considering the mass fractions of $H_2$, $CO$ and $CH_4$ in the mixture according to the following expression:

$$LHV_{syngas} = LHV_{CO}CO + LHV_{H_2}H_2 + LHV_{CH_4}CH_4$$

In particular the LHV of the components are equal to $10.1 MJ/kg$ for $CO$, $120.1 MJ/kg$ for $H_2$ and $50 MJ/kg$ for $CH_4$. The feedstock LHV is calculated on the basis of the ultimate analysis of the biomass according to the correlations shown in references [56, 57]. In particular, the HHV is calculated as:

$$HHV_{feedstock} = 0.3491{*}C{+}1.1783{*}H{+}0.1005{*}S{-}0.1034{*}O{-}0.0151{*}N{-}0.0211{*}A$$

where for C, H, S, O, N and A it is referred to the carbon, hydrogen, sulfur, oxygen, nitrogen and ash mass fraction in the feedstock. As noted by the author of the correlation, the average absolute error for this correlation is around 1.45%, as long as the range of applicability are respected (C<92.25%, H<25.15%, O<50.00%, N<5.60%, S<94.08%, A<71.40%) [56]. The LHV is finally calculated as:

$$LHV_{feedstock} = HHV_{feedstock} - 10.55(W + 9H)$$

where W is the weight% of moisture in the fuel and H is the weight% of hydrogen in the fuel, the correlation gives the LHV in $Btu/b$ [57].

### 5.4.1 Scenarios description

Four main scenarios are simulated using this model, in an effort to cover some of the possible modalities of functioning of the system. These scenarios are synthesized in Table 9.

Some additional scenarios may include hazardous solid wastes and oily sludges, as long as information on their proximate and ultimate analysis are obtained, which is not trivial and may require dedicated sampling campaigns. The range of mass flow rates investigated are based on the data provided by the literature coupled to the characteristics in terms of passengers of the vessel considered as model, the carnival Freedom [17, 40]. In particular, taken

**Table 9:** Scenarios considered for the simulations using the plasma gasification model.

| Scenario | Description | Mass flow rate (kg/hr) | Feedstock Composition |
|---|---|---|---|
| 1 | Solid waste(SW) only; total mass flow rate varied | 200 - 425 | 100% SW |
| 2 | Solid waste and sewage sludge (SWG); total mass flow rate fixed | 300 | 0.0 - 33.3 % SWG<br>100.0 - 67.7 % SW |
| 3 | Solid waste and plastic (PLS); total mass flow rate fixed | 300 | 0.0 - 16.7 % PLS<br>100.0 - 83.3 % SW |
| 4 | Solid waste, plastic and sewage sludge; total ass flow rate fixed | 300 | 0.0 - 16.7 % PLS<br>0.0 - 33.3 % SWG<br>100.0 - 50.0 % SW |

into account the cruise ship waste generation, the system is modeled to operate around a median value of 300 kg/hr of waste.

**Scenario 1**

In scenario 1 the system is fed by a stream of solid wastes, while the other streams are redirected away. The main objective of this scenario is to assess how the system operates if provided with only food wastes and domestic wastes, but also to investigate different values of mass flow rates for the feedstock, in order to identify a possible range of operability. This range, which will be identified by a maximum value and a minimum value of feedstock mass flow rate, is expected to be correlated to the size and number of the plasma torches providing air to the system. As preliminary concept, five plasma generators capable of providing 54 kg/hr of air are considered, for a maximum of 270 kg/hr. The critical condition for the identification of the minimum feedstock mass flow rate is expected to be related to the electrical balance of the system, which we want to be non-negative.

**Scenario 2**

In scenario 2 the system is fed by two streams: solid wastes and sewage sludge, while the plastic stream is redirected away. A value of mass flow rate is fixed, chosen on the basis on the analysis performed in scenario 1, and

the composition of the two fractions is varied to investigate the effects of the addition of sewage sludge to the feedstock. The addition of sewage sludge requires the operation of a new component, the dryer, which will require heat from the heat recovery system; for this reason, the heat recovered from the system is expected to be fairly reduced.

**Scenario 3**

In scenario 3 the system is also fed by two streams: solid wastes and plastics, while the sewage sludge stream is redirected away. A value of mass flow rate is fixed, chosen on the basis on the analysis performed in scenario 1, and the composition of the two fractions is varied to investigate the effects of the addition of plastics to the feedstock. Plastics are generally characterized by an high content of carbon and hydrogen, therefore it is expected an sharp increase of the LHV of both the waste mixture and the syngas; the amount of plastic wastes generated are reduced with respect to the amount of solid wastes, as part of them are unfeasible and some others are offloaded for recycling.

**Scenario 4**

In scenario 4 the system is fed by all the three streams previously considered, in varying compositions. A value of mass flow rate is fixed, chosen on the basis on the analysis performed in scenario 1; the results are expected to be similar to the previous two scenarios depending on the fractions of sewage sludge and plastics.

### 5.4.2 Scenarios results

In the next paragraphs the most important results for each scenarios will be shown, starting from the description of the criteria followed for the optimization of the results. The outputs provided by the Aspen Plus simulations were post-processed using the software Matlab, version 2019b.

**Optimization process**

The first raw results obtained from the simulations are not optimized, as the mass flow rates of the plasma gas, combustion air and the sorbent consumption are initially assumed. After the initial run, three sensitivity analysis are performed, and the approach employed is the following: the first

parameter optimized is the gasification air flow rate, as it influences the syngas composition, its LHV, the formation of contaminant, which in turn affect the other parameters to be optimized. Once the gasification air flow rate and in turn the raw syngas composition have been optimized, the sorbent consumption rates are investigated, as the syngas cleaning is the direct subsequent step. The $ZnO$ and $Na_2CO_3$ consumption rates are optimized based on the rational of reducing the contamination by $H_2S$ and $HCl$ as much as possible, without employing more sorbent than needed. Lastly, as bottom process, the mass flow rate of the combustion air is optimized based on the mechanical power that can be produced, the temperature in the combustor and the NOx emissions, as compromises must be made between technical strains, environmental issues and the system overall efficiency. Examples of the sensitivity analysis are shown in Figures 15(a) and (b), in which the key parameters discussed are varied as function of the respective ERs; as example of the process, Figure 15(b) show quantities that are evaluated based on the optimization performed using 15(a).

**Scenario 1**

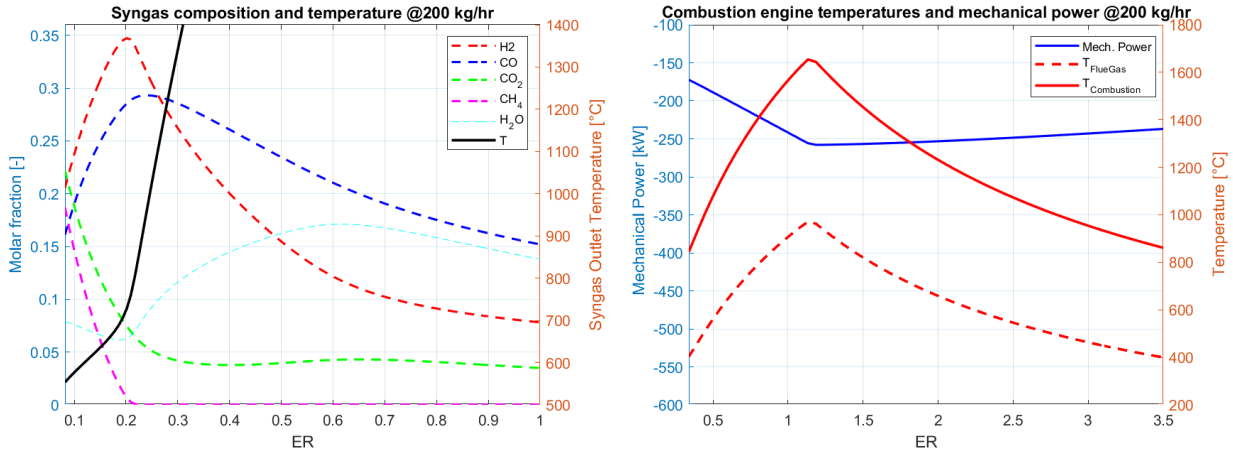


**(a)** **(b)**

**Figure 15:** (a) Syngas composition and syngas outlet temperature; (b) Mechanical power, combustion temperature and temperature of the gases leaving the gas engine at 200 kg/hr of feedstock mass flow rate.

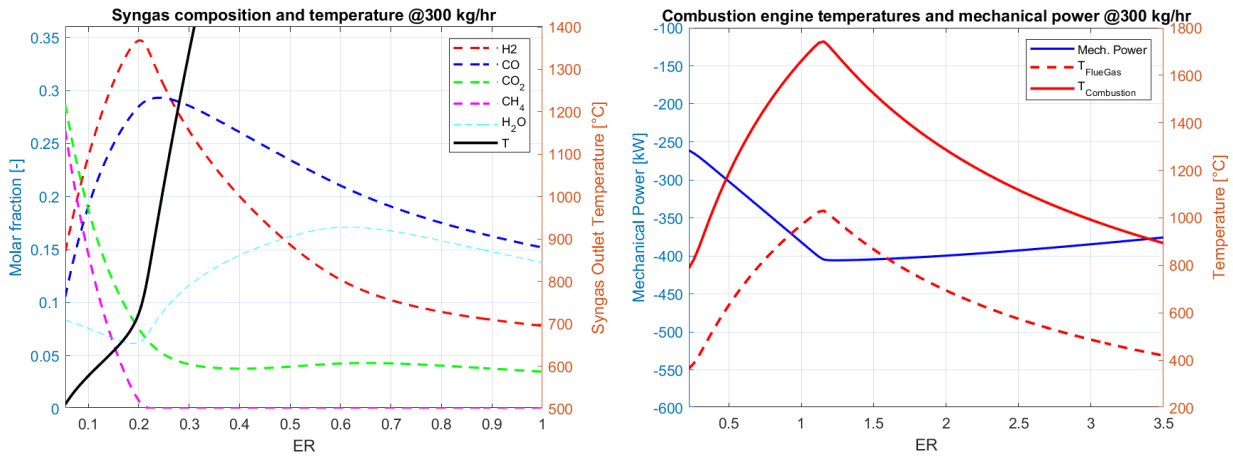


**(a)** **(b)**

**Figure 16:** (a) Syngas composition and syngas outlet temperature; (b) Mechanical power combustion temperature and temperature of the gases leaving the gas engine at 300 kg/hr of feedstock mass flow rate.

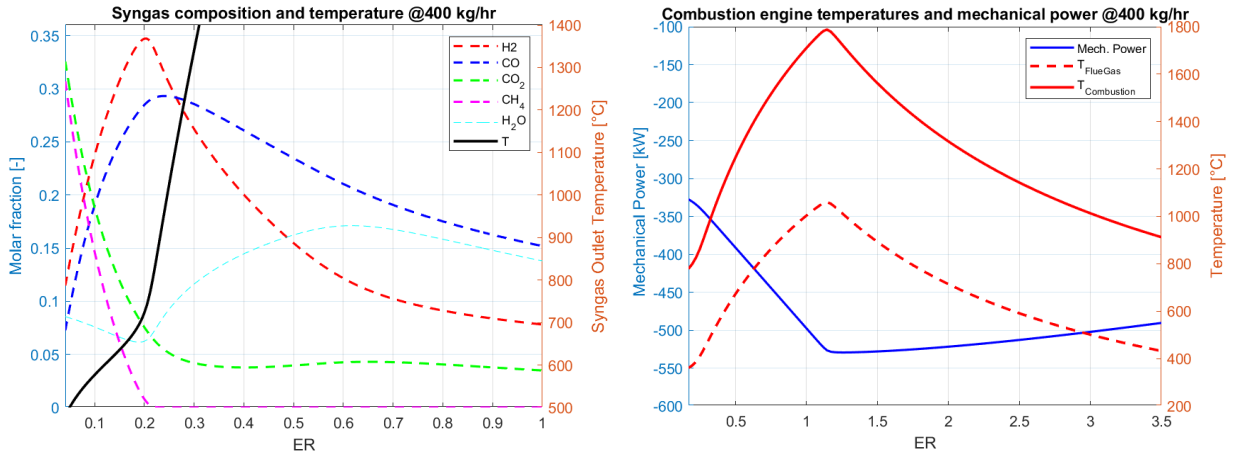


**(a)** **(b)**

**Figure 17:** (a) Syngas composition and syngas outlet temperature; (b) Mechanical power, combustion temperature and temperature of the gases leaving the gas engine at 400 kg/hr of feedstock mass flow rate.

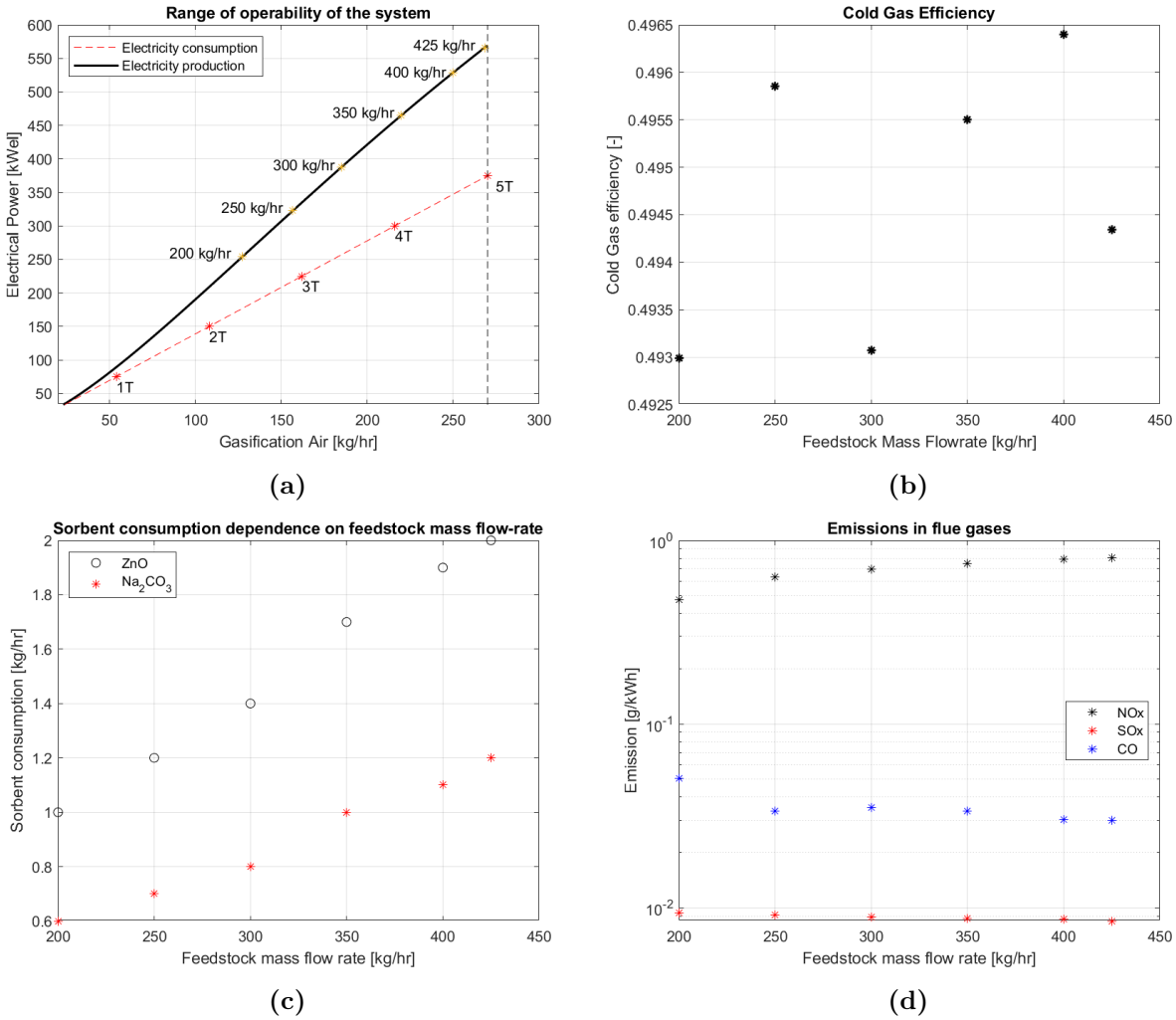


**Figure 18:** (a) Range of operability of the system, as function of the gasification air mass flow rate; (b) Cold gas efficiency as function of the feed-stock mass flow rate; (c) Sorbent consumption as function of the feedstock mass flow rate; (d) SOx, NOx and CO emissions as function of the feedstock mass flow rate.

**Table 10:** Heat recovered from different units and ash flow rate as function of the feedstock mass flow rate (Q: Ash quench, SC: Syngas cleaning unit, ICE: Internal combustion engines unit).

| $\dot{m}_{feed}[kg/hr]$ | 200 | 250 | 300 | 350 | 400 | 425 |
|---|---|---|---|---|---|---|
| $\dot{m}_{ashes}[kg/hr]$ | 9.2 | 12.1 | 14.0 | 16.2 | 18.5 | 19.6 |
| $\dot{Q}_Q$ [kW] | 4.43 | 5.54 | 6.65 | 7.76 | 8.87 | 9.42 |
| $\dot{Q}_{SC}$ [kW] | 8.73 | 18.91 | 28.52 | 45.1 | 62.52 | 66.2 |
| $\dot{Q}_{ICE}$ [kW] | 350.68 | 444.58 | 541.54 | 638.10 | 732.68 | 780.64 |

**Scenario 1 comments**

As it can be seen from Figures 15(a), 16(a) and 17(a), the mass flow rate of the feedstock does not impact the syngas composition, which is optimal in the neighborhood of $ER = 0.21$, as the molar fraction of $H_2$ reaches a peak of 34.7% while the molar fraction of CO reaches 28.6%. An higher content of Hydrogen in the syngas is beneficial, as it increases the LHV of the mixture and subsequently the cold gas efficiency. It can be noted that for increasing values of ER the production of $H_2O$ and $CO_2$ is increased, reducing the molar fractions of $CO$ and $H_2$. This is because as the ER value increases towards 1, the environment becomes richer in oxidant and $H_2O$ and $CO_2$ productions are enhanced. It can also be noted that the syngas outlet temperature increases sharply for higher ERs, due to increasing widespread oxidation. This effect that may cause technological difficulties from the point of view material integrity. Figures 15(b), 16(b) and 17(b) and 18(a) show the dependency of the mechanical power produced by both the gas engines with respect to the feedstock mass flow rate: as the mass flow rate increases so does the mechanical power and accordingly the electrical power. The mechanical power also decreases for ER >1.2, due to the high content of air, which affects combustion thus reducing the combustion temperature .The electrical power is calculated on the basis of the electrical efficiency of the generator which is provided by the constructor [54], in this case equal to $\eta_{el} = 0.963$. The peak electrical power (considering both engines) are the following: 254 kW at 200 kg/hr of feedstock, 391 kW at 300 kg/hr and 530 kW at 400 kg/hr. Figure 18(a) is especially interesting as it shows an increasing difference between the interpoled electrical power produced (black line) and the electric power consumed by the plasma torches (red dotted line); all the points on the black solid line represent fully optimized conditions for the feedstock mass flow rates with a gasification ER equal to 0.21, and as the mass flow rate is increased, the bigger the surplus of electrical power produced by the system. The red solid line is drawn on the assumption that every plasma generator is rated 75 kWel for electrical power and capable of providing a maximum of 54 kg/hr or air, thus for an ensemble of 5 torches the maximum air flow rate that can be reached is equal to 270 kg/hr, which inevitably draws an upper bound for the feedstock mass flow rate: a maximum of 425 kg/hr of wastes can be treated by the system; a lower bound is also identified, which corresponds to the condition electrical consumption higher than the electricity production,

around 30kg/hr of feedstock. This means that the system must treat a suitable amount of wastes to not fall in the negative electrical balance region, which may be a disadvantage from the point of view of flexibility. However, a storage system could tackle this issue allowing to keep the feedstock flow constant. This range, for real life systems, may be more limited, due to the presence on losses not modelled, neglected auxiliary systems and components, possibly worse performances in terms of gasification and combustion and overall due to simplifying assumptions; it was not possible to validate the results of these simulations in this work, due to the necessity of complex and expensive experimental apparatuses, but it would be very valuable, especially for what concerns the plasma gasification unit. Regarding Figures 18(b), (c) and (d), it can be observed that as expected, the sorbent consumption increases as the mass flow rate increases, given that a bigger stream of gas must be cleaned. The $NOx$ emissions increase, while on the other hand $SOx$ and $CO$ decrease according to the feedstock mass flow rate. Regarding $NOx$ emissions, according to Annex VI of MARPOL there are limits prescribed for diesel engines of power superior to 130 kW for both liquid and dual fuel [19]; in particular, corresponding to tier II standards (related to the amendment introduced in 2008), for engines of operating speed (n) in the range 130 <n <2000 rpm, the following equation should be used:

$$NOx_{limit}[g/kWh] = 44 * n^{-0.23}$$

Corresponding to 1800 rpm the limit is therefore 7.84 g/kWh, which is satisfied according to the simulations. Finally, the cold gas efficiency values are not very consistent, however the differences between the six cases are very small and the average value is around 49.47%. These oscillations could be related to slight variations in the optimization process in each case. While no graph is provided for the heat recovered, it is expected to show a behavior similar to the one of the mechanical power, that is increasing with increasing feedstock mass flow rate. This is shown in Table 10, and as expected the main source of heat comes from the flue gas heat recovery system, followed by the syngas cleaning heat recovery system and the ash quench. Naturally, the ash flow rate increases with the feed stock mass flow rate. Given these results, the focus will be now shifted to the investigation of different compositions of the feedstock, by integration of varying quantities of dried sewage sludge and plastic. The overall feesdstock mass flow rate will be fixed to 300 kg/hr, as it

was shown to be the median value of the operability range, and the fractions of the three types of wastes will be varied accordingly. It must be noted that solid wastes will be the main mass fraction in any case, as those are the most abundant types of wastes generated on cruise ships, followed by dried sewage sludge (max 100 kg/hr considered) and plastics (max 50 kg/hr considered).

### Scenario 2

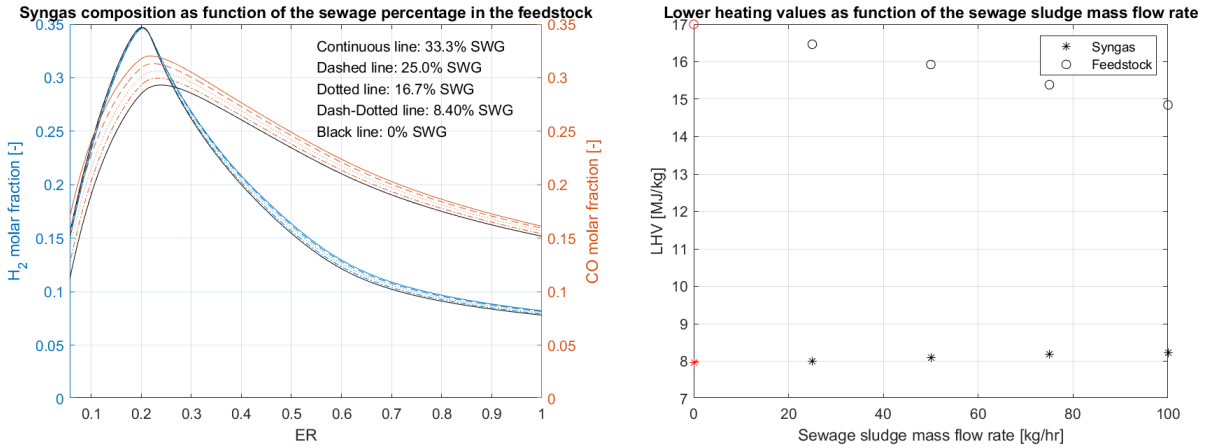


**(a)** **(b)**

**Figure 19:** (a) Molar concentrations of $H_2$ and $CO$ as function of swg. sludge percentage in the feedstock; (b) Lower Heating Values (LHV) of the syngas and the feedstock as function of the swg. sludge mass flow rate.

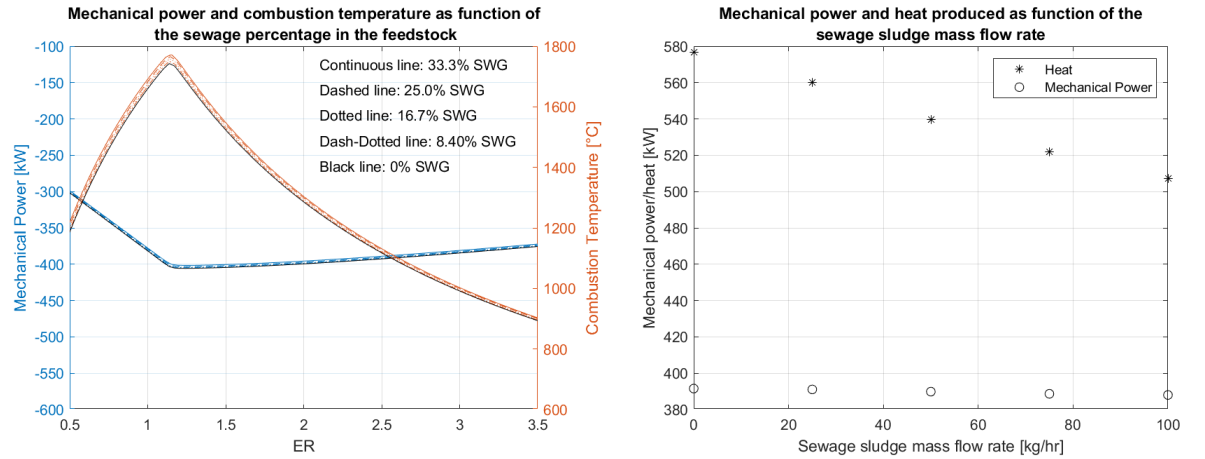


**(a)** **(b)**

**Figure 20:** (a) Mechanical power and combustion temperature as function of swg. sludge percentage in the feedstock; (b) Mechanical power and heat produced as function of the swg. sludge mass flow rate.

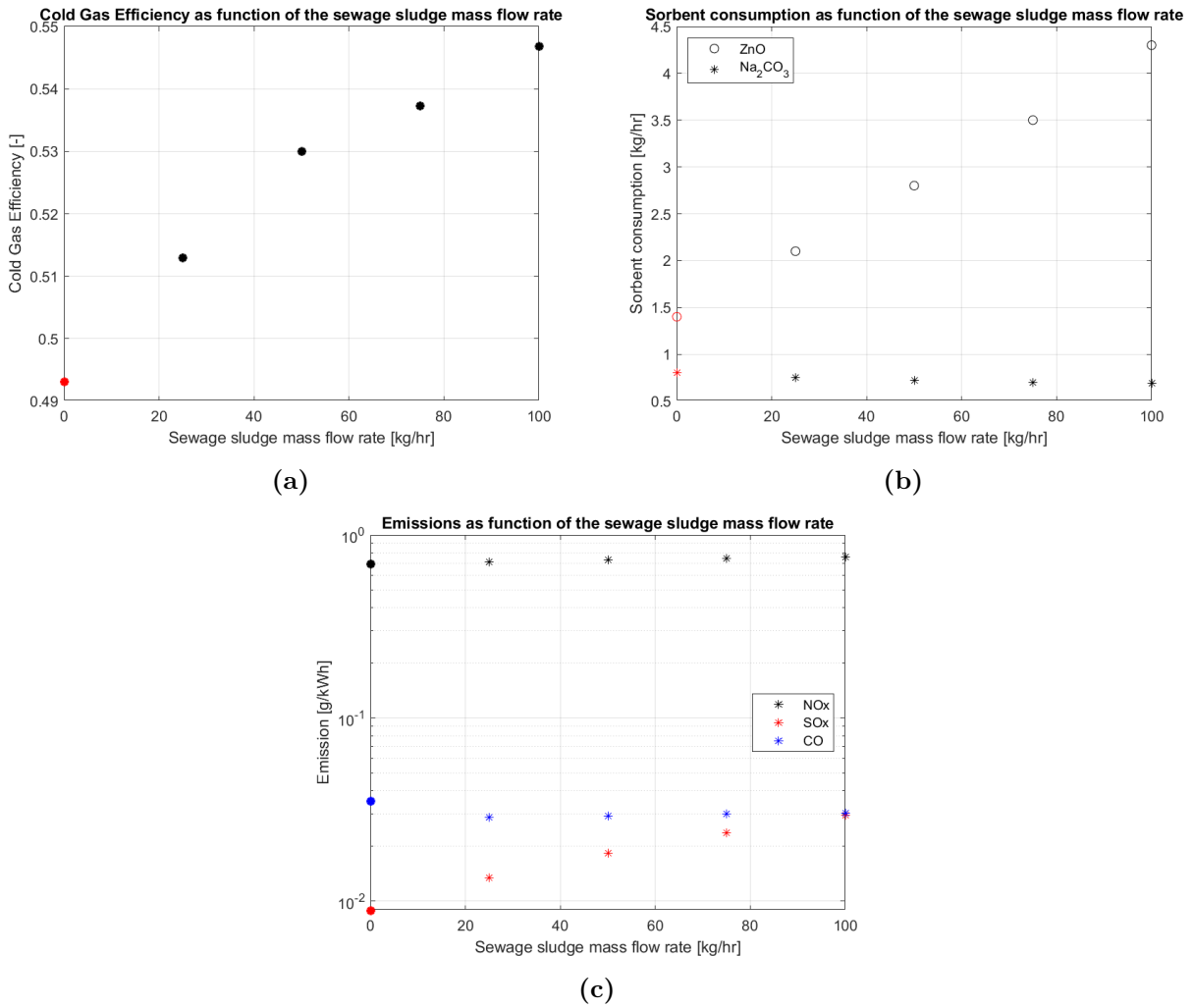


**Figure 21:** (a) Cold gas efficiency dependence on sewage sludge mass flow rate; (b) Sorbent consumption dependence on sewage sludge mass flow rate; (c) Emission dependence on sewage sludge mass flow rate.

**Scenario 2 comments**

In this second scenario, dried sewage sludge is mixed with the main stream of solid wastes in different and increasing percentages, for a maximum of 100 kg/hr of sewage sludge corresponding to 33.3% of the overall mass flow. This maximum value has been assumed based on the data obtained from literature, but higher fractions could be considered and integrated, as long as the drier and more generally the pre-treatment machines are sized accordingly. These simulations will try to give a general idea of the major effects obtained when integrating sewage sludge to the main flow. According to Figure 19(a), the molar fraction of $H_2$ does not really change with increasing sewage sludge

fraction, while the $CO$ molar fraction reaches a peak of 31.7% at 33% of sewage sludge integration. The direct consequence of this effect is shown in Figure 19(b): the lower heating value of the syngas increases slowly for increased sewage sludge mass flow rates, despite the lower heating value of the feedstock being increasingly lower. As shown in Figure 20(a), despite the optimization processes, the mechanical power produced remains almost constant and close to the scenario without sewage sludge, due to the small increase in syngas LHV. This is being displayed also in Figure 20(b), in which the reduction of recovered heat for increasing sewage sludge mass flow rates is apparent, as the drying process requires part of the useful recovered heat. The last three graphs provide further important information: first of all, according to Figure 21(a), the cold gas efficiency tend to increase with increasing sewage sludge fraction, effect that is linked to the syngas LHV increase and the feedstock LHV decrease, up to a peak value of 54.6%. This is without a doubt a beneficial consequence, as it means that the gasification process is slightly more efficient in this case than in the previous one without sewage sludge. Two negative effects are shown in the subsequent Figures 21(b) and 21(c). In fact, the consumption rate of ZnO is sharply increased due to the higher content of sulfur in the stream (4.3 kg/hr of ZnO at 100 kg/hr of sewage sludge), which favors the formation of the undesired $H_2S$ during gasification and SOx during the combustion process. $Na_2CO_3$ consumption does not change much (around 0.7 kg/hr at 100 kg/hr of sewage sludge). Regarding the prescribed limits on $SOx$, according to Annex VI of MARPOL, the value 6 gSOx/kWh should be not surpassed and according to the simulations the condition is met even in the worst scenario considered. Overall, keeping in mind the assumptions made regarding the sewage sludge composition, the introduction of this waste stream can have both beneficial and negative effects. After all, the main objective of this system is not to produce huge quantities of heat to tackle heating demands of the ship, but to be able to handle a large enough variety of waste streams and reduce the burdens linked to waste management, while also ideally reducing the environmental impacts usually produced by normal waste management systems. Indeed, the results obtained by this simulation show that it is possible to introduce fractions of sewage sludge in the main waste stream without incurring in major complications.

## Scenario 3

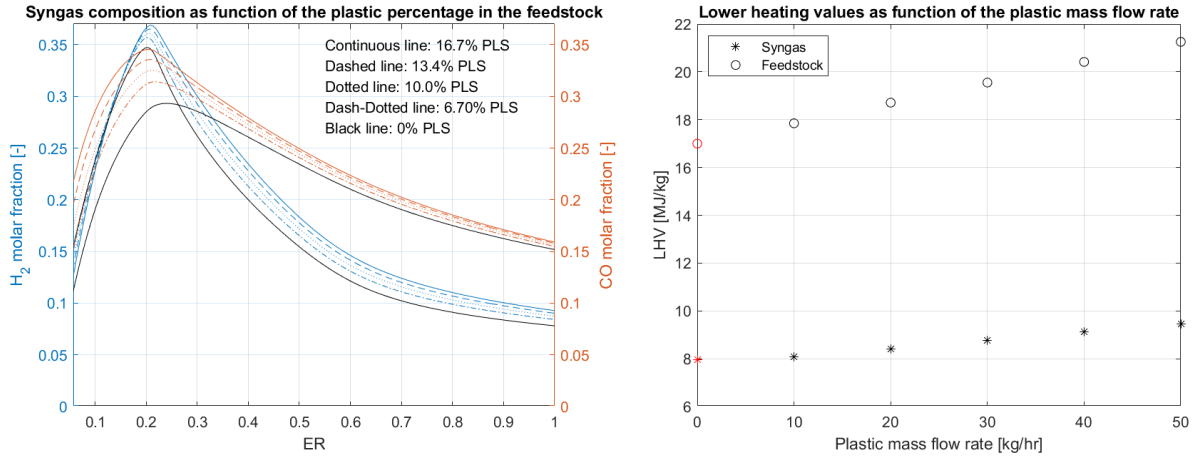


**(a)** **(b)**

**Figure 22:** (a) Molar concentrations of $H_2$ and $CO$ as function of plastic percentage in the feedstock; (b) Lower Heating Values (LHV) of the syngas and the feedstock as function of the plastic mass flow rate.

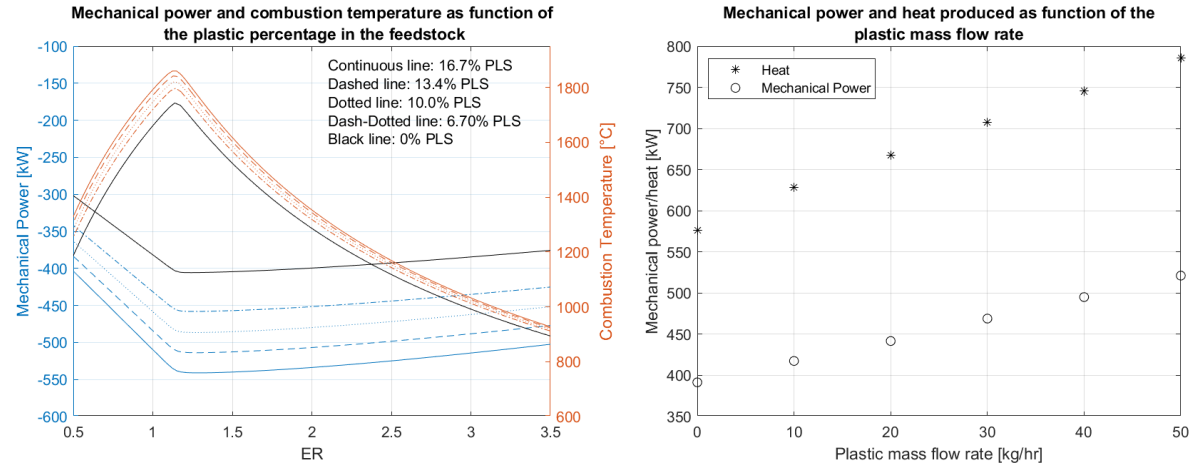


**(a)** **(b)**

**Figure 23:** (a) Mechanical power and combustion temperature as function of plastic percentage in the feedstock; (b) Mechanical power and heat produced as function of the plastic mass flow rate.

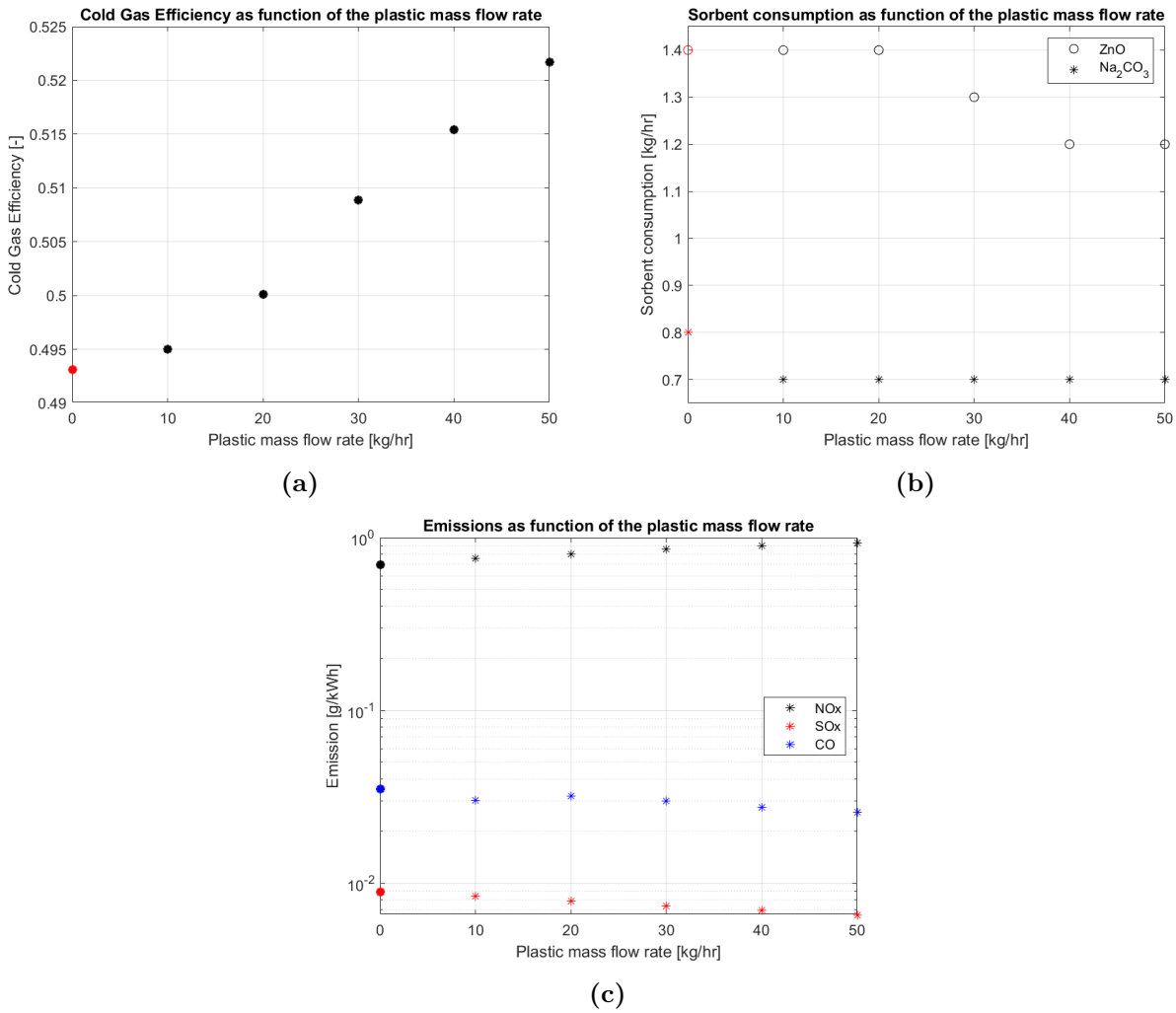


**Figure 24:** (a) Cold gas efficiency dependence on plastic mass flow rate; (b) Sorbent consumption dependence on plastic mass flow rate; (c) Emission dependence on plastic mass flow rate.

**Scenario 3 comments**

Similar to scenario 2, in scenario 3 unrecoverable, non-recyclable and chlorine-free plastic wastes (such as dirty plastics and LDPE plastic bags) are mixed with the main solid waste stream in varying and increasing fractions, for a maximum of 50 kg/hr corresponding to 16.7% of the overall mass flow. As for sewage sludge, this maximum value has been chosen based on the data from literature, which provided an average of 55.2 kg/hr of undefined plastic wastes produced on cruise ships, but the treatable fraction is bound to be lower when considering the removal of the clean, recyclable and chlorinated (like PVC) fraction. The goal of the simulations performed is to give a general idea of the main effects related to the integration of plastics in the main

flow, using diagrams similar to the one employed in scenario 2. In particular, Figure 22(a) shows the variations of $H_2$ and $CO$ molar fractions as function of the gasification equivalence ratio and plastic fraction, and it can be easily noted that both curves tend to have higher peaks for higher values of plastic percentages: at 16.7% of plastic integration the peak molar fraction of $H_2$ reaches 36.8% and the peak molar fraction of $CO$ reaches 34.1%. This effect is related to the higher content of Hydrogen and Carbon in the feed. This is beneficial from the point of view of the lower heating value of the syngas, as shown in Figure 22(b). With respect to the sewage sludge case, the increase in the syngas lower heating value is much sharper, moreover the feedstock LHV is also increasing, as plastics are generally characterized by higher mass fractions of Carbon and Hydrogen (peak values are 21.25 MJ/kg for the LHV of the feedstock and 9.44 MJ/kg for the LHV of te syngas). Figures 23(a) and 23(b) show significant increases in the mechanical power produced by the gas engine as well as in the combustion temperature for increasing plastic fractions, effects that are most likely linked to the higher LHV of the syngas. In fact, we see a +33.21% increase to mechanical power at 16.7% integration, compared to scenario 1, and a +36.21% increase to the heat recovered. In this case the heat recovered grows, as no drying pre-treatment process is needed. The graphs displayed in Figures 24(a), (b) and (c) provide further information on key parameters such as cold gas efficiency, emissions and sorbent consumption. In particular, the cold gas efficiency increases strongly, and we have a peak of 52.21% for 16.7% of plastic integration, which means that the cold gas efficiency increases faster compared to the sewage sludge case, in which up to 100 kg/hr of sewage were integrated. From the point of view of sorbent consumption, plastic integration seems beneficial since around the same amount of material is needed compared to the case with no plastic, as the Sulphur content in the feedstock is reduced (1.2 - 1.4 kg/hr of $ZnO$). NOx emissions are slightly increased, while SOx and CO levels slightly decrease, but still everything inside the prescribed limits. Overall, the introduction of plastics, which are normally characterized by high intrinsic chemical energy, seems to be possible and even beneficial for the process, and the positive net electric energy balance is also guaranteed, as discussed in scenario 1. Potential issues linked to plastic involvement that cannot be simulated with the present model, such as dioxine generation, enhanced tars production and slag/ashes toxicity will require real life experiments.

## Scenario 4

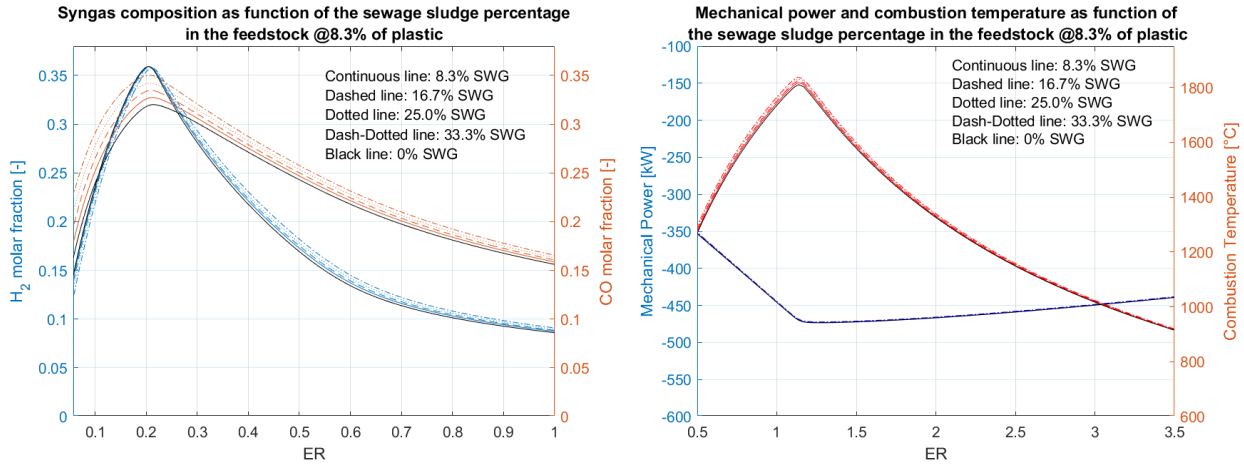


**(a)** **(b)**

**Figure 25:** (a) Molar concentrations of $H_2$ and $CO$ as function of sewage sludge percentage in the feedstock at 8.3% fraction of plastic; (b) Mechanical power and combustion temperature as function of sewage sludge percentage in the feedstock at 8.3% fraction of plastic.

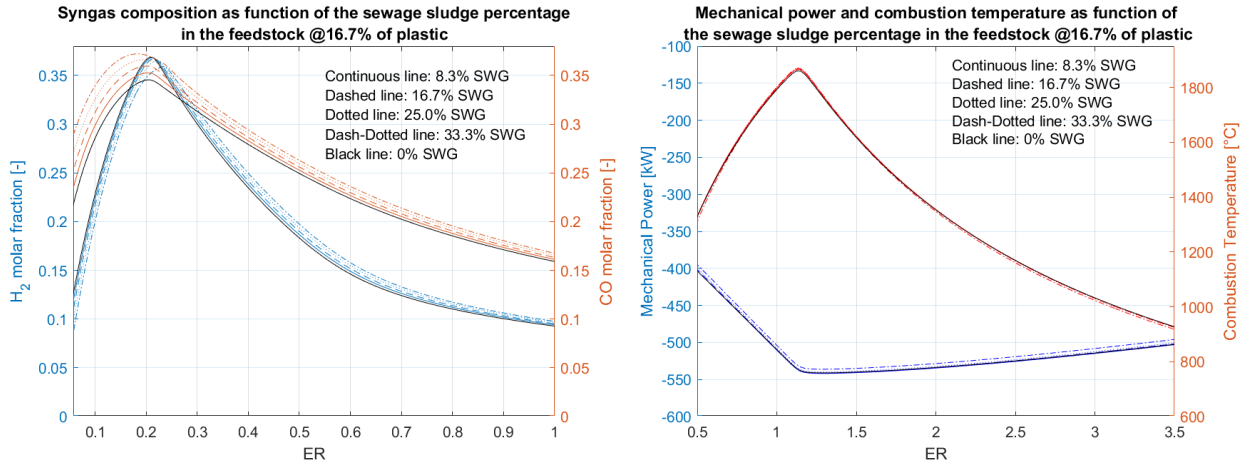


**(a)** **(b)**

**Figure 26:** (a) Molar concentrations of $H_2$ and $CO$ as function of sewage sludge percentage in the feedstock at 16.7% fraction of plastic; (b) Mechanical power and combustion temperature as function of sewage sludge percentage in the feedstock at16.7% fraction of plastic.

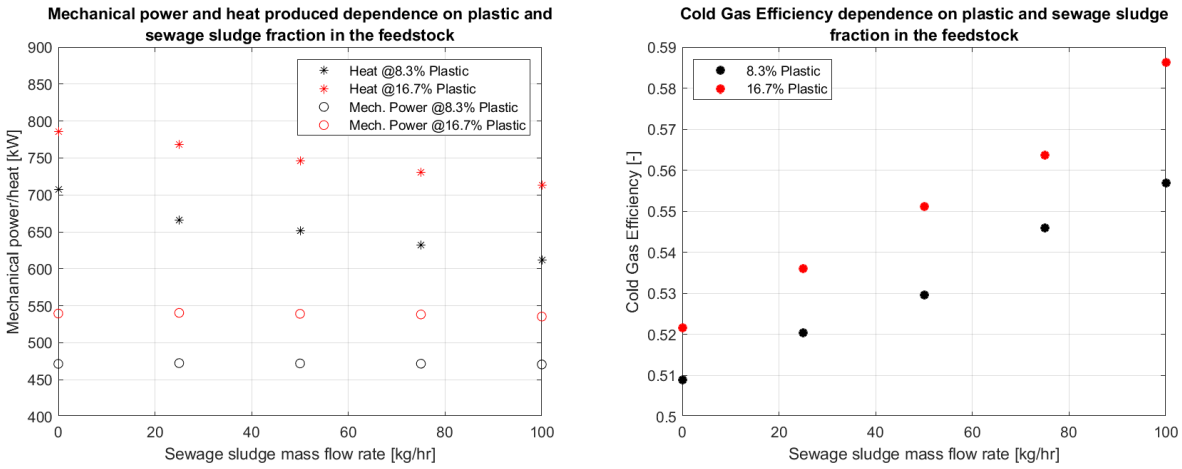


(a)




(b)

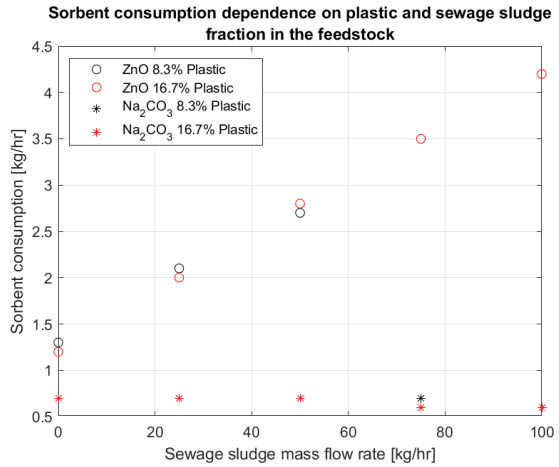


(c)

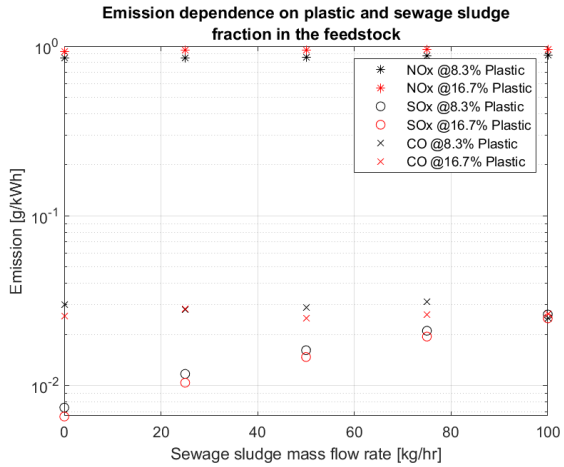


(d)

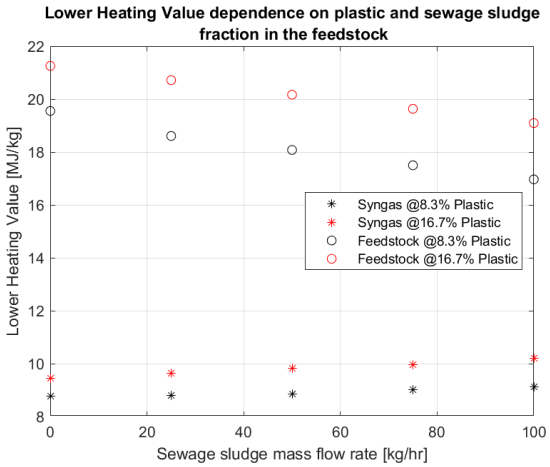


(e)

**Figure 27:** (a) Mechanical power and heat produced as function of sewage sludge and plastic fraction; (b) Cold gas efficiency as function of sewage sludge and plastic fraction; (c) Sorbent consumption as function of sewage sludge and plastic fraction; (d) SOx, NOx and CO emissions as function of sewage sludge and plastic fraction. (e) Lower heating value as function of sewage sludge and plastic fraction.

**Scenario4 comments**

In this last scenario the previous two cases are combined, as both plastic and sewage sludge are mixed together in the main feedstock stream. The maximum values introduced are retained, 100 kg/hr of sewage sludge and 50 kg/hr of plastic. Nevertheless, two values of plastic fraction are fixed for the simulation, 25 kg/hr and 50 kg/hr, or in percentage 8.3% and 16.7%, while sewage sludge is varied in the same way of scenario 2. It is expected a combination of the effects observed in the previous cases, and this can be noticed in Figures 25(a), (b) and 26(a), (b). In fact, the mechanical power is observed to remain almost constant when varying sewage sludge at fixed plastic fraction but sharply increasing when instead the plastic fraction is increased, as noted in scenario 2 and 3. The same behavior can be noticed for the syngas composition, as sewage sludge tends to increase only the $CO$ molar fraction, while an increase in plastic produces higher quantities of hydrogen in the gas mixture. Corresponding to 33.3% of sewage sludge and 16.7% of plastic, at ER = 0.21, the molar fraction of $H_2$ reaches 36.9% while the molar fraction of $CO$ reaches 37.0%, the highest value found. According to Figure 27 some further considerations can be made: as already displayed, the mechanical power increases strongly with plastic and weakly with sewage sludge, while the heat recovered decreases for increasing sewage sludge due to the drying process, although the presence of plastic can compensate this effect. In case of 16.7% of plastic and 33.3% of sewage sludge the mechanical power increases of +32.19% compared to scenario 1, while the heat recovered by +23.66%. The maximum value of cold gas efficiency is reached for the maximum percentage of both plastics and sewage sludge, around 58.65%, meaning that the most efficient gasification process is achieved for a reduced amount of solid wastes. This is mostly related to the increase in the syngas LHV and the reduction in the feedstock LHV. The $ZnO$ consumption is strongly affected by the sewage sludge percentage, and with varying plastic content no significant variations are observed (peak value of 4.3 kg/hr), while $Na_2CO_3$ consumption remains relatively constant (around 0.7 kg/hr). The emissions too are mainly affected by the the sewage sludge integration, which is especially true for $SOx$, while $CO$ and $NOx$ remain relatively constant, and still the prescribed limits are satisfied. The maximum value of syngas LHV corresponds to the condition of higher cold gas efficiency, that is for 16.7% plastic and 33.3% sewage sludge (10.2 MJ/kg). Overall, the integration of

both streams in the main feedstock appears to be even more beneficial than the two previous scenarios, as some negative effects like the reduced recovered heat are compensated by the increased overall syngas LHV. The simulations have shown that it is indeed possible for the system to theoretically handle a variety of different waste streams, which is a excellent thing from the point of view of flexibility.

## 5.5 Chapter summary

In this chapter the preliminary design and modeling of a plasma gasification unit for maritime applications, in particular for cruise ships, was performed, with the use of the process modeling software Aspen Plus and MatLab for the post-processing phase. The system was split into five main sub-units, according to the function they perform: the waste pre-treatment unit, for the preliminary treatment of the feedstock with the function of increasing the syngas yield and to simplify the subsequent processes. The gasification unit, in which the feedstock is converted into raw syngas and bottom slag/ashes. The syngas cleaning unit, in which the raw syngas is cleaned and removed of deleterious contaminants such as $H_2S$ and $HCl$. The gas engine, for the conversion of the chemical energy stored in the cleaned syngas to thermal, then mechanical and then electric energy. The heat recovery system, characterized by several heat exchangers whose function is to collect waste heat from the 4 previous units. Four scenarios of operation of the system were investigated, the first one being a solid waste-pure feedstock, the second one integrating dried sewage sludge, the third one integrating plastic wastes and the fourth one a combination of second and third scenario. The results of these simulations, which were accurately optimized, showed a good flexibility for the system modeled, capable of handling varying compositions of solid feedstock without incurring in cases of negative net electric energy balance, which is a crucial outcome that needed to be demonstrated. Several other different outputs were also produced: from the point of view of gasification efficiency, the cold gas efficiency was evaluated for every scenario, and the results varied in a range of $49.3\% \div 58.65\%$ depending on the composition of the feedstock chosen. The SOx, NOx and CO emissions at the flue gases were also evaluated, as well as the consumption rate of the sorbents used in the syngas cleaning system. The LHV of the syngas and of the feedstock

were also calculated as necessary for the evaluation of the cold gas efficiency, and these LHV are based respectively on the mass composition of the syngas and the ultimate analysis of the treated feedstock, which was obtained from the literature.

# 6 Conclusions

The research work aimed to develop a comprehensive model for the treatment of waste on mobile applications, in particular cruise ships, through the employment of plasma gasification. The model, split into two macro unit, which are the plasma generator section and the plasma gasification system section, was developed using the software COMSOL and Aspen Plus respectively, while MATLAB and Microsoft Excel were used for the results processing. The main scope of the model was to ultimately investigate the possibility of operating similar systems in condition of positive net electricity balance at steady state and in different conditions of feedstock composition, while also trying to assess the gaseous emissions to the environment. Furthermore, such a model could aid the development of real systems by providing preliminary data for the design (in terms of temperatures involved, mass flow rates of feed, water, air, ashes, sorbents, feedstock composition, mechanical power produced, heat recovered), however validation of the model should be performed. The model development was done following some logical steps: first of all, the waste management issues and the environmental impacts linked to the waste streams on cruise ships were investigated, and the average waste generation and its characteristics were also assessed. After that, the waste-to-energy approaches were described, in order to justify the choice of the plasma gasification technology. The modeling phase started with the section related to the modeling of the RF plasma torch, fundamental component of the system, and the scope of the section was to produce output results (temperature, plasma gas mass flow rate, electrical power consumption) to be fed to the following section, related to the modeling of the whole waste treatment unit. The system was split into five sub units, each performing a definite function: waste pre-treatment, plasma gasification, syngas cleaning, energy conversion, heat recovery. The waste pre-treatment unit received as input the information obtained from the cruise ship waste generation assessment and characterization, while the gasification unit received inputs from the plasma modeling section. The scope of the research project was fulfilled, as the system modeled is able, for sufficiently high feedstock mass flow rates, to operate in conditions of electric energy gain. Furthermore, through the use of different feedstock scenarios, the flexibility of the system was also as-

sessed, as the possibility of treating wastes with varying concentrations of sewage sludge and plastic, besides typical solid wastes, appeared beneficial. In particular, the cold gas efficiency was observed to be increasing in these cases. The plasma torch simulations performed show also reasonable results, as the temperatures obtained are within the ranges provided in the literature and the typical effects on the magnetic field penetration are also observed. Having said so, a lot of improvements to the study can be made, by increasing the overall complexity of the system and the physics involved. Some of these improvements could be foreseen for future works: for starting, direct audits or surveys in cooperation with cruise liners would allow to better characterize the feedstock, coupled with specific studies on their proximate and ultimate analysis. The gasification model could be improved by including tars and dioxins formation and the effects of free radicals on the efficiency of the gasification process. Regarding the syngas cleaning unit, considering the kinetics of the adsorption reactions would give better results. It could be also possible to consider the cold syncas cleaning approach instead of the hot one. Furthermore, sizing of the units and inclusion of the spatial dependence in the gasification model would improve the results in the optics of more structured designs. Inclusion of time dependent studies and accidental conditions. Economic analysis more precise preliminary designs would for sure improve the quality of the model. Naturally, it would be absolutely crucial to design experimental setups to validate both the gasification model and the plasma torch model and to verify that some real life technical issues, like tars clogging, wearing of plasma torches components such as excitation coils/electrodes, hot syngas cleaning feasibility, are not deal-breakers. These are only some of the main problems that will need to be targeted in potential future research works to increase the reliability of the simulations and to identify possible critical issues.

# References


[1] Cruise Lines international Association (2018). '2019 Cruise Trends & Industry'.
https://cruising.org/news-and-research/research/2018/december/2019-state-of-the-industry (last seen on 18/05/2020)

[2] Business Research & Economic Advisors (2018). 'The Global Economic Contribution of Cruise Tourism 2017', prepared for CLIA.
https://cruising.org/news-and-research/research/2017/december/the-global-economic-contribution-of-cruise-tourism-2017 (last seen on 18/05/2020)

[3] Timothy MacNeill, David Wozniak (2018). 'The economic, social, and environmental impacts of cruise tourism', *Tourism Management*, Vol. 66, pp. 387-404.
https://doi.org/10.1016/j.tourman.2017.11.002

[4] David Johnson (2002). 'Environmentally sustainable cruise tourism: a reality check', *Marine Policy*, Vol. 64, no. 4, pp. 261-270.
https://doi.org/10.1016/S0308-597X(02)00008-8

[5] Aida Kaldas, Isabelle Picard, Christos Chronopoulos, Philippe Chevalier, Pierre Carabin, Gillian Holcroft, Gary Alexander, Joseph Spezio, Jim Mann, Henry Molintas (2006). 'Plasma Arc Waste Destruction System (PAWDS) A novel approach to Waste elimination aboard ships', *Naval Engineers Journal*, Vol. 118, no. 3, pp. 139-150(12).
https://doi.org/10.1111/j.1559-3584.2006.tb00470.x

[6] CruiseMapper.com (2015). 'Cruise Ship Passenger Capacity'.
https://www.cruisemapper.com/wiki/761-cruise-ship-passenger-capacity-ratings (last seen on 18/05/2020)

[7] RoyalCaribbean International Press Center (2020). 'Symphony of the Seas Fast Facts'.
https://www.royalcaribbeanpresscenter.com/fact-sheet/31/symphony-of-the-seas (last seen on 18/05/2020)

[8] Cruise Lines international Association (2020). '2021 State Of the Cruise Industry Outlook'.

https://cruising.org/en-gb/news-and-research/research/2020/december/state-of-the-cruise-industry-outlook-2021 (last seen on 21/04/2021)

[9] Robert J. Kwortnik (2008). 'Shipscape Influence on the Leisure Cruise Experience', *International Journal of Culture Tourism and Hospitality Research*, Vol. 2, no. 4, pp. 289-311.
http://doi.org/10.1108/17506180810908961

[10] James E.N. Sweeting, Scott L. Wayne, The Center for Environmental Leadership in Business (2003). 'A shifting tide: environmental challenges and cruise industry responses'.
https://eldis.org/document/A12448 (last seen on 18/05/2020)

[11] Ben Lyons, CruiseCritic.com (2020). 'How Do Cruise Ships Work?'.
https://www.cruisecritic.com/articles.cfm?ID=1546 (last seen on 18/05/2020)

[12] Tom Stieghorst, travelweekly.com (2019). 'The beauty of batteries: Hurtigruten's Roald Amundsen'.
https://www.travelweekly.com/Blogs/Dispatch/Sailing-on-Hurtigruten-ship-Roald-Amundsen (last seen on 18/05/2020)

[13] Xiuxiu Sun, Xingyu Liang, Gequn Shu, Hanzhengnan Yu, Hai Liu (2019). 'Development of surrogate fuels for heavy fuel oil in marine engine', *Energy*, Vol. 185, pp. 961-970.
https://doi.org/10.1016/j.energy.2019.07.085

[14] Lasse Johansson, Jukka-Pekka Jalkanen, Jaakko Kukkonen (2017). 'Global assessment of shipping emissions in 2015 on a high spatial and temporal resolution', *Atmospheric Environment*, Vol. 167, pp. 403-415.
https://doi.org/10.1016/j.atmosenv.2017.08.042j

[15] Marjorie Mulhall (2009). 'Saving the Rainforests of the Sea: An Analysis of International Efforts to Conserve Coral Reefs', *Duke Environmental Law & Policy Forum*, Vol. 19, pp. 321-351.
https://scholarship.law.duke.edu/delpf/vol19/iss2/6 (last seen on 18/05/2020)

[16] Jones Ross (2011). 'Environmental Effects of the Cruise Tourism Boom: Sediment Resuspension from Cruise Ships and the Possible Effects of In-

creased Turbidity and Sediment Deposition on Corals (Bermuda)', *Bulletin of Marine Science*, Vol. 87, no. 3, pp. 659-679.
https://doi.org/10.5343/bms.2011.1007

[17] Michael Herz, Joseph Davis, The Ocean Concervancy (2002). 'A Report on How Cruise Ships Affect the Marine Environment'.
Retrieved from http://www.cruiseresearch.org/MR.html (last seen on 18/05/2020)

[18] United States Environmental Protection Agency (2011). 'Graywater Discharges from Vessels'.
https://www.epa.gov

[19] International Maritime Organization, 'MARPOL - International Convention for the Prevention of Pollution from Ships, Amended by Resolutions MEPC.111(50), MEPC.115(51) and MEPC.116(51)'.
http://www.imo.org/en/Pages/Default.aspx

[20] Paul F. Kingston (2002). 'Long-term Environmental Impact of Oil Spills', *Spill Science & Technology Bulletin*, Vol. 7, nos. 1-2, pp. 53-61.
https://doi.org/10.1016/S1353-2561(02)00051-8

[21] Nickie Butt (2007). 'The impact of cruise ship generated waste on home ports and ports of call: A study of Southampton', *Marine Policy*, Vol. 31, pp. 591–598.
https://doi.org/10.1016/j.marpol.2007.03.002

[22] United States Environmental Protection Agency (2008). 'Cruise Ship Discharge Assessment Report', EPA842-R-07-005.
https://www.epa.gov

[23] Merica Sliskovic Helena Ukić BoljatH Igor Gorana Jelic-Mrcelic (2018). 'Review of Generated Waste from Cruisers: Dubrovnik, Split, and Zadar Port Case Studies', *Resources* , Vol. 7, no. 4, 72.
https://doi.org/10.3390/resources7040072

[24] CE Delft, CHEW (2016) prepared for European Maritime Safety Agency. 'The Management of Ship-Generated Waste On-board Ships'.

http://www.emsa.europa.eu/news-a-press-centre/external-news/item/2925-the-management-of-ship-generated-waste-on-board-ships.html (last seen on 18/05/2020)

[25] International Maritime Organization (2014), 'RESOLUTION MEPC.244(66), 2014 STANDARD SPECIFICATION FOR SHIP-BOARD INCINERATORS'.
http://www.imo.org/en/Pages/Default.aspx

[26] Intergovernmental Panel on Climate Change (2013). 'Anthropogenic and Natural Radiative Forcing' in 'Climate Change 2013: The Physical Science Basis. Contribution of Working Group I to the Fifth Assessment Report of the Intergovernmental Panel on Climate Change', Stocker, T.F., D. Qin, G.-K. Plattner, M. Tignor, S.K. Allen, J. Boschung, A. Nauels, Y. Xia, V. Bex and P.M. Midgley (eds.).
https://www.ipcc.ch/report/ar5/wg1/anthropogenic-and-natural-radiative-forcing (last seen on 18/05/2020)

[27] European Parliament and European Council, 19 November 2008. 'DIRECTIVE 2008/98/EC on waste and repealing certain Directives'.
http://data.europa.eu/eli/dir/2008/98/2018-07-05

[28] Pooja Ghosh, Subhanjan Sengupta, Lakhveer Singh, Arunaditya Sahay (2020). 'Chapter 8 - Life cycle assessment of waste-to-bioenergy processes: a review', *Bioreactors*, Elsevier, ISBN 9780128212646, pp. 105-122, Lakhveer Singh, Abu Yousuf, Durga Madhab Mahapatra (Ed.).
https://doi.org/10.1016/B978-0-12-821264-6.00008-5

[29] Fre´de´ric Fabry, Christophe Rehmet, Vandad Rohani, Laurent Fulcheri (2013). 'Waste Gasification by Thermal Plasma: A Review', *Waste and Biomass Valorization*, Vol. 4, pp. 421–439.
https://doi.org/10.1007/s12649-013-9201-7

[30] E. J. Lopes, Layssa Aline Okamura, Carlos Itsuo Yamamoto (2015). ' Formation Of Dioxins And Furans During Municipal Solid Waste Gasification ', *Brazilian Journal of Chemical Engineering*, Vol. 31, no. 1 pp. 87-97.
https://doi.org/10.1590/0104-6632.20150321s00003163

[31] Biswajit Ruj, Subhajyoti Ghosh (2014). 'Technological aspects for thermal plasma treatment of municipal solid waste—A review', *Fuel Processing Technology* Vol. 126, pp. 298-308.
https://doi.org/10.1016/j.fuproc.2014.05.011

[32] Michal Hlína, Milan Hrabovsky, Tetyana Kavka, Miloš Konrád (2014). 'Production of high quality syngas from argon/water plasma gasification of biomass and waste', *Waste Management*, Vol. 34, no. 1, pp. 63-66.
https://doi.org/10.1016/j.wasman.2013.09.018

[33] Gary C. Young (2010). 'Introduction to Gasification/Pyrolysis and Combustion Technology(s)' in 'Municipal Solid Waste to Energy Conversion Processes', G.C. Young (Ed.).
https://doi.org/10.1002/9780470608616.ch1

[34] Siwen Xue, Pierre Proulx, Maher I Boulos (2001). 'Extended-field electromagnetic model for inductively coupled plasma', *Journal of Physics D: Applied Physics*, Vol. 34, no. 12, 1897.
https://doi.org/10.1088/0022-3727/34/12/321

[35] T. Billoux, Y. Cressault, Ph. Teulet1, A. Gleizes (2012). 'Calculation of the net emission coefficient of an air thermal plasma at very high pressure', *Journal of Physics: Conference Series*, 12th High-Tech Plasma Processes Conference (HTPP-12), Vol. 146, pp. 21-29.
https://doi.org/10.1088/1742-6596/406/1/012010

[36] COMSOL AC/DC Module User's Guide.
https://doc.comsol.com/5.5/docserver (last seen on 03/07/2020)

[37] COMSOL Heat Transfer Module User's Guide.
https://doc.comsol.com/5.5/docserver (last seen on 03/07/2020)

[38] COMSOL CFD Module User's Guide.
https://doc.comsol.com/5.5/docserver (last seen on 03/07/2020)

[39] Liuyang Bai, Jiaping, Yuge Ouyang, Wenfu Liu, Huichao Liu, Haizi Yao, Zengshuai Li, Jun Song, Yinling Wang, Fangli Yuan (2019). 'Modeling and Selection of RF Thermal Plasma Hot-Wall Torch for Large-Scale Production of Nanopowders', *Materials*, Vol. 12, no. 13, 2141
https://doi.org/10.3390/ma12132141

[40] Fincantieri, 'Carnival Liberty, Carnival Freedom, Carnival Splendor technical data'.
https://www.fincantieri.com/it/prodotti-servizi/navi-crociera/carnival-freedom (last seen on 18/05/2020)

[41] Hui Zhou, Aihong Meng, Yanqiu Long, Qinghai Li, Yanguo Zhang (2014). 'Classification and comparison of municipal solid waste based on thermochemical characteristics', *Journal of the Air & Waste Management Association*, Vol. 64, no. 5, pp. 597-616.
https://doi.org/10.1080/10962247.2013.873094

[42] Ayşe Sever Akdağ, Onur Atak, Aysel T. Atimtay, Faika Dilek Sanin (2018). 'Co-combustion of sewage sludge from different treatment processes and a lignite coal in a laboratory scale combustor', *Energy*, Vol. 158, pp. 417-426.
https://doi.org/10.1016/j.energy.2018.06.040

[43] Hui Zhou, AiHong Meng, YanQiu Long, QingHai Li, YanGuo Zhang (2014). 'An overview of characteristics of municipal solid waste fuel in China: Physical, chemical composition and heating value', *Journal of Sustainable Tourism*, Vol. 36, pp. 107-122.
https://doi.org/10.1016/j.rser.2014.04.024

[44] Massimiliano Materazzi, Paola Lettieri, Luca Mazzei, Richard Taylor, Chris Chapman (2015). 'Reforming of tars and organic sulphur compounds in a plasma-assisted process for waste gasification', *Fuel Processing Technology*, Vo. 137, pp. 259-268.
https://doi.org/10.1016/j.fuproc.2015.03.007

[45] Siyi Luo, Bo Xiao, Zhiquan Hu, Shiming Liu, Yanwen Guan, Lei Cai (2010). 'Influence of particle size on pyrolysis and gasification performance of municipal solid waste in a fixed bed reactor', *Bioresource Technology*, Vol. 101, no. 16, pp. 6517-6520.
https://doi.org/10.1016/j.biortech.2010.03.060

[46] Isam Janajreh, Syed Shabbar Raza, Arnar Snaer Valmundsson (2013). 'Plasma gasification process: Modeling, simulation and comparison with conventional air gasification', *Energy Conversion and Management*, Vol.

65, pp. 801–809.
https://doi.org/10.1016/j.enconman.2012.03.010 ,

[47] Andrei Veksha, Apostolos Giannis, Wen-Da Oh, Victor W.-C. Chang, Grzegorz Lisak, Teik-Thye Lim (2018). 'Catalytic activities and resistance to HCl poisoning of Ni-based catalysts during steam reforming of naphthalene', *Applied Catalysis A, General*, Vol. 557, pp. 25-38.
https://doi.org/10.1016/j.apcata.2018.03.005

[48] World Health Organization (2016). 'Dioxins and their effects on human health'.
https://www.who.int/news-room/fact-sheets/detail/dioxins-and-their-effects-on-human-health (last seen on 18/05/2020)

[49] K. Suzuki, Eiki Kasai, Teruhiko Aono, H. Yamazaki, Katsuya Kawamoto (2004). 'De novo formation characteristics of dioxins in the dry zone of an iron ore sintering bed', *Chemosphere*, Vol. 54, pp. 97-104.
https://doi.org/10.1016/S0045-6535(03)00708-2

[50] Nicola Verdone, Paolo De Filippis (2006). 'Reaction kinetics of hydrogen chloride with sodium carbonate', *Chemical Engineering Science*, Vol. 61, no. 22, pp. 7487 – 7496.
https://doi.org/10.1016/j.ces.2006.08.023

[51] Joseph Lee, Bo Feng (2012). 'A thermodynamic study of the removal of HCl and H2S from syngas', *Frontiers of Chemical Science and Engineering* , Vol. 6, pp 67-83.
https://doi.org/10.1007/s11705-011-1162-4

[52] Nourredine Abdoulmoumine, Sushil Adhikari, Avanti Kulkarni, Shyamsundar Chattanathan, (2015). 'A review on biomass gasification syngas cleanup', *Applied Energy*, Vol. 155, pp. 294-307.
https://doi.org/10.1016/j.apenergy.2015.05.095

[53] Prasad Kaparaju, Jukka Rintala (2013). 'Generation of heat and power from biogas for stationary applications: boilers, gas engines and turbines, combined heat and power (CHP) plants and fuel cells' in 'The Biogas Handbook'.
https://doi.org/10.1533/9780857097415.3.404

[54] Siemens AG, 'SGE-S series gas engines and gen-sets natural gas'. https://www.siemens-energy.com/global/en/offerings/power-generation/gas-engines/sl-engines.html (last seen on 27/04/2021)

[55] Chung K. Law (2006). 'Combustion Physics', Cambridge University press. https://doi.org/10.1017/CBO9780511754517

[56] S.A. Channiwala, P.P. Parikh (2002). 'A unified correlation for estimating HHV of solid, liquid and gaseous fuels', *Fuel*, Vol. 81, no. 8, pp. 1051-1063. https://doi.org/10.1016/S0016-2361(01)00131-4

[57] United States Environmental Protection Agency (2007). 'Methodology for Thermal Efficiency and Energy Input Calculations and Analysis of Biomass Cogeneration Unit Characteristics', EPA-HQ-OAR-2007-0012. https://www3.epa.gov